

FIG. 1A

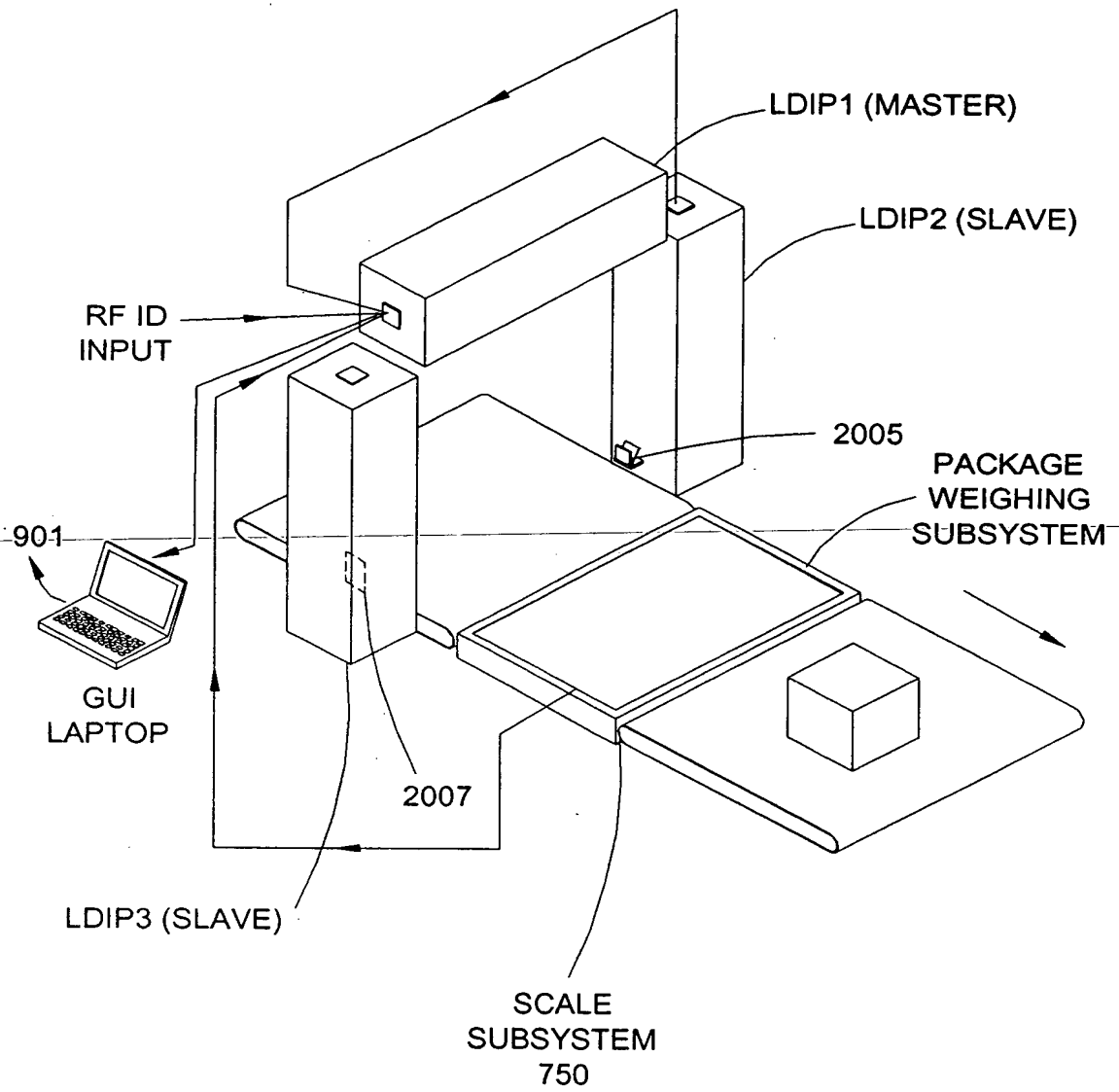
3-SIDED TUNNEL
SYSTEM

FIG. 1B

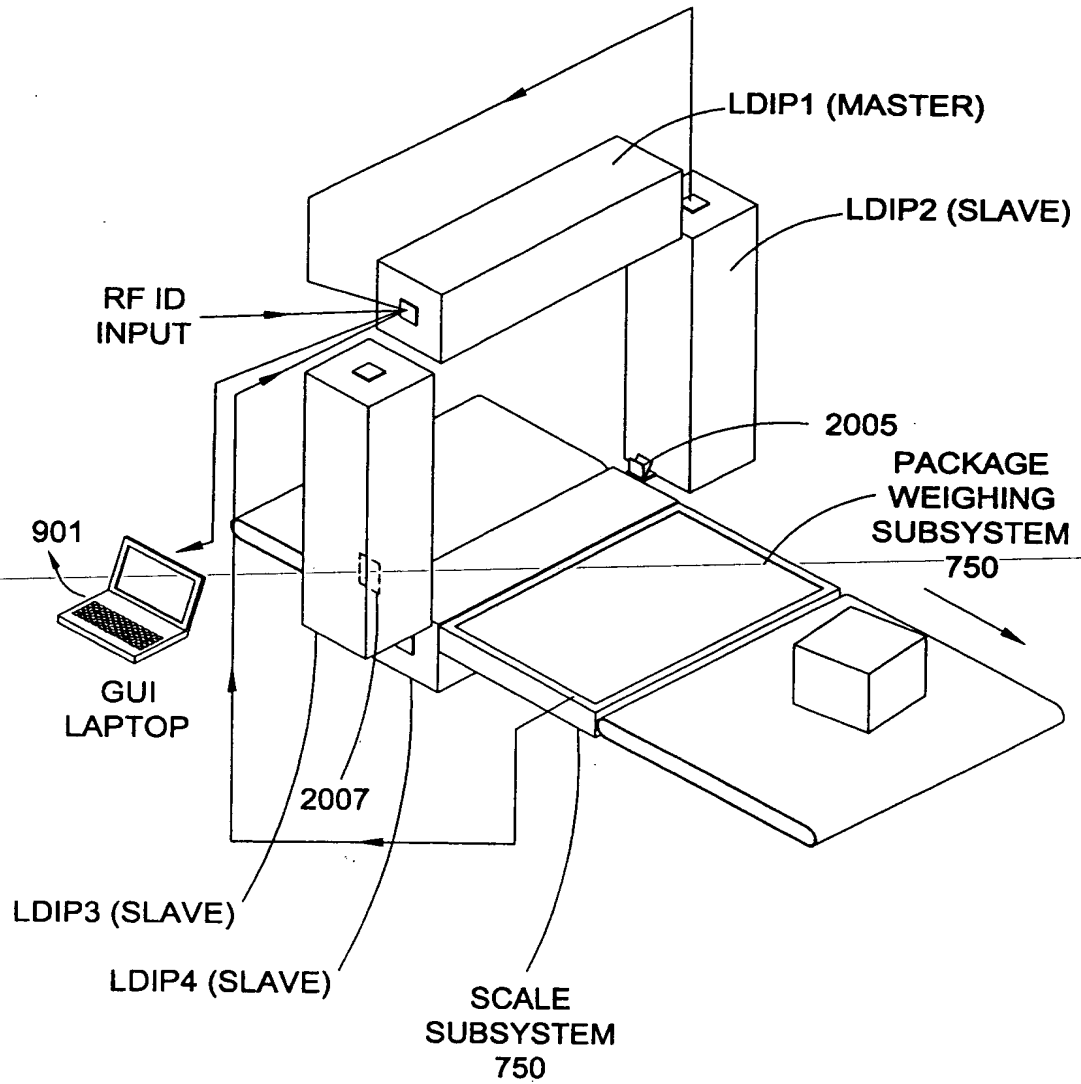
4-SIDED TUNNEL
SYSTEM

FIG. 1C

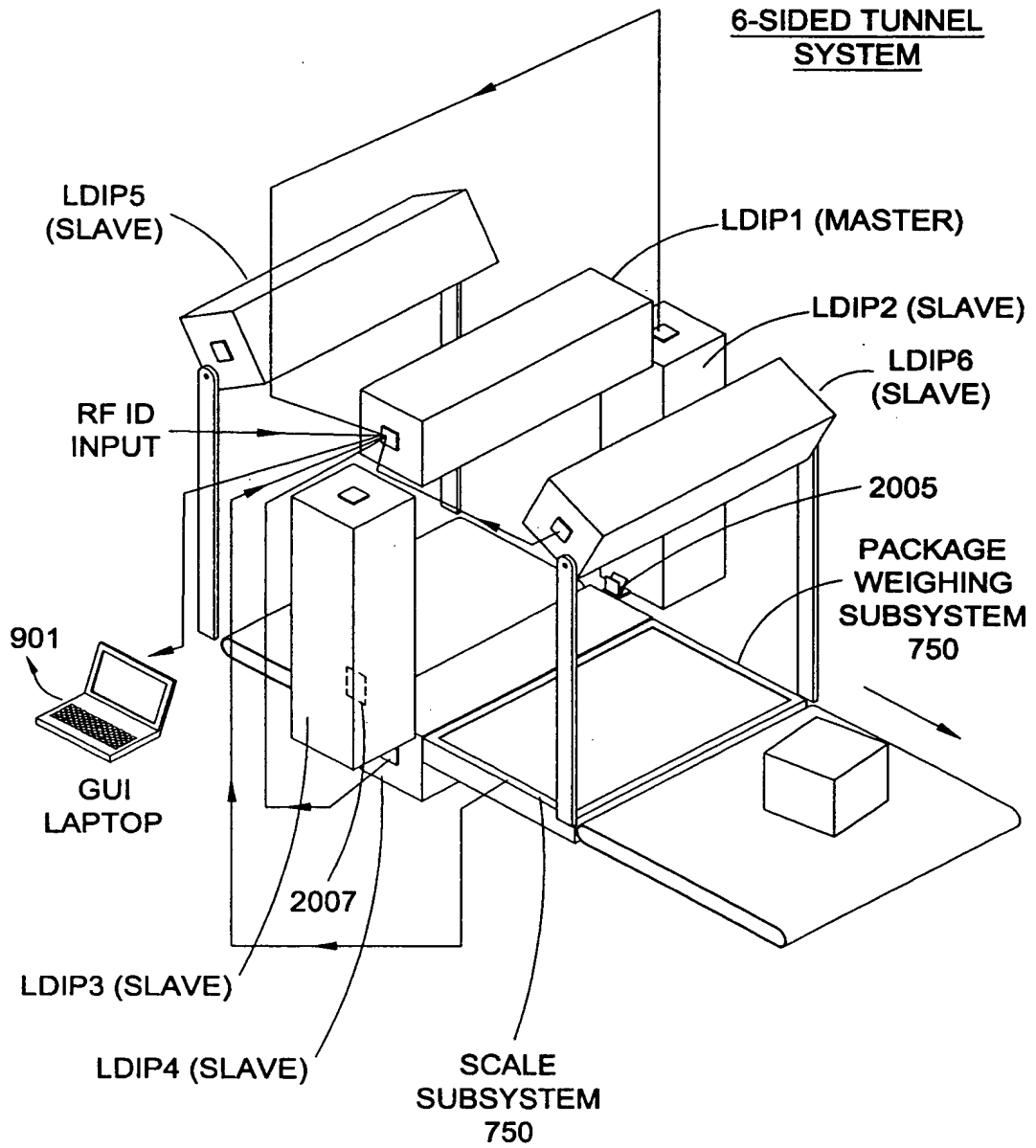


FIG. 1D

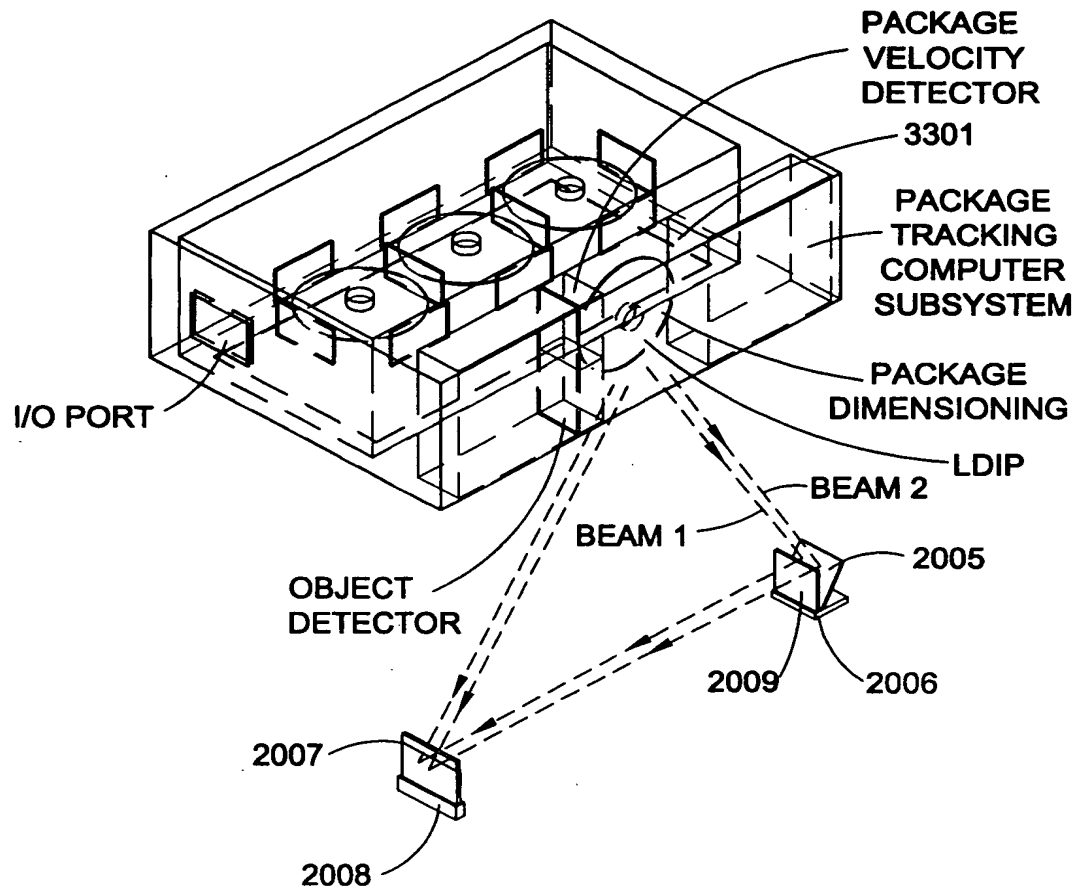


FIG. 2A

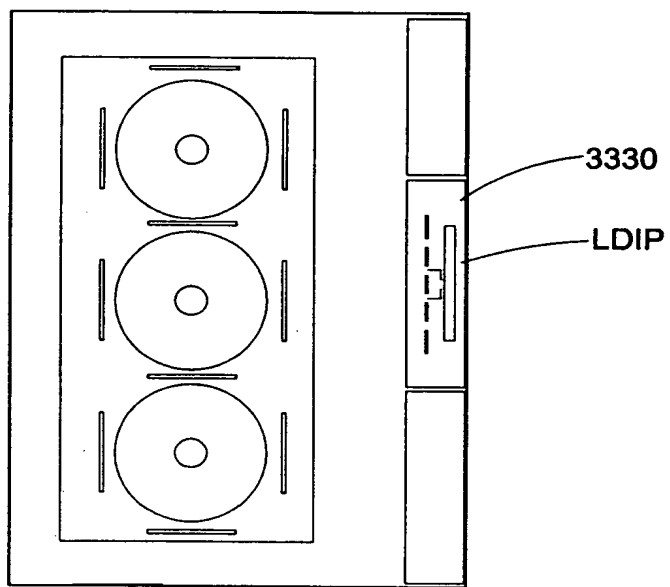


FIG. 2B

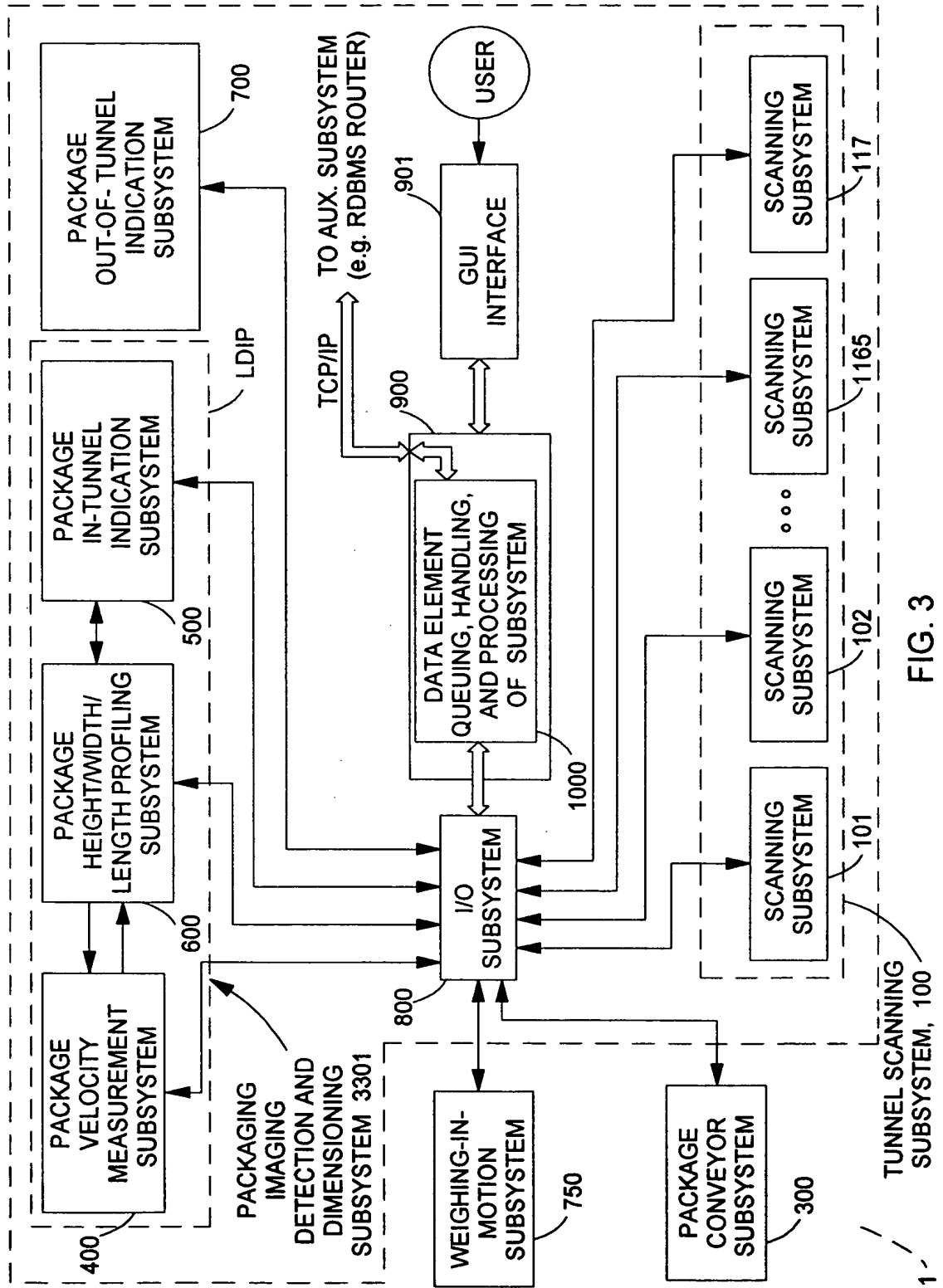


FIG. 3

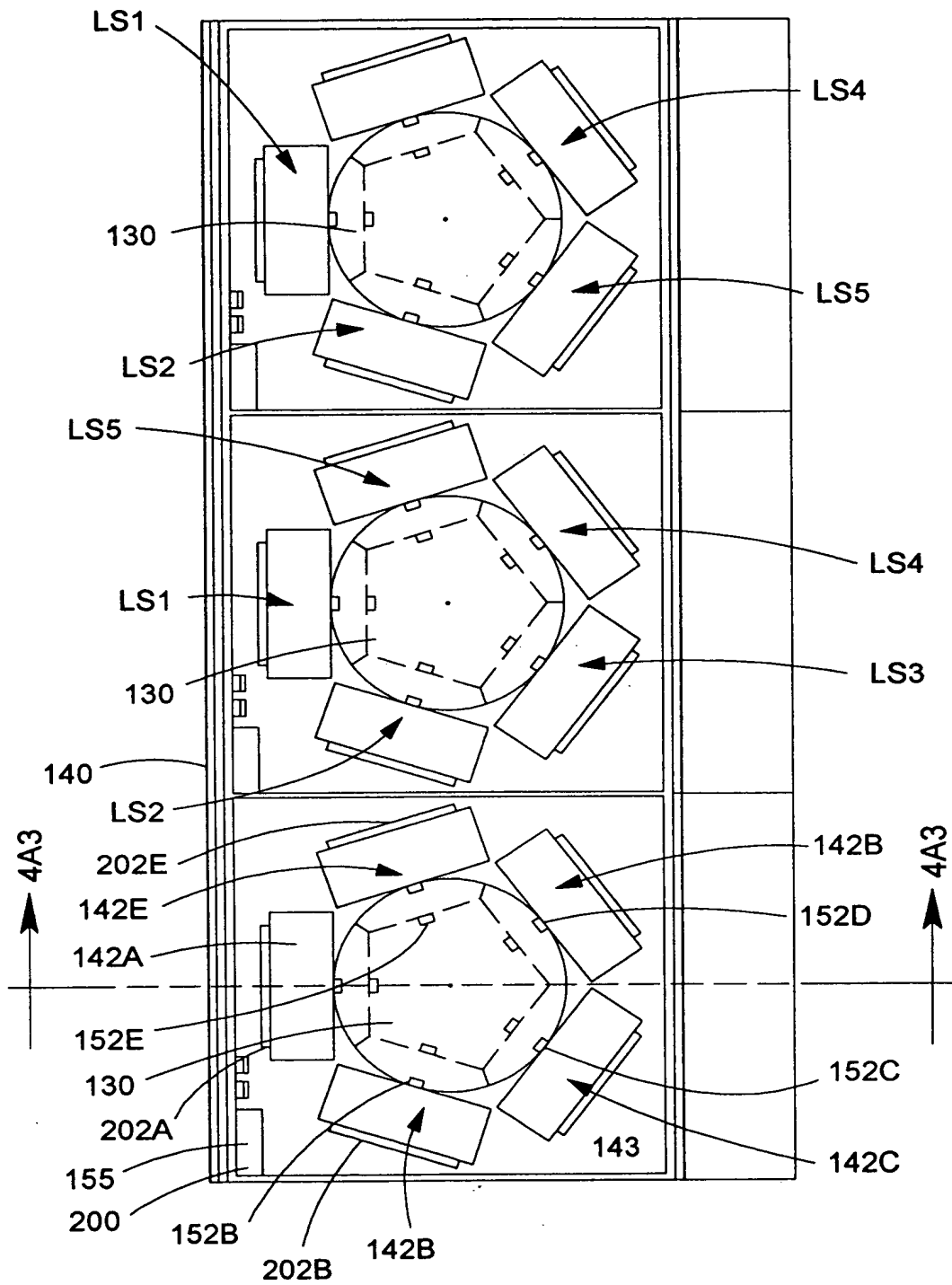


FIG. 4A1

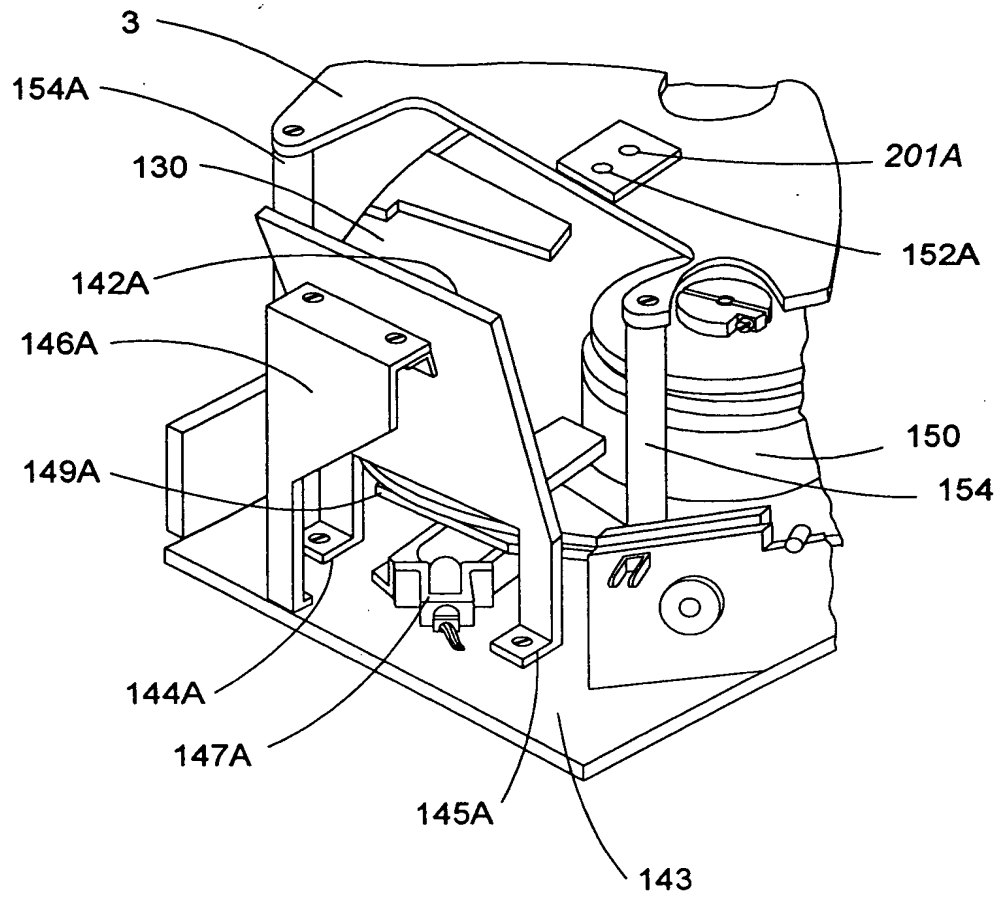


FIG. 4A2

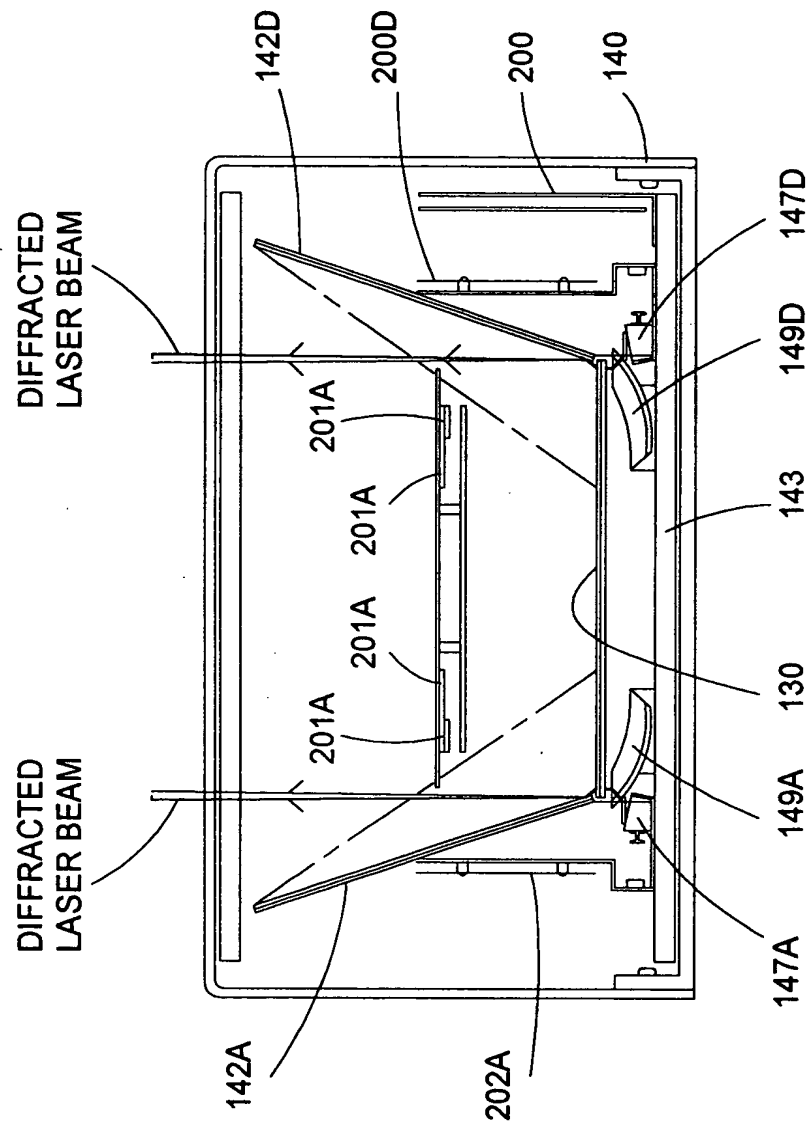


FIG. 4A3

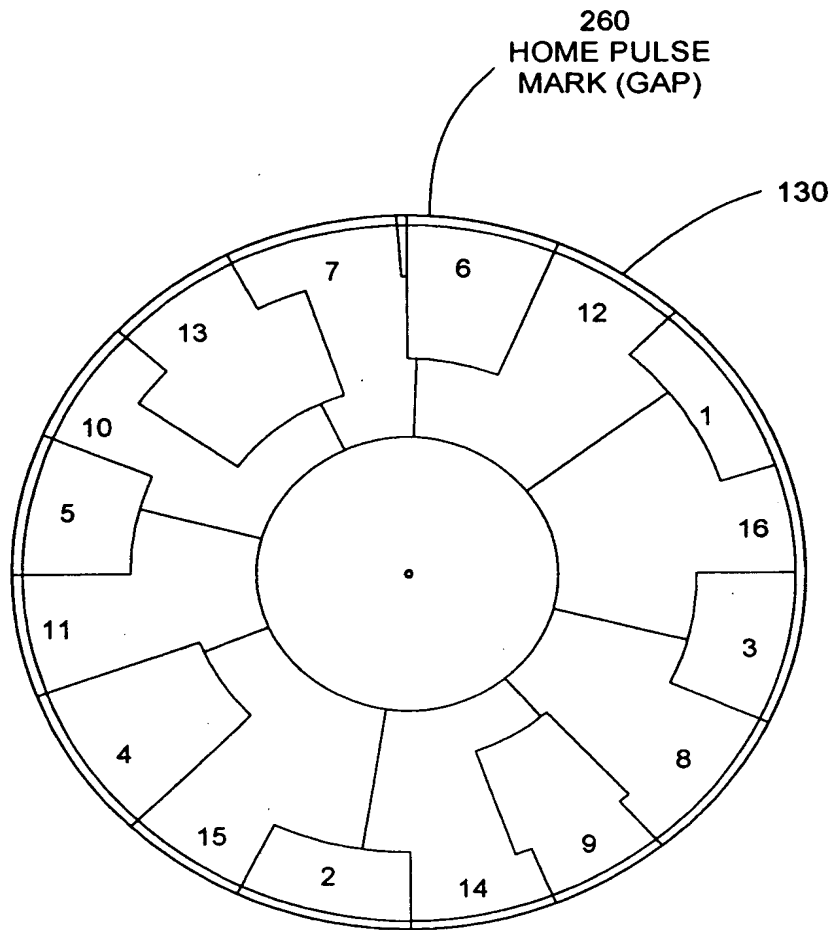
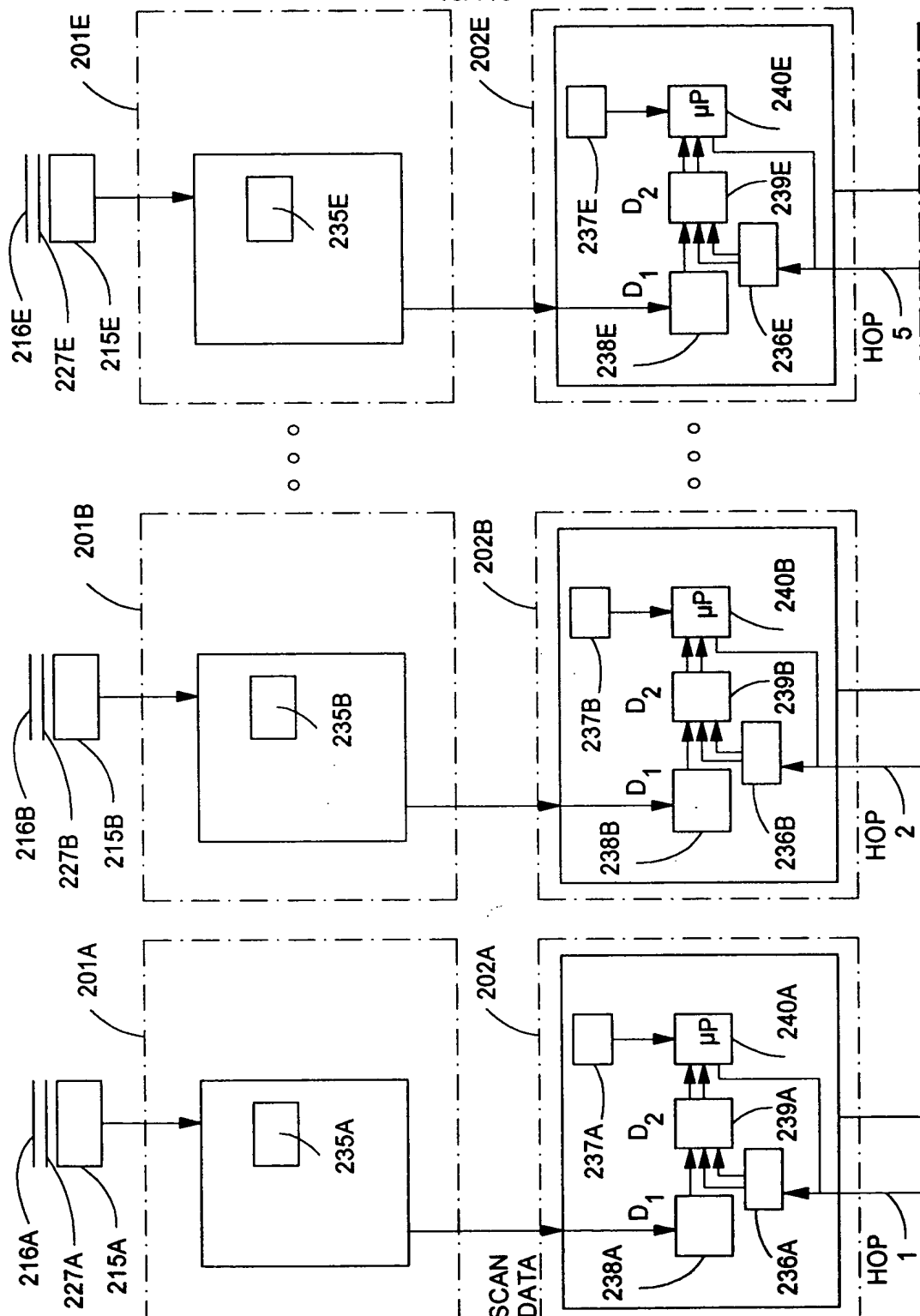


FIG. 4A4

FACET	DIFFRACTION FOCAL LENGTH (INCHES)	GEOMETRICAL FOCAL LENGTH (INCHES)	ANGLE A (DEGREE)	ANGLE B (DEGREE)	ANGLE OF DIFFRACTION (DEGREES)	ANGLE OF BEAM FROM VERTICAL (DEGREES)	SCAN ANGLE (DEGREES)	SCAN MULT. FACTOR (m)	ROTATION ANGLE (DEGREES)
1	49.57	49.76	45.9	61.06	28.94	-3.06	29.61	1.26	23.51
2	49.54	49.73	45.9	55.62	34.38	2.38	29.62	1.34	22.10
3	49.96	50.16	45.9	50.23	39.77	7.77	29.39	1.41	20.77
4	50.81	51.01	45.9	44.97	45.03	13.03	28.92	1.48	19.52
5	49.57	49.76	45.9	61.06	28.94	-3.06	29.61	1.26	23.51
6	49.54	49.73	45.9	55.62	34.38	2.38	29.62	1.34	22.10
7	49.96	50.16	45.9	50.23	39.77	7.77	29.39	1.41	20.77
8	50.81	51.01	45.9	44.97	45.03	13.03	28.92	1.48	19.52
9	59.06	59.38	45.9	60.56	29.44	-2.56	25.01	1.25	55.73
10	59.04	59.36	45.9	56.00	34.00	2.00	25.02	1.32	55.73
11	59.39	59.72	45.9	51.47	38.53	6.53	24.88	1.39	55.73
12	60.10	60.44	45.9	47.01	42.99	10.99	24.59	1.44	55.73
13	59.06	59.38	45.9	60.56	29.44	-2.56	25.01	1.25	55.89
14	59.04	59.36	45.9	56.00	34.00	2.00	25.02	1.32	55.89
15	59.39	59.72	45.9	51.47	38.53	6.53	24.88	1.39	55.89
16	60.10	60.44	45.9	47.01	42.99	10.99	24.59	1.44	55.89

FIG. 4A5



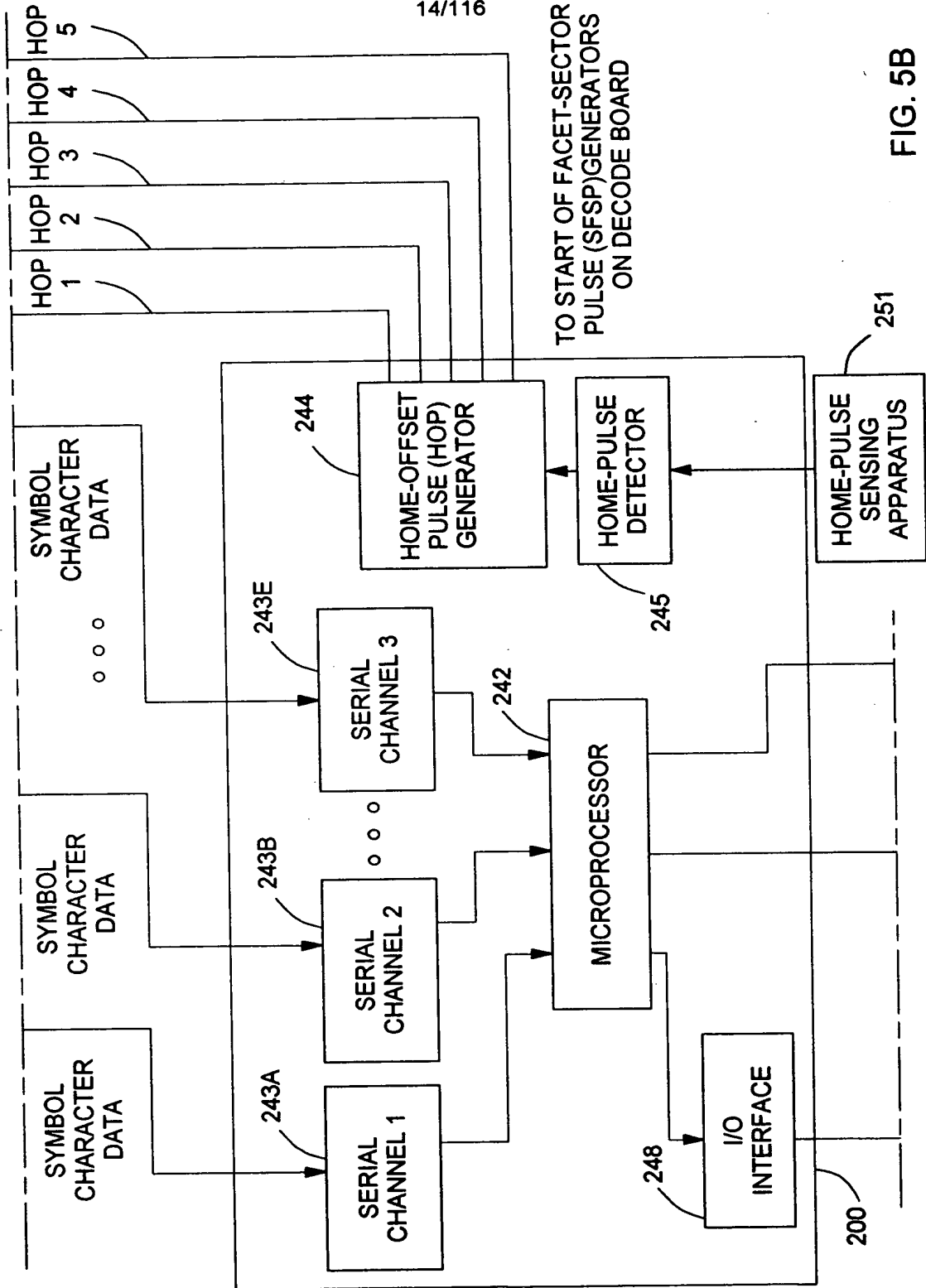


FIG. 5B

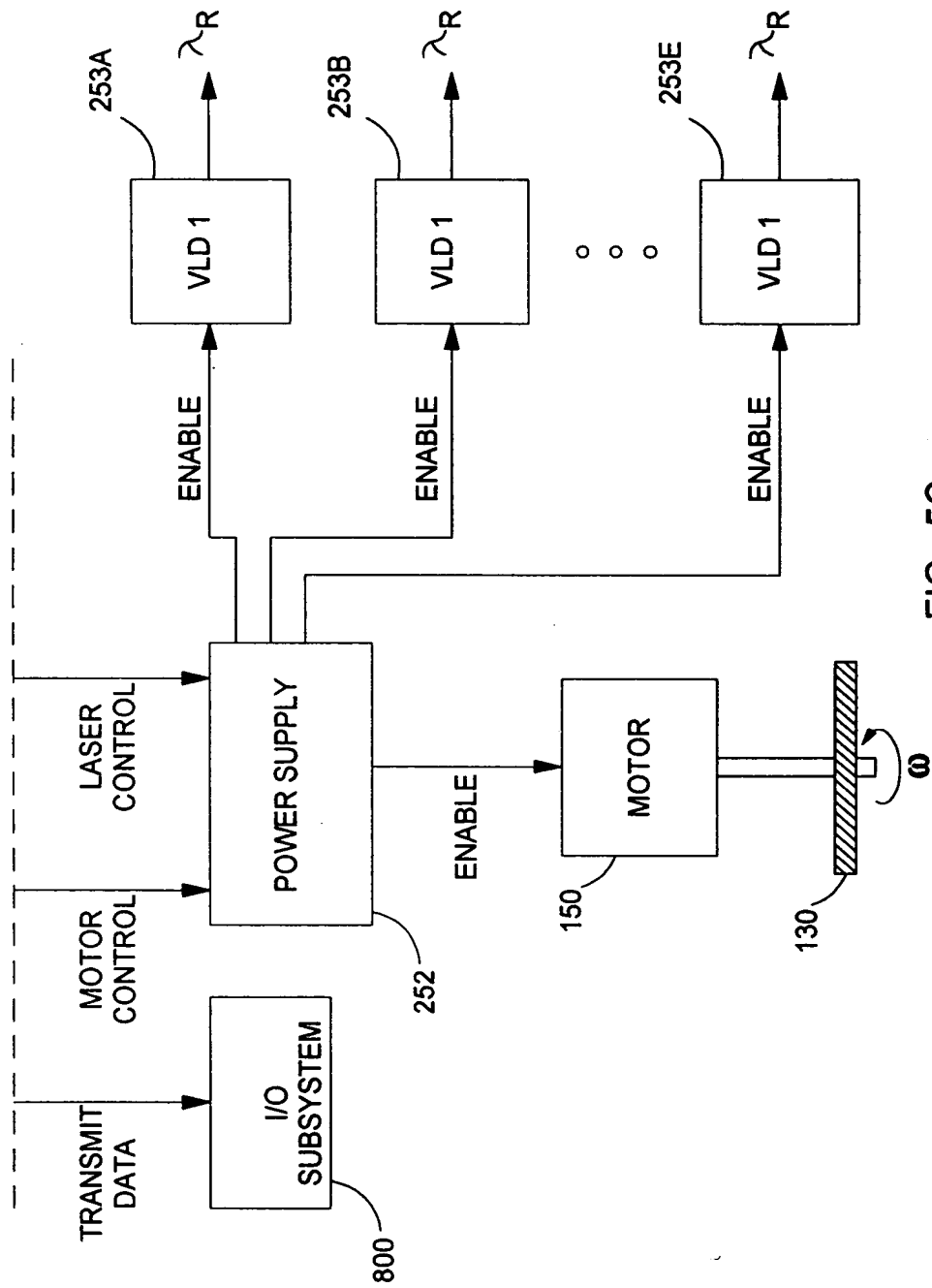


FIG. 5C

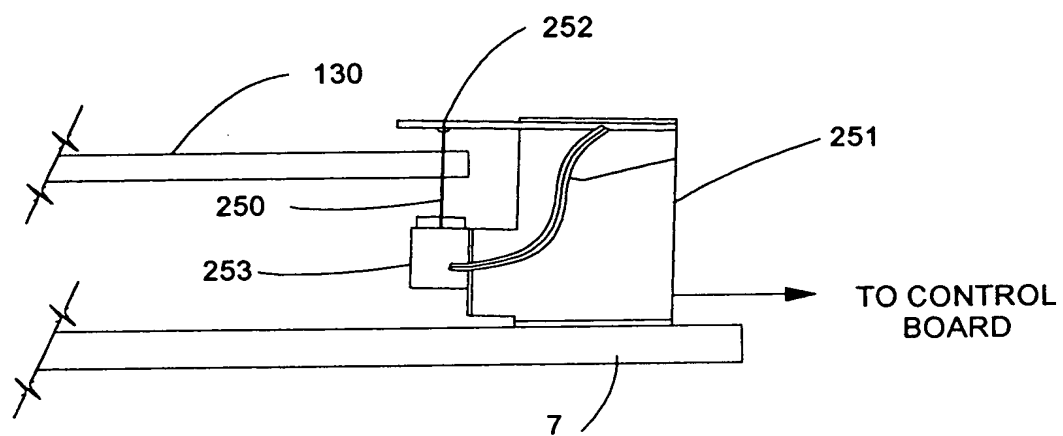


FIG. 6A

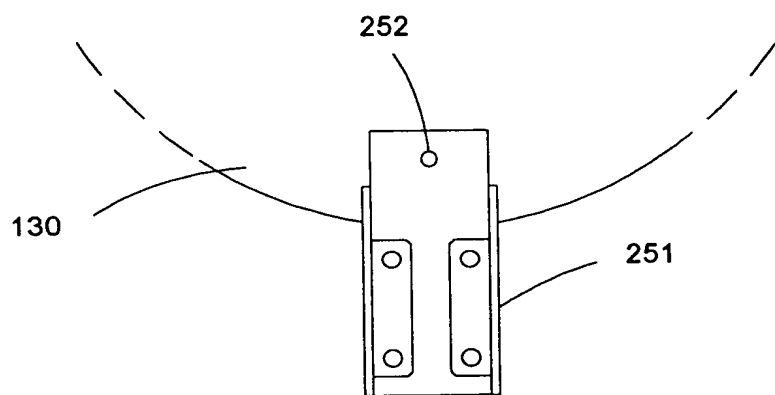


FIG. 6B

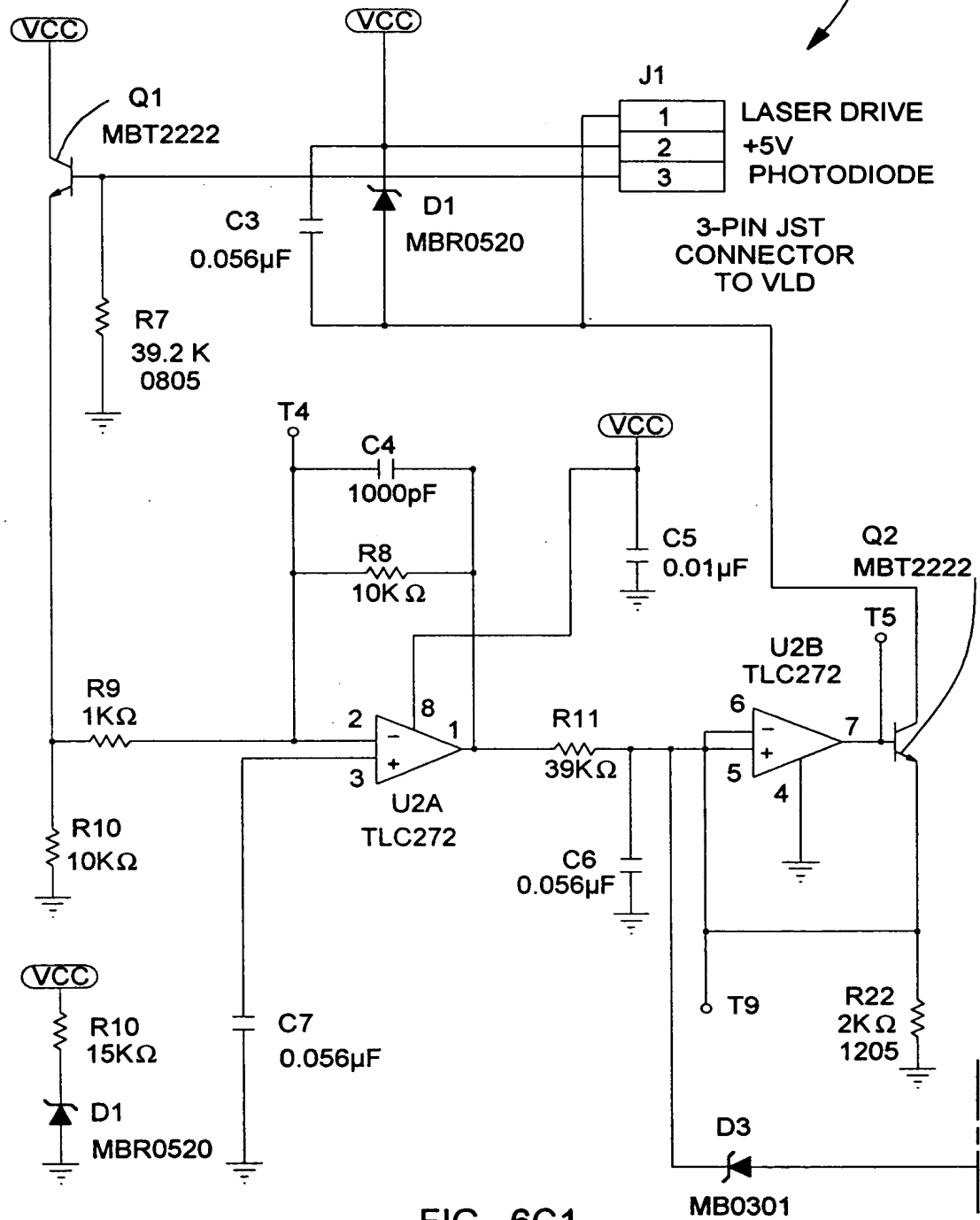


FIG. 6C1

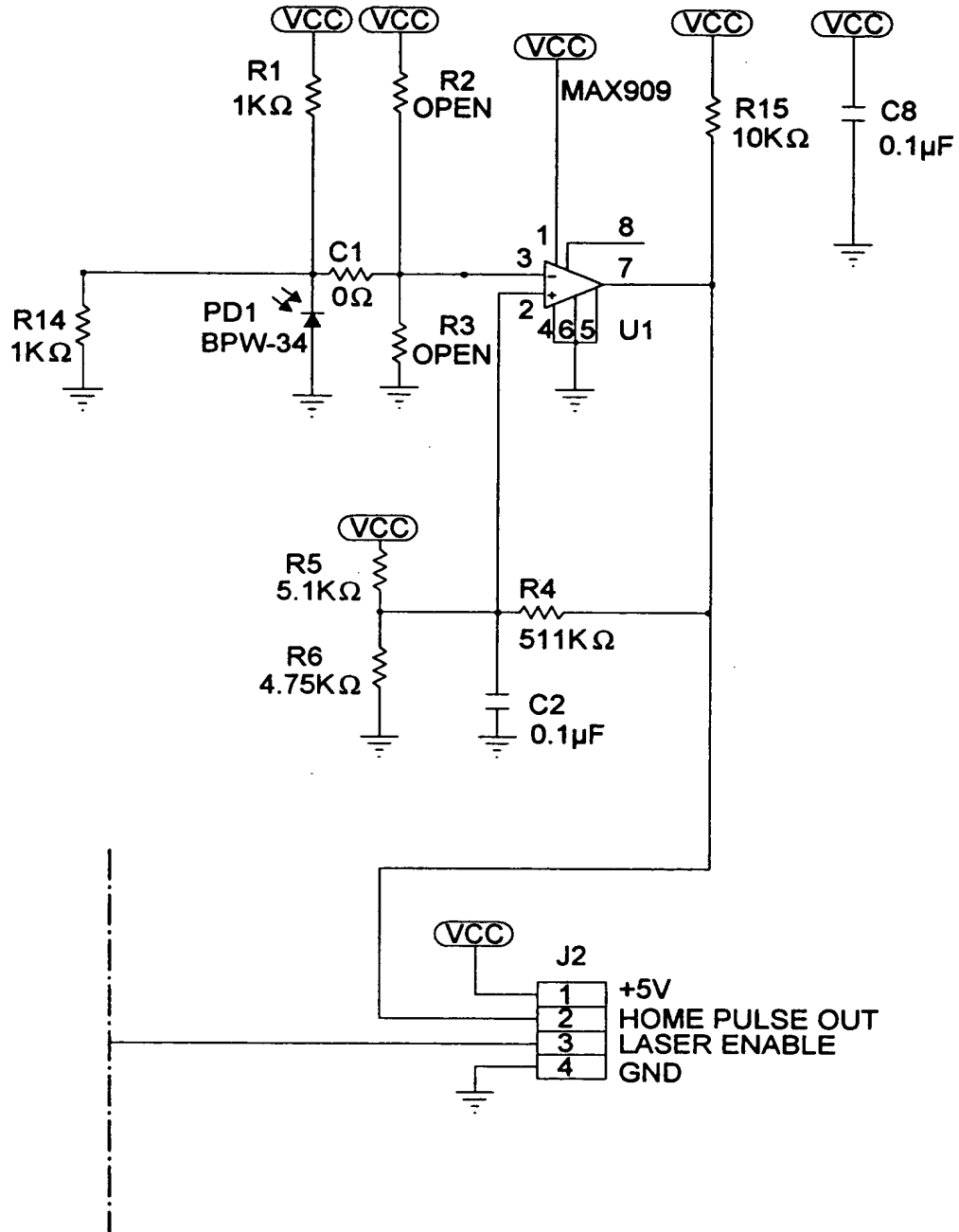


FIG. 6C2

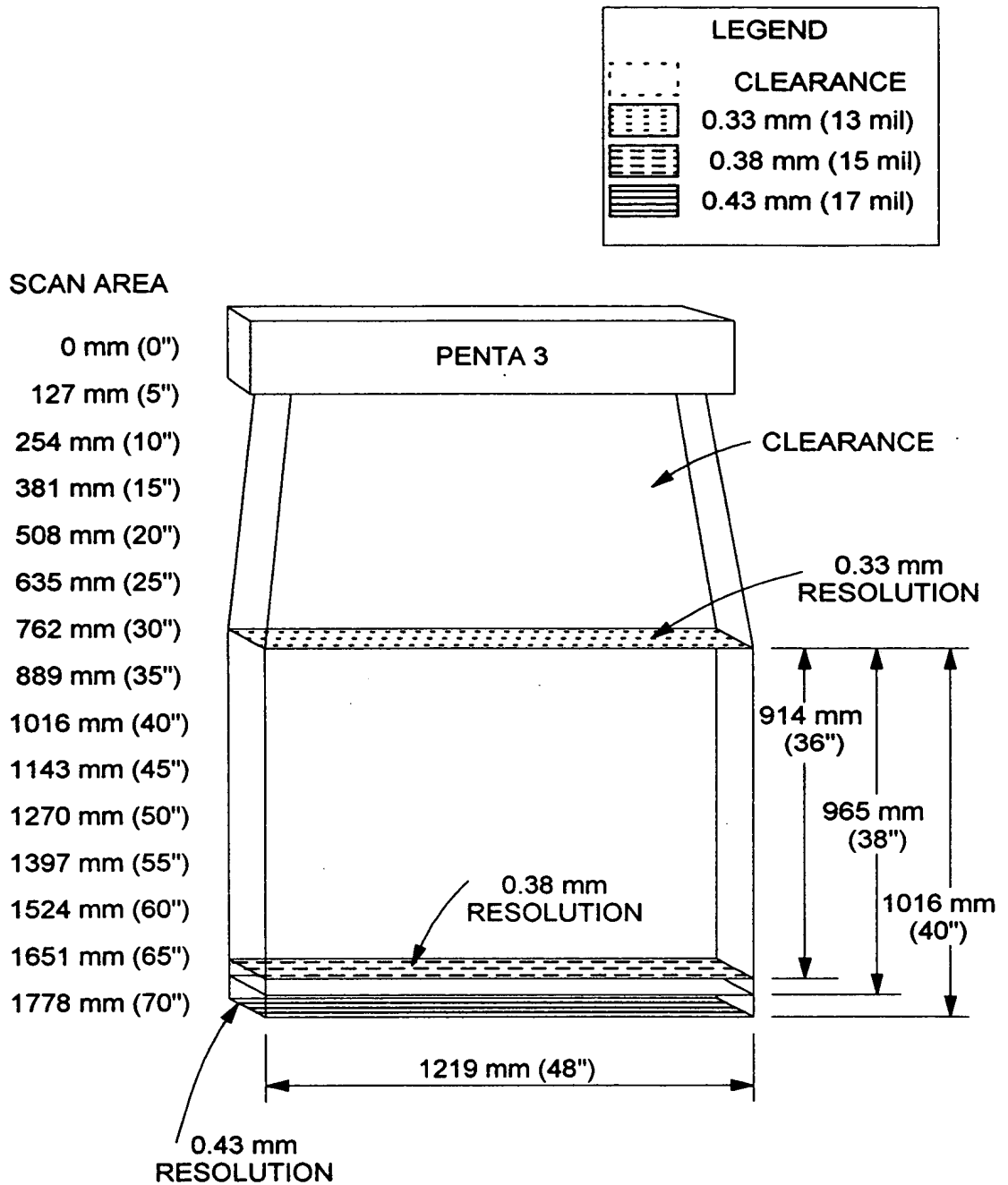


FIG. 7A

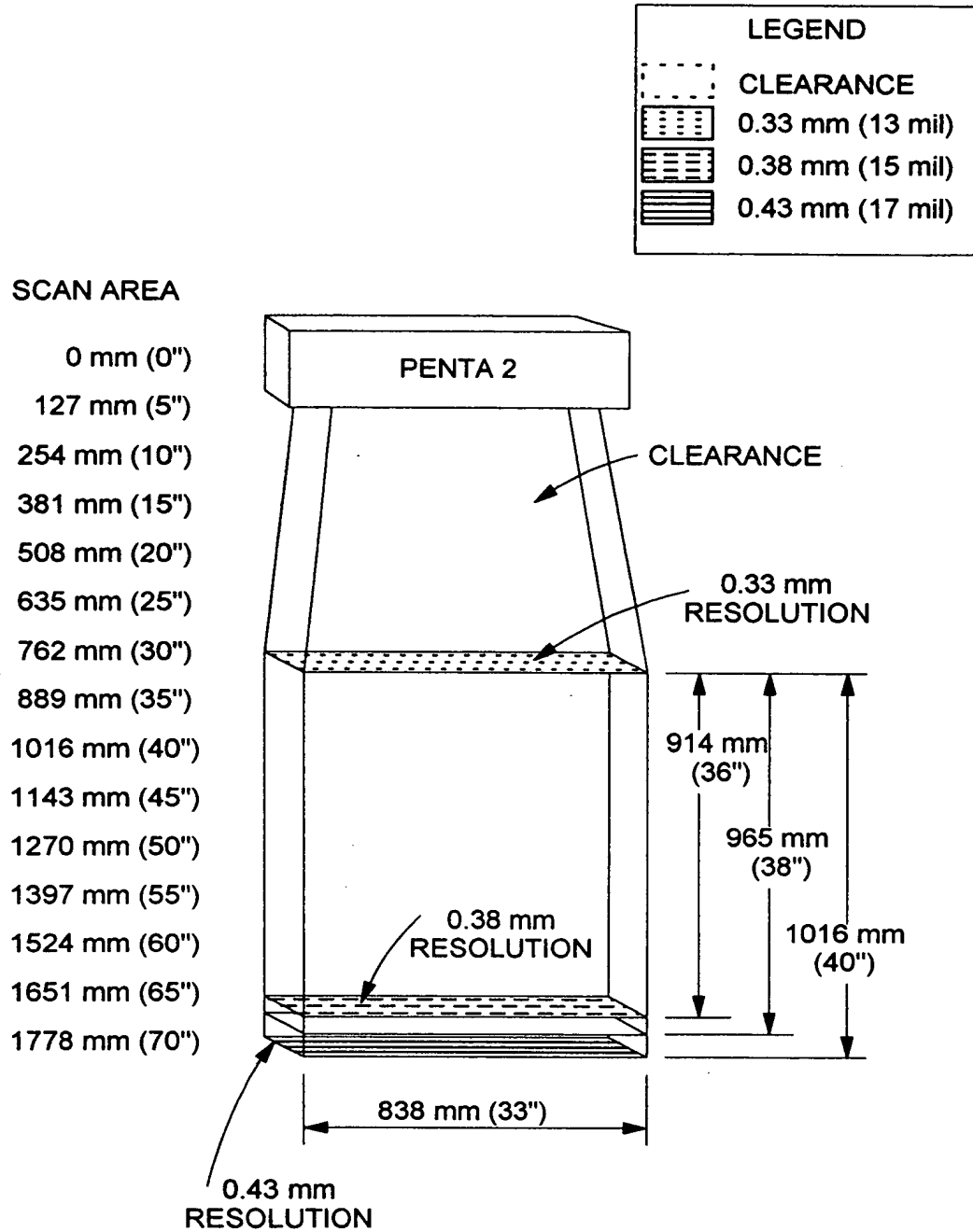


FIG. 7B

SCAN AREA

0 mm (0")
 127 mm (5")
 254 mm (10")
 381 mm (15")
 508 mm (20")
 635 mm (25")
 762 mm (30")
 889 mm (35")
 1016 mm (40")
 1143 mm (45")
 1270 mm (50")
 1397 mm (55")
 1524 mm (60")
 1651 mm (65")
 1778 mm (70")

0.43 mm
RESOLUTION

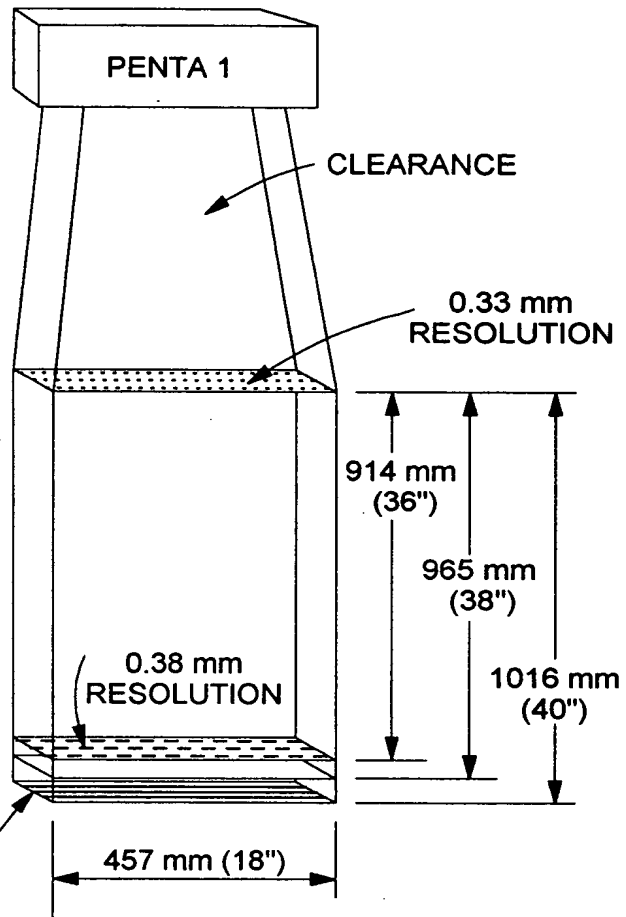


FIG. 7C

SPECIFICATIONS FOR PENTA 1, PENTA 2, PENTA 3 SCANNERS**OPERATIONAL**

LIGHT SOURCE	5 VISIBLE LASER DIODES 858 + 5mm
LASER POWER	8.4mW (PEAK): LESS THAN 1 mW AVERAGE POWER
DEPTH OF SCAN FIELD	914mm (36") FOR 0.33 mm (13mil) BAR CODES 965mm (38") FOR 0.38 mm (15mil) BAR CODES 1,016mm (40") FOR 0.43 mm (17mil) BAR CODES
WIDTH OF SCAN FIELD	PENTA 1 : 457mm (18") PENTA 2 : 838mm (33") PENTA 3 : 1219mm (48")
SCAN SPEED	PENTA 1 : 6,930 SCAN LINES PER SECOND PENTA 2 : 13,860 SCAN LINES PER SECOND PENTA 3 : 20,790 SCAN LINES PER SECOND
SCAN PATTERN	OMNIDIRECTIONAL 5-SIDED PENTAGON SCAN PATTERN PENTA 1: 20 SCAN LINES REPEATED AT FOUR DISTANCES (80 TOTAL) PENTA 2: 40 SCAN LINES REPEATED AT FOUR DISTANCES (160 TOTAL) PENTA 3: 60 SCAN LINES REPEATED AT FOUR DISTANCES (240 TOTAL)
MINIMUM BAR WIDTH	0.33 mm (13mil)
DECODE CAPABILITY	AUTODISCRIMINATES ALL STANDARD BAR CODES
SYSTEM INTERFACES	RS 232. POINT TO POINT. RS422. LIGHT PEN EMULATION
PRINT CONTRAST	35% MINIMUM REFLECTANCE DIFFERENCE
NUMBER CHARACTERS READ	UP TO 60 DATA CHARACTERS. (MAXIMUM NUMBER WILL VARY BASED ON SYMBOLOGY AND DENSITY)
ASPECT RATIO	UP TO 2.6 TO 1

FIG. 8

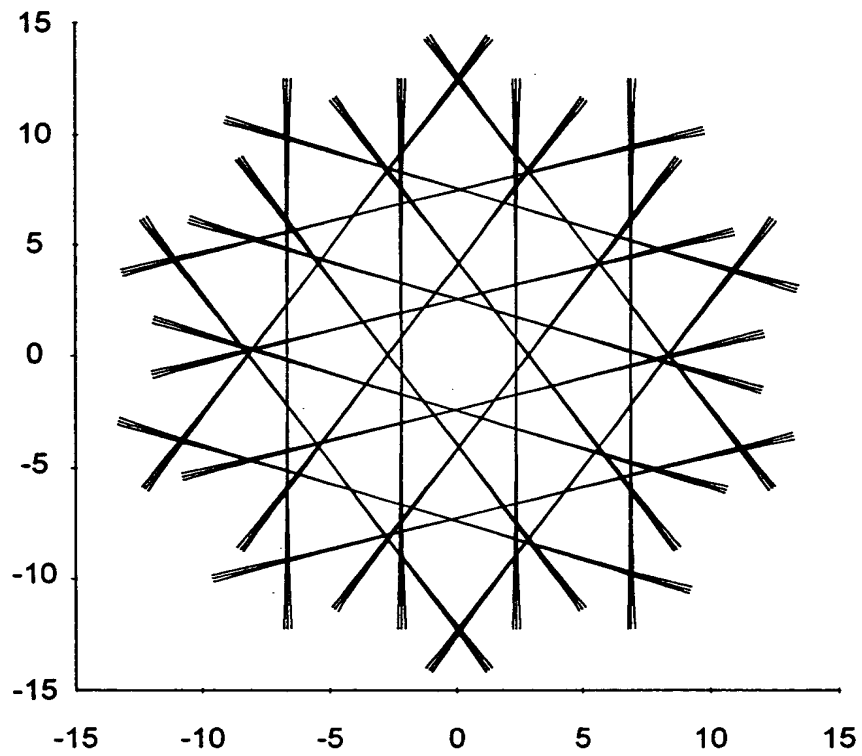


FIG. 9A

PENTA TRIPLE SCANNER FOCAL PLANE SCAN PATTERN

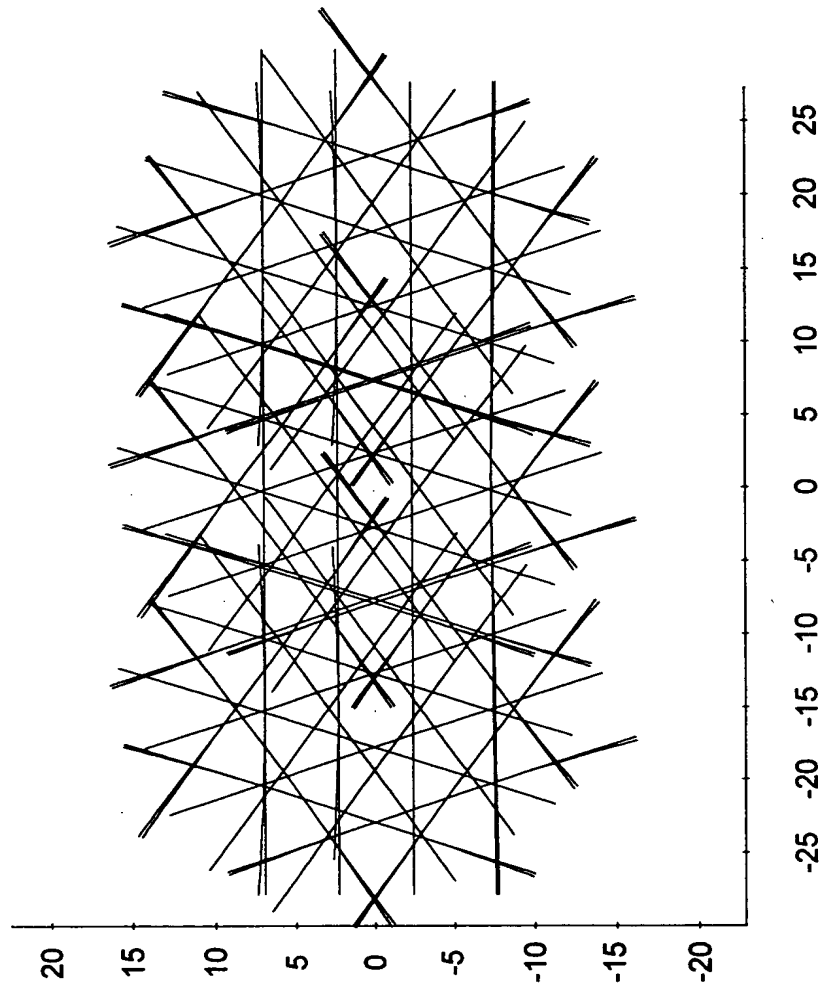


FIG. 9B

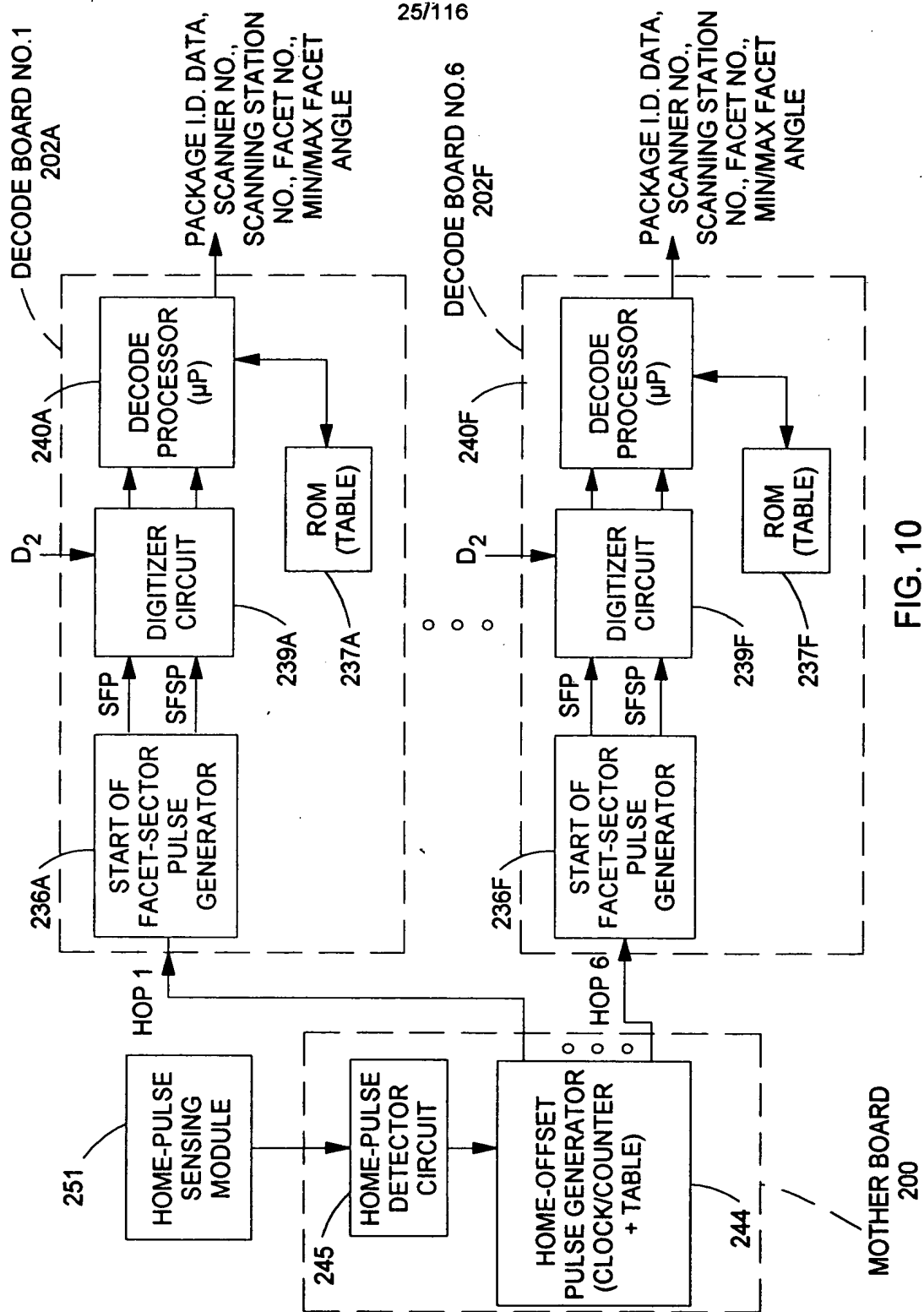


FIG. 10

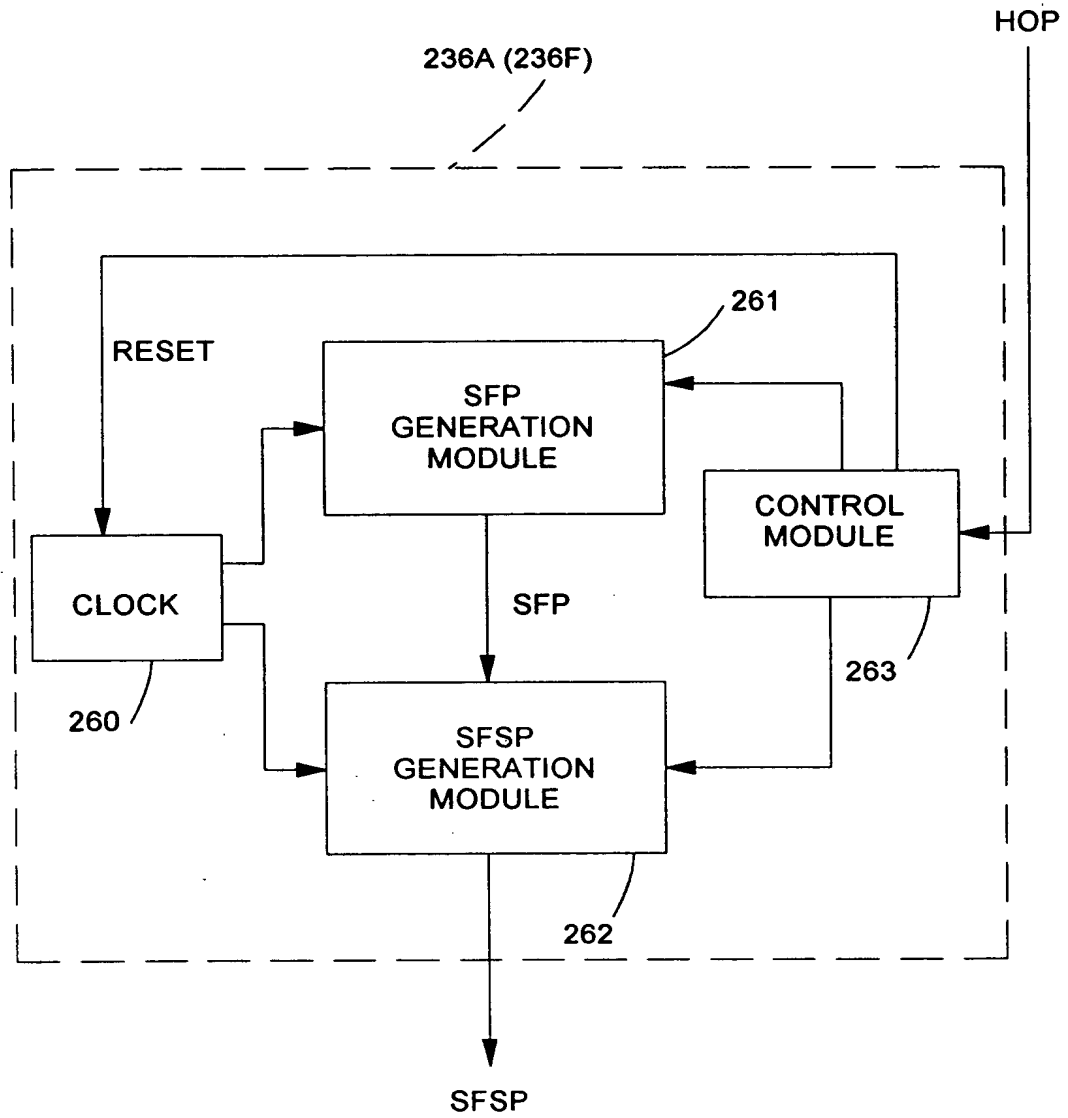


FIG. 10A

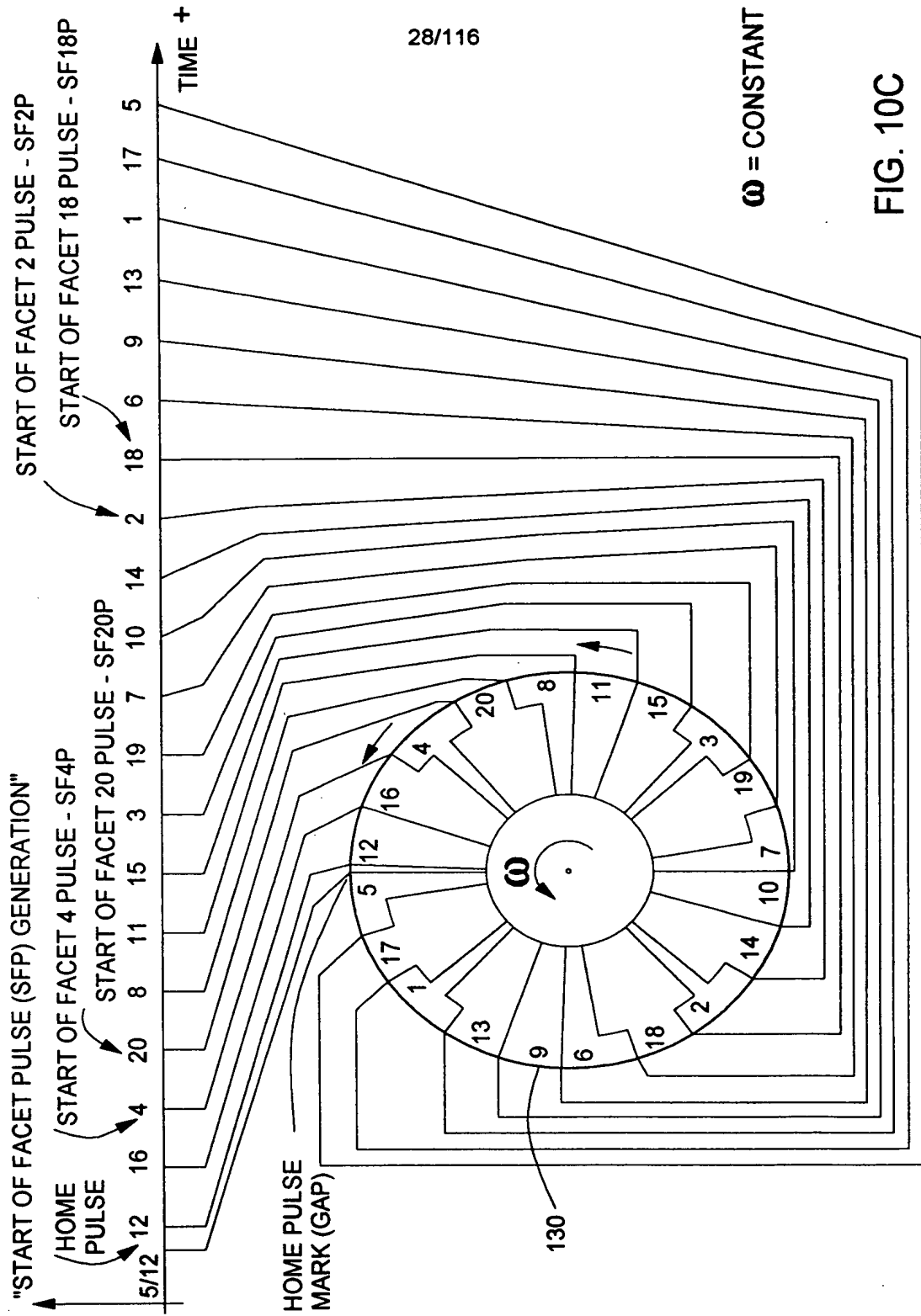
**DATA TABLE EMBODIED IN SFP GENERATOR ON DECODE
PROCESSOR BOARD**

SCANNING FACET NO.	TRIGGERING EVENT WHEN THE CLOCK PULSE COUNT ATTAINS THE VALUE EQUAL TO THE COUNT VALUE SET FORTH BELOW	PULSE EVENT FROM SFP MODULE
12	7	SF12P
16	146	SF16P
4	271	SF4P
20	4467	SF20P
8	561	SF8P
11	716	SF11P
15	855	SF15P
3	980	SF3P
19	1155	SF19P
7	1270	SF7P
10	1425	SF10P
14	1564	SF14P
2	1689	SF2P
18	1864	SF18P
6	1979	SF6P
9	2134	SF9P
13	2273	SF13P
1	2398	SF1P
17	2573	SF17P
5	2688	SF5P

W = 5200 RPM

CLOCK PULSE WIDTH = 4 μ SEC

FIG. 10B



$\omega = \text{CONSTANT}$

FIG. 10C

**TABLE EMBODIED IN SFSP GENERATOR DECODE
PROCESSOR BOARD**

SCANNING FACET NO.	SFSP TRIGGERING EVENT	PULSE EVENT FROM SFSP MODULE .
12	RULES 1 - 4 IN FIGS.	SFSP 12/1P SFSP 12/2P SFSP 12/3P SFSP 12/4P
16	RULES 1 - 4 IN FIGS.	SFSP 16/1P SFSP 16/2P SFSP 16/3P SFSP 16/4P
4	RULES 1 - 4 IN FIGS.	SFSP 4/1P SFSP 4/2P SFSP 4/3P SFSP 4/4P
20	RULES 1 - 4 IN FIGS.	SFSP 20/1P SFSP 20/2P SFSP 20/3P SFSP 20/4P
8	RULES 1 - 4 IN FIGS.	SFSP 8/1P SFSP 8/2P SFSP 8/3P SFSP 8/4P
11	RULES 1 - 4 IN FIGS.	SFSP 11/1P SFSP 11/2P SFSP 11/3P SFSP 11/4P
○ ○ ○		
17	RULES 1 - 4 IN FIGS.	SFSP 17/1P SFSP 17/2P SFSP 17/3P SFSP 17/4P
5	RULES 1 - 4 IN FIGS.	SFSP 5/1P SFSP 5/2P SFSP 5/3P SFSP 5/4P

FIG. 10D

RULE 1: FOR GENERATING SFSP/1P TYPE PULSES

FOR EACH FACET X BEFORE WHICH IS LOCATED FACET X-1
AND BEYOND WHICH IS LOCATED FACET X+1 (ABOUT THE
SCANNING DISC), THE SFSP GENERATION MODULE
GENERATES SFSX/1P TYPE PULSES WHEN THE COUNT
IS EQUAL TO:

COUNT (SFSP)

RULE 2: FOR GENERATING SFSX/2P TYPE PULSES

FOR EACH FACET X BEFORE WHICH IS LOCATED FACET
X-1 AND BEYOND WHICH IS LOCATED FACET X+1 (ABOUT
THE SCANNING DISC), THE SFSP GENERATION MODULE
GENERATES SFSX/2P TYPE PULSES WHEN THE COUNT
IS EQUAL TO:

$$\text{COUNT (SFSP) +1} \left[\frac{\text{COUNT (SFX+1P) - COUNT (SFXP)}}{4} \right]$$

FIG. 10E1

RULE 3: FOR GENERATING SFSP/3P TYPE PULSES

FOR EACH FACET X BEFORE WHICH IS LOCATED FACET X-1
AND BEYOND WHICH IS LOCATED FACET X+1 (ABOUT THE
SCANNING DISC), THE SFSP GENERATION MODULE
GENERATES

SFSX/3 TYPE PULSES WHEN THE COUNT IS EQUAL TO:

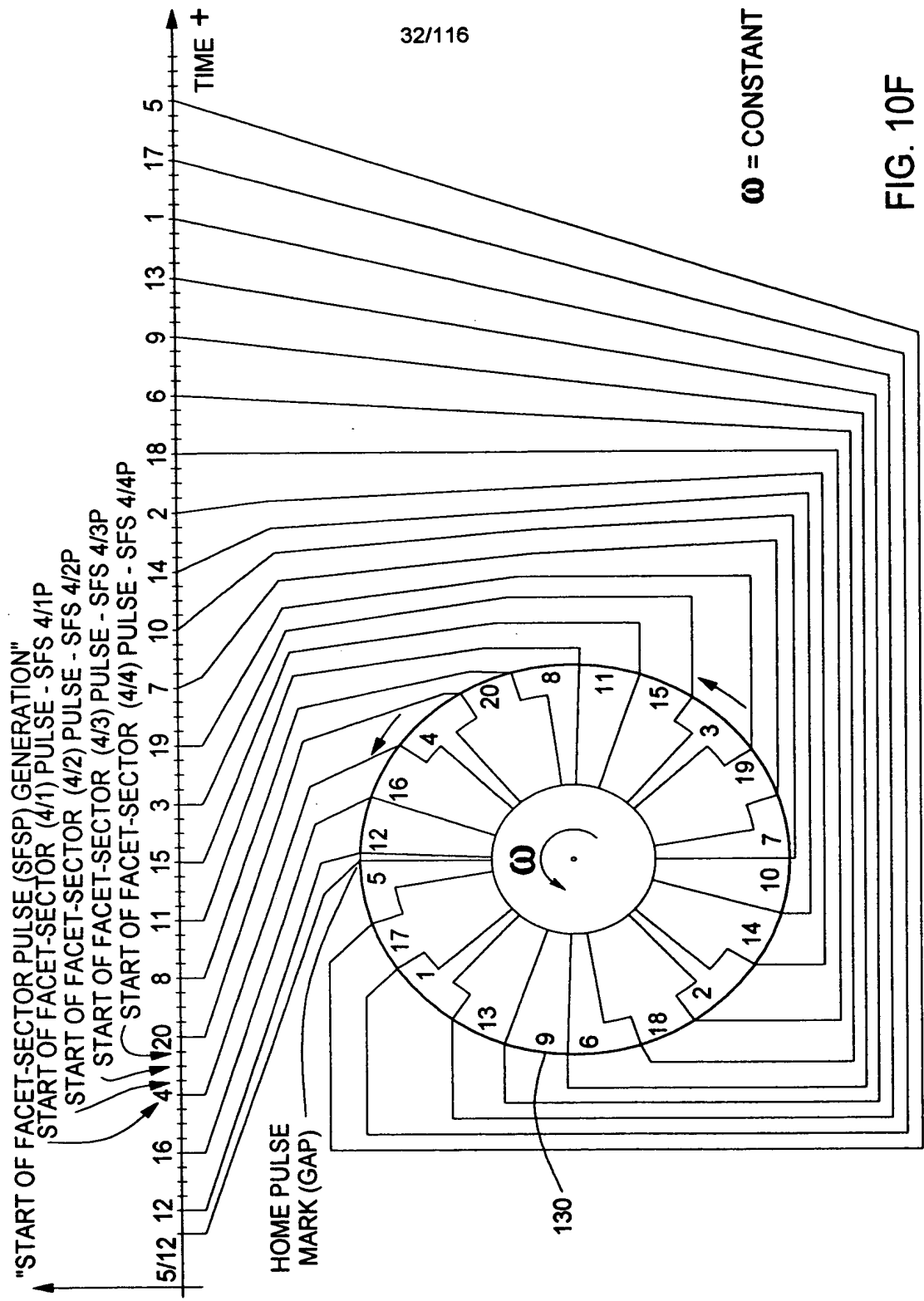
$$\text{COUNT (SFSP)} + 2 \left[\frac{\text{COUNT (SFX+1P)} - \text{COUNT (SFXP)}}{4} \right]$$

RULE4: FOR GENERATING SFSX/4P TYPE PULSES

FOR EACH FACET X BEFORE WHICH IS LOCATED FACET X-1 AND
BEYOND WHICH IS LOCATED FACET X+1 (ABOUT THE SCANNING
DISC), THE SFSP GENERATION MODULE GENERATES
SFSX/4 TYPE PULSES WHEN THE COUNT IS EQUAL TO:

$$\text{COUNT (SFSP)} + 3 \left[\frac{\text{COUNT (SFX+1P)} - \text{COUNT (SFXP)}}{4} \right]$$

FIG. 10E2



32/116

ω = CONSTANT

FIG. 10F

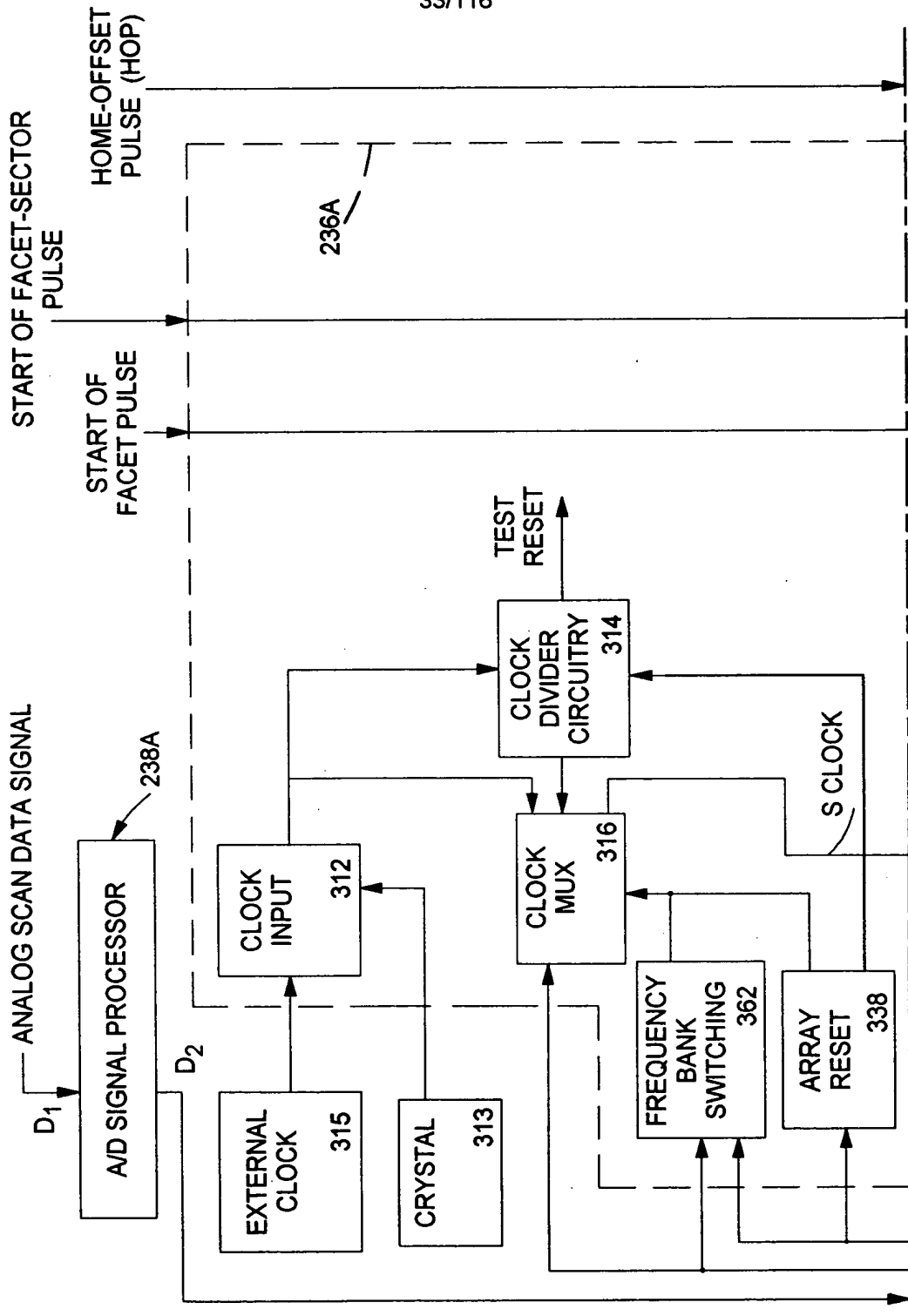


FIG. 11A1

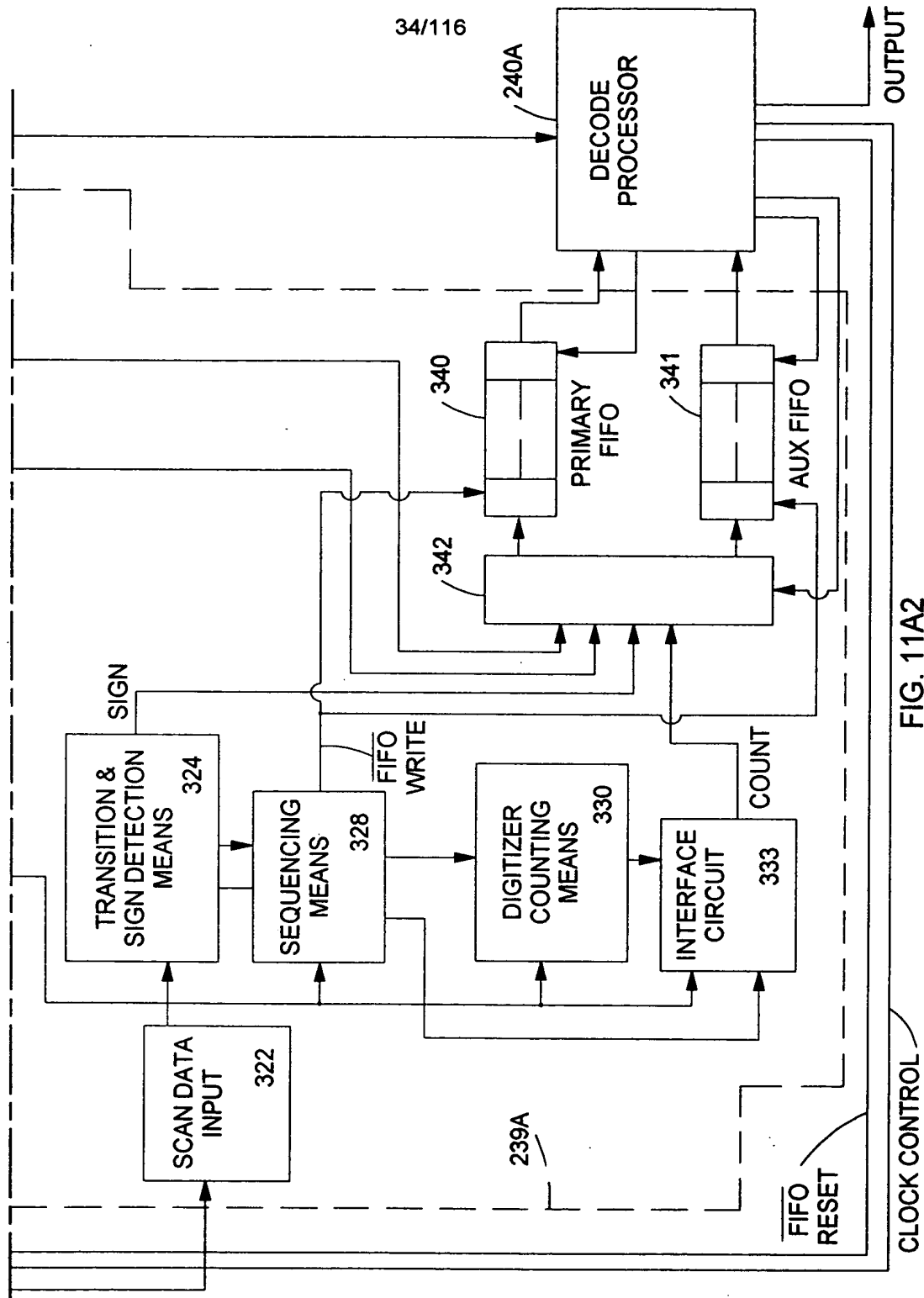
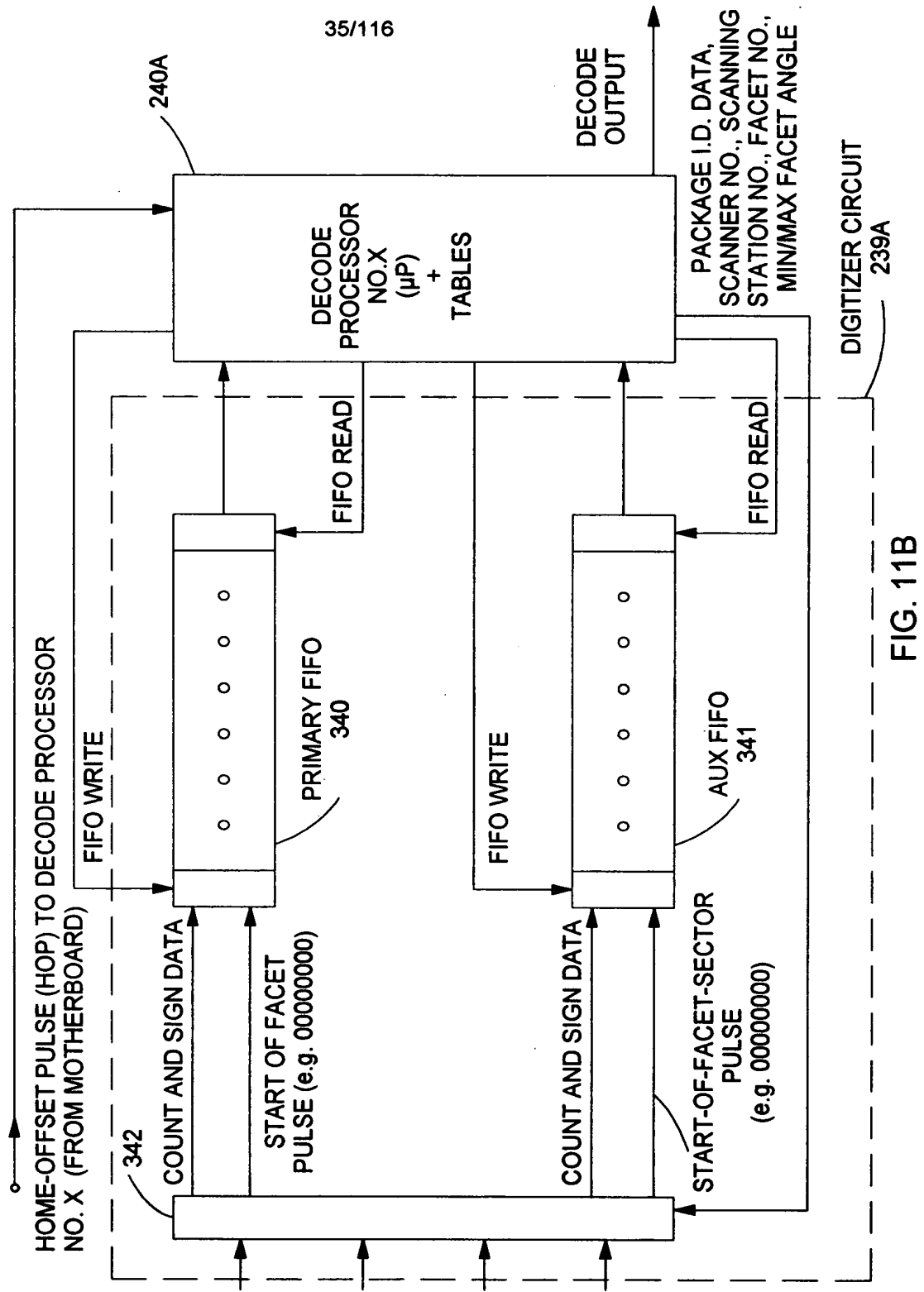


FIG. 11A2



SCANNER NO.	TOTAL NO. OF FACETS ON DISC
NO. OF SECTORS / FACET	SCANNING STATION NO.

FIG. 11C1

SCANNING FACET NO.	TRIGGERING EVENT WHEN THE CLOCK PULSE COUNT ATTAINS THE VALUE EQUAL TO THE COUNT VALUE SET FORTH BELOW	PULSE EVENT FROM SFP MODULE
12	7	SF12P
16	146	SF16P
4	271	SF4P
20	4467	SF20P
8	561	SF8P
11	716	SF11P
15	855	SF15P
3	980	SF3P
19	1155	SF19P
7	1270	SF7P
10	1425	SF10P
14	1564	SF14P
2	1689	SF2P
18	1864	SF18P
6	1979	SF6P
9	2134	SF9P
13	2273	SF13P
1	2398	SF1P
17	2573	SF17P
5	2688	SF5P

TABLES EMBODIED IN DECODE PROCESSOR
CLOCK PULSE WIDTH = 4 μ SEC
W = 5200 RPM

FIG. 11C2

TABLE EMBODIED IN DECODE PROCESSOR

			MINIMUM AND MAXIMUM FACET ANGLES CORRESPONDING TO FACET-SECTOR IDENTIFIED BY SFSP EVENT
SCANNING FACET NO.	SFS TRIGGERING EVENT	PULSE EVENT FROM SFSP MODULE .	
12	RULES 1 - 4 IN FIGS.	SFSP 12/1P	$\theta_{ROT MIN}$, $\theta_{ROT MAX}$
		SFSP 12/2P	
		SFSP 12/3P	
		SFSP 12/4P	
16	RULES 1 - 4 IN FIGS.	SFSP 16/1P	
		SFSP 16/2P	
		SFSP 16/3P	
		SFSP 16/4P	
4	RULES 1 - 4 IN FIGS.	SFSP 4/1P	
		SFSP 4/2P	
		SFSP 4/3P	
		SFSP 4/4P	
20	RULES 1 - 4 IN FIGS.	SFSP 20/1P	
		SFSP 20/2P	
		SFSP 20/3P	
		SFSP 20/4P	
8	RULES 1 - 4 IN FIGS.	SFSP 8/1P	
		SFSP 8/2P	
		SFSP 8/3P	
		SFSP 8/4P	
11	RULES 1 - 4 IN FIGS.	SFSP 11/1P	
		SFSP 11/2P	
		SFSP 11/3P	
		SFSP 11/4P	
○ ○ ○			
17	RULES 1 - 4 IN FIGS.	SFSP 17/1P	
		SFSP 17/2P	
		SFSP 17/3P	
		SFSP 17/4P	
5	RULES 1 - 4 IN FIGS.	SFSP 5/1P	
		SFSP 5/2P	
		SFSP 5/3P	
		SFSP 5/4P	

FIG. 11D

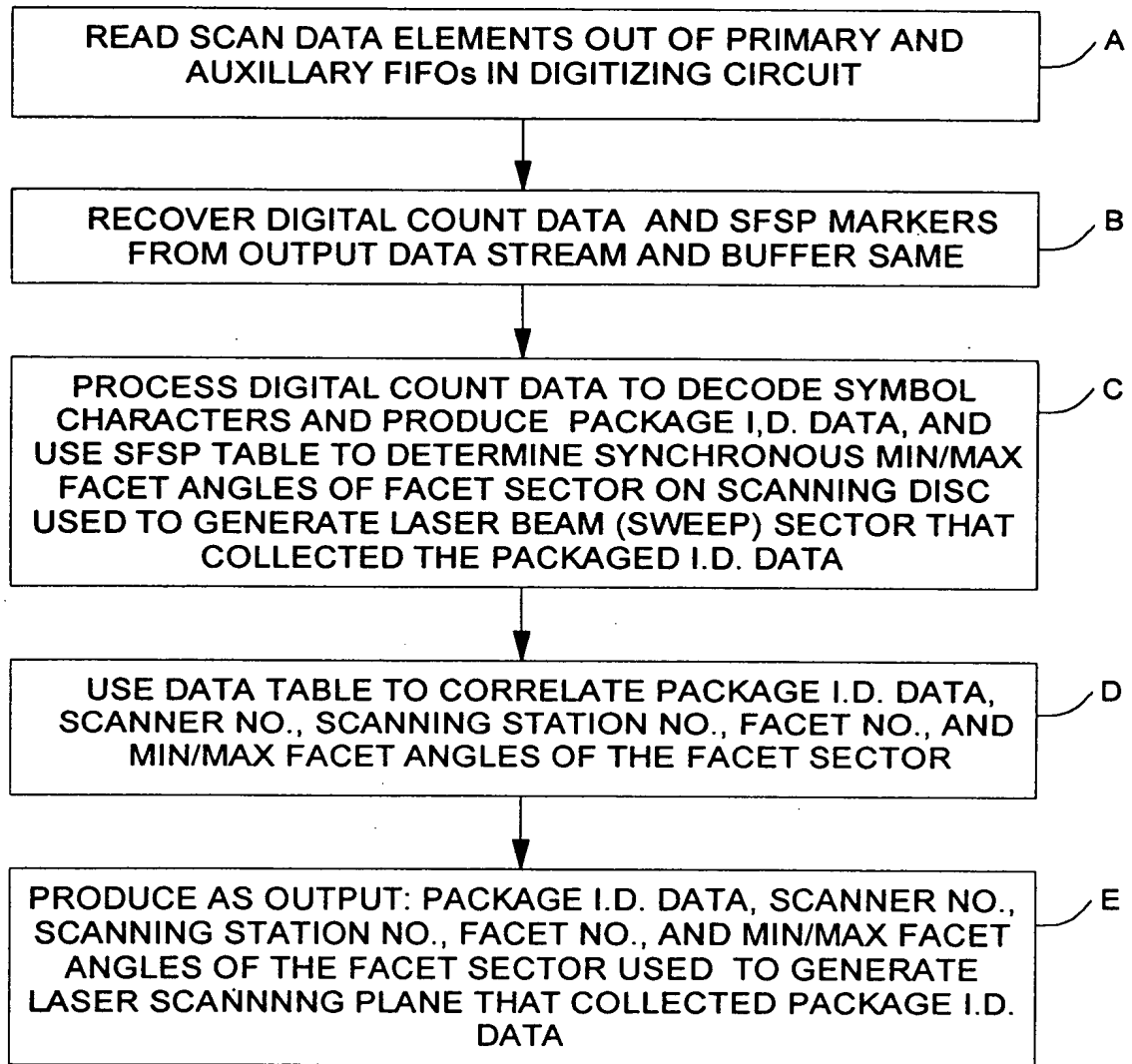


FIG. 11E

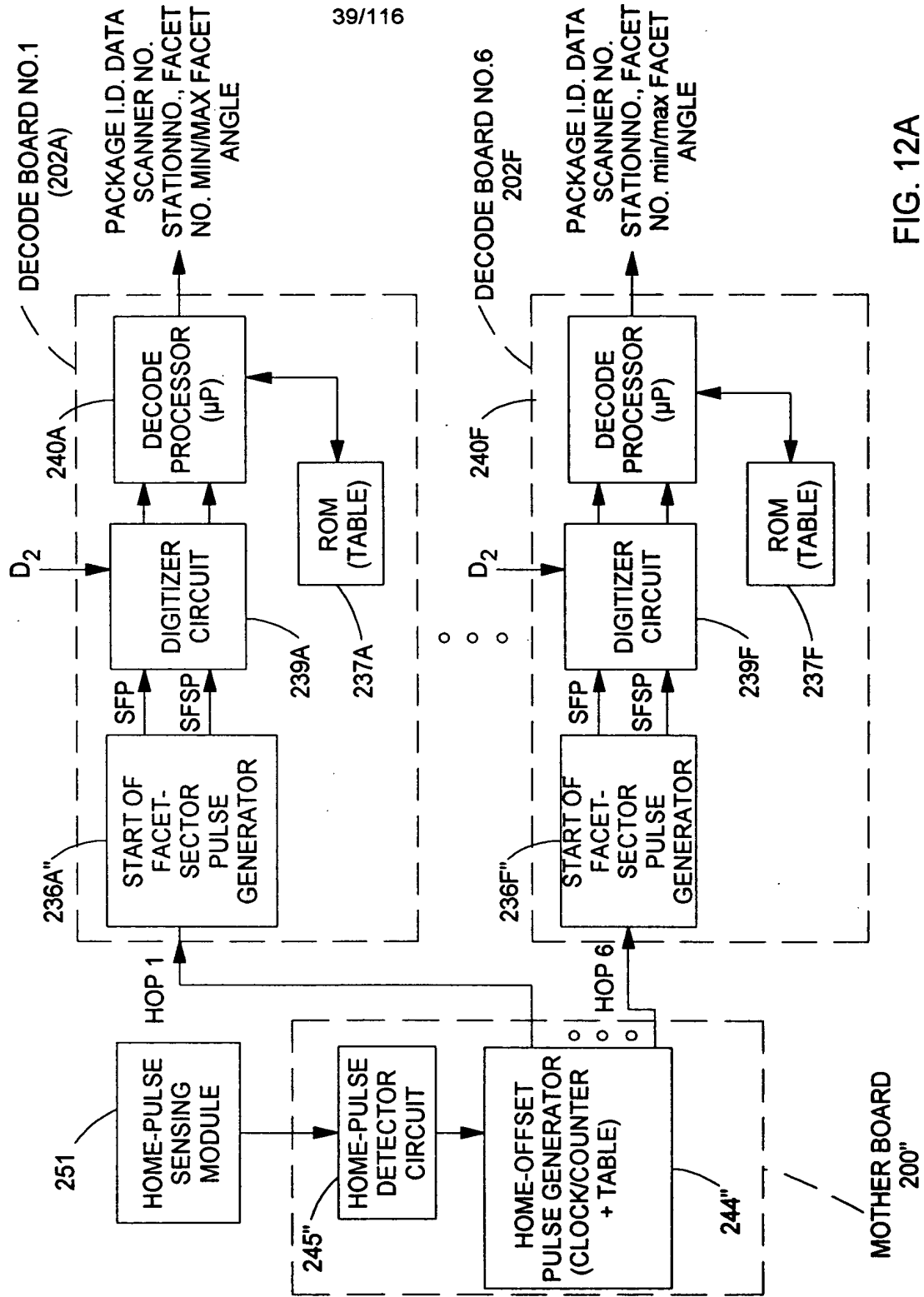


FIG. 12A

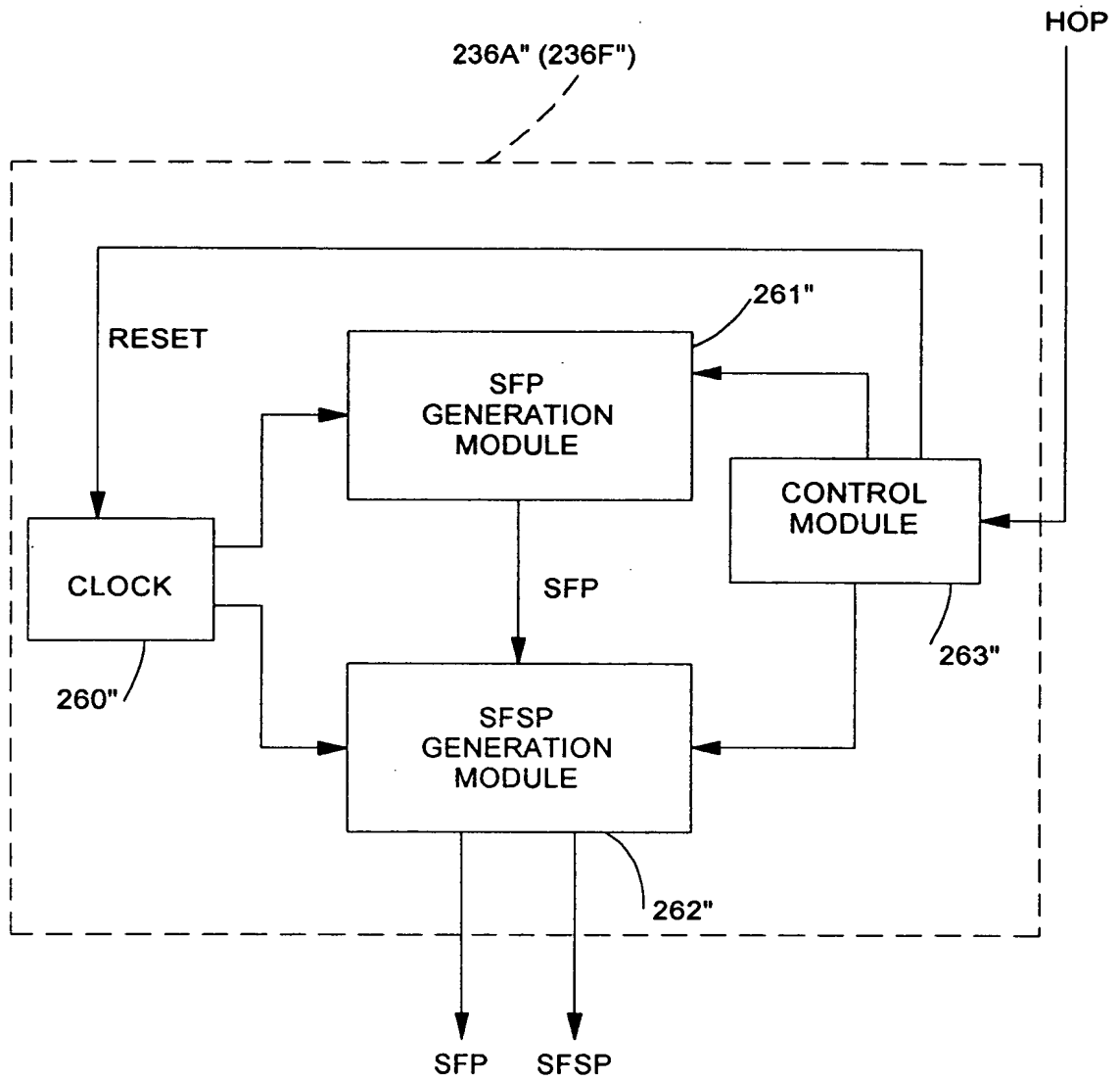


FIG. 12B

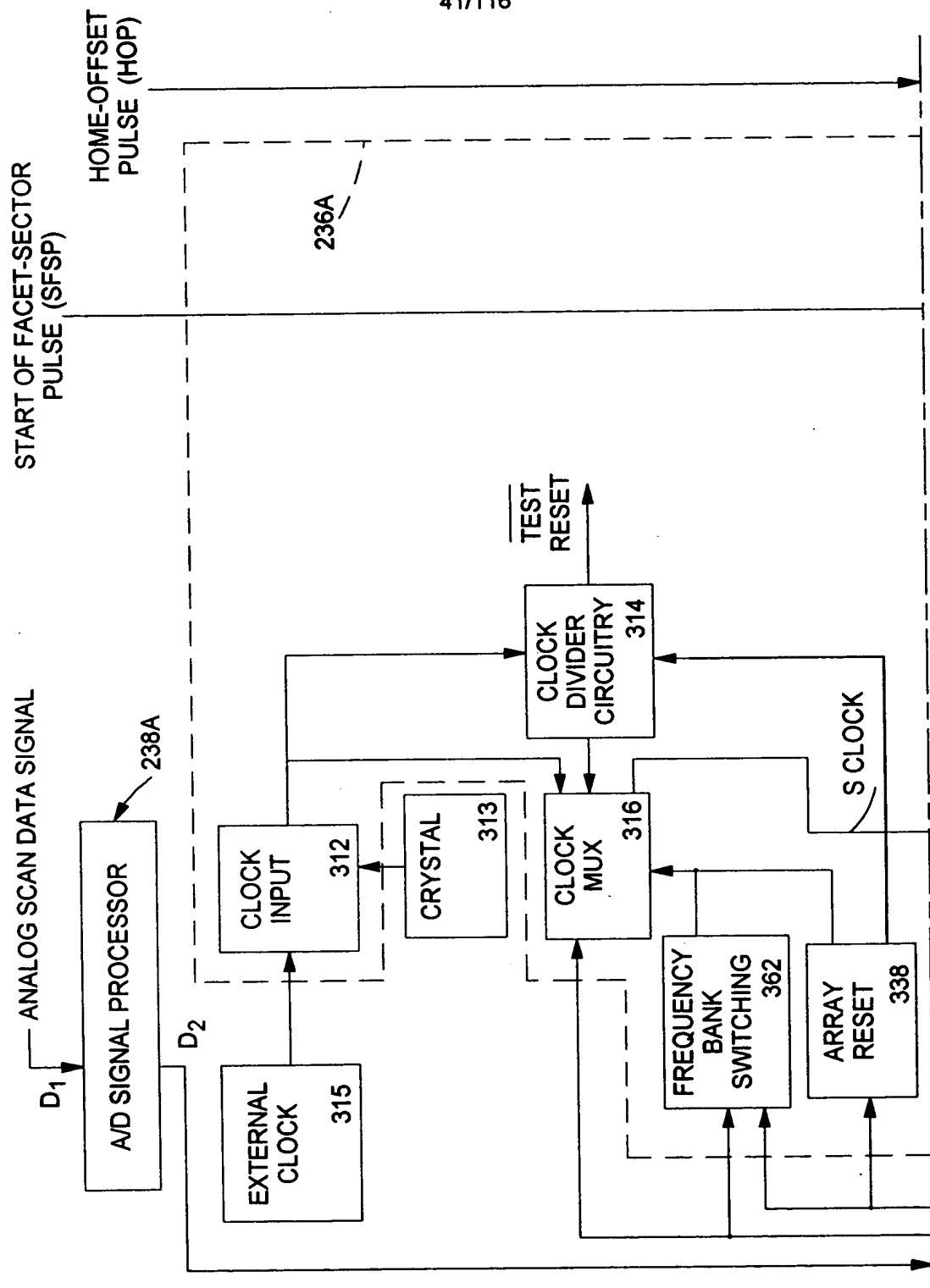
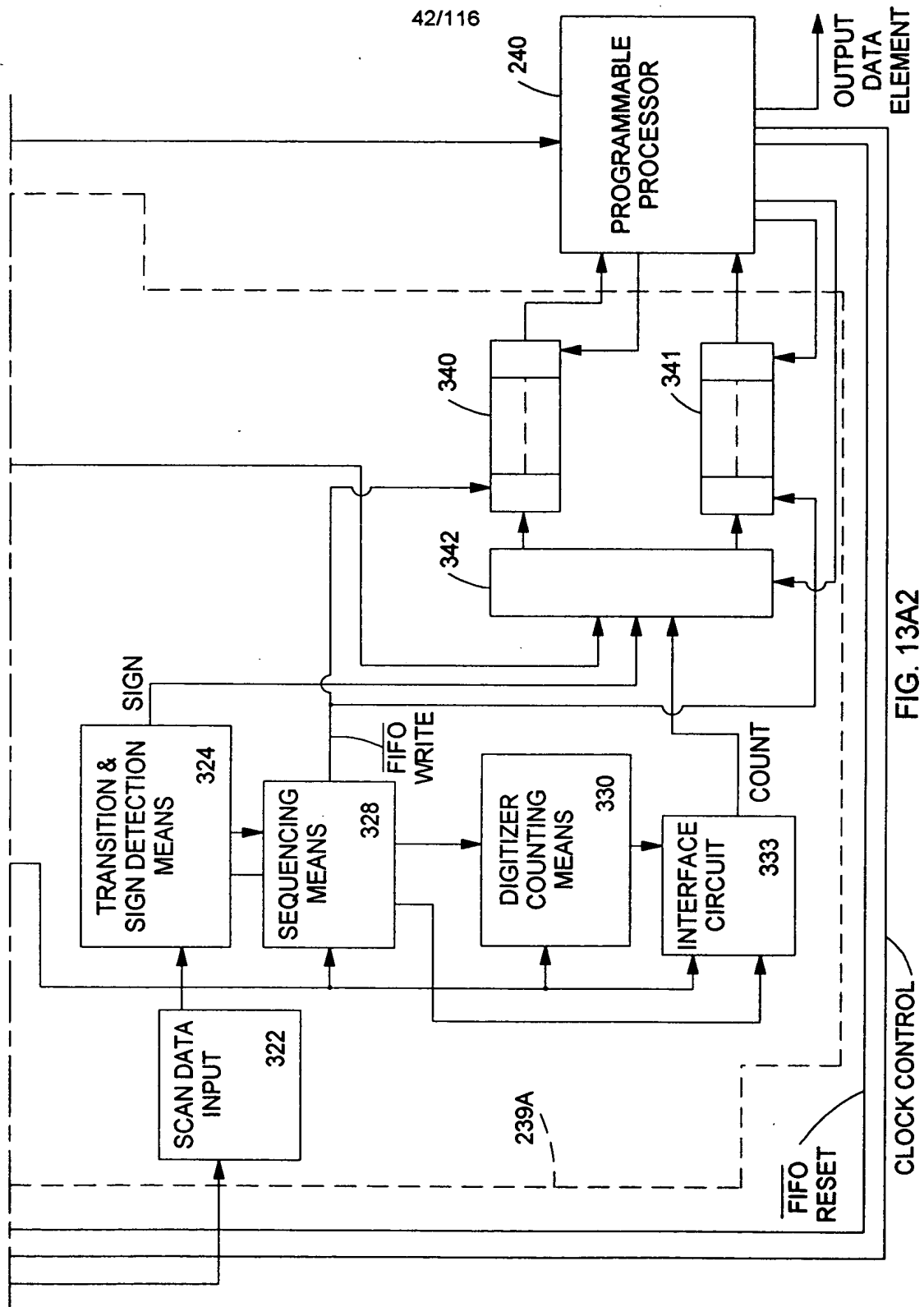


FIG. 13A1



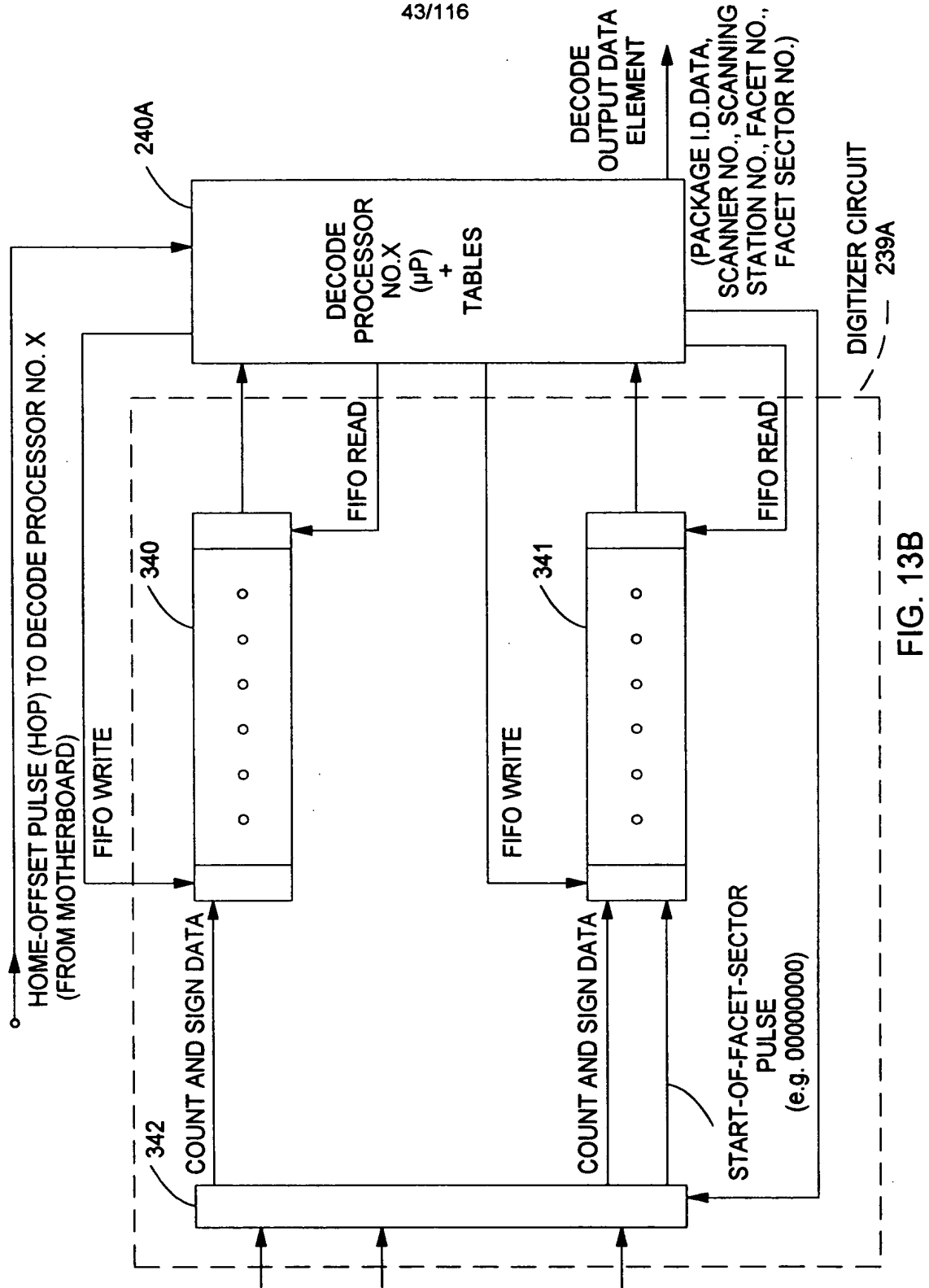


FIG. 13B

HOP GENERATION ALGORITHM

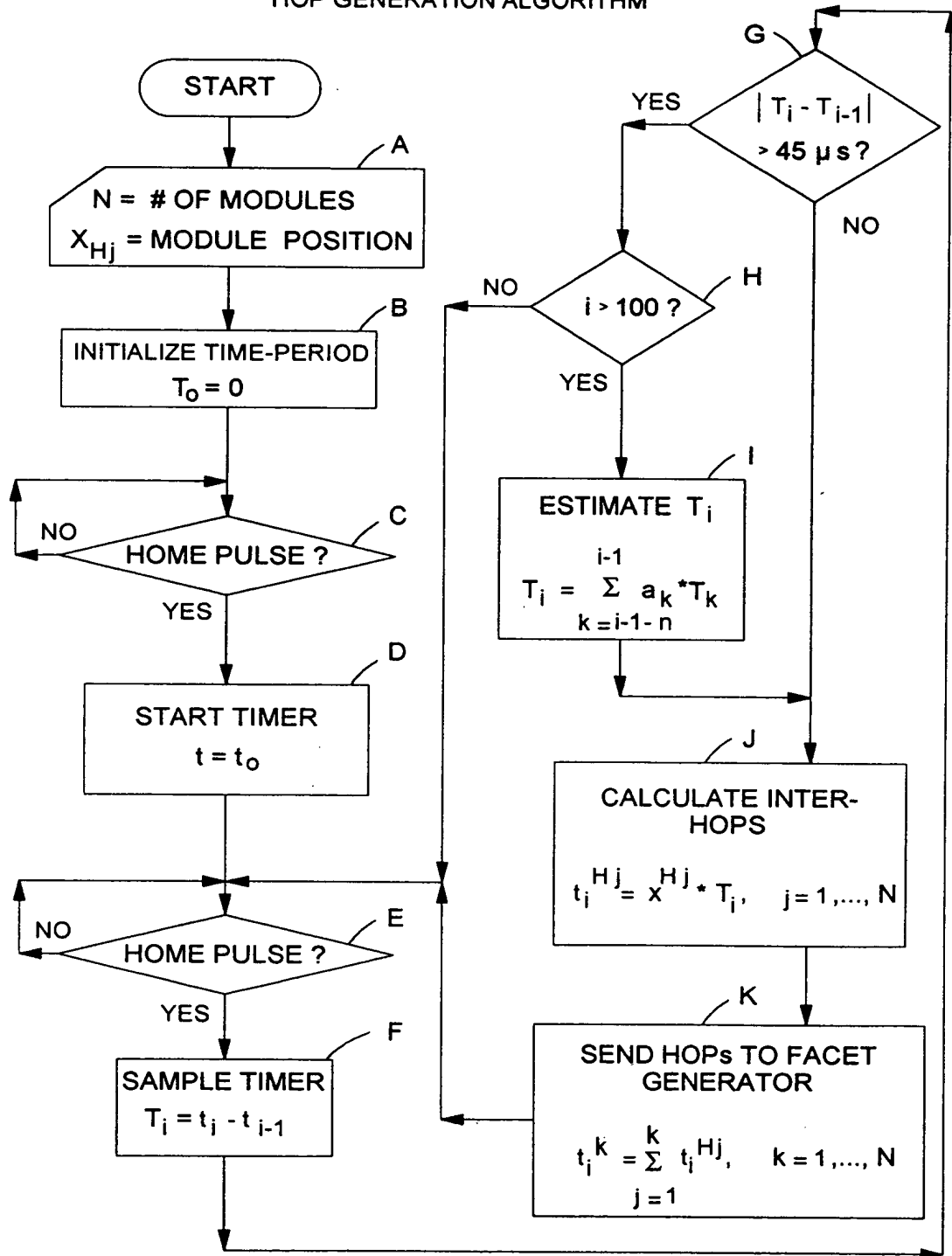


FIG. 14A

FACET / TICK GENERATION ALGORITHM

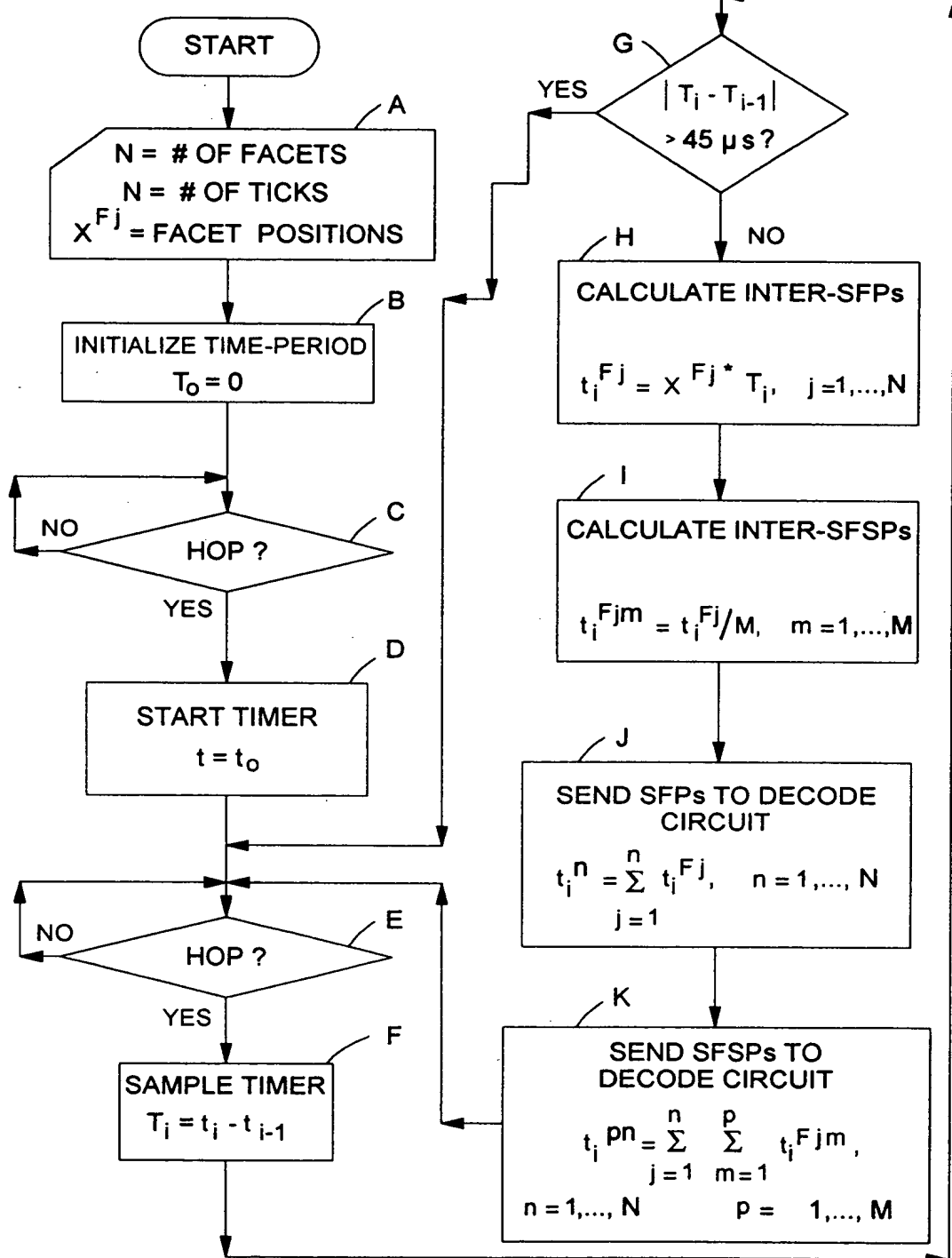


FIG. 14B

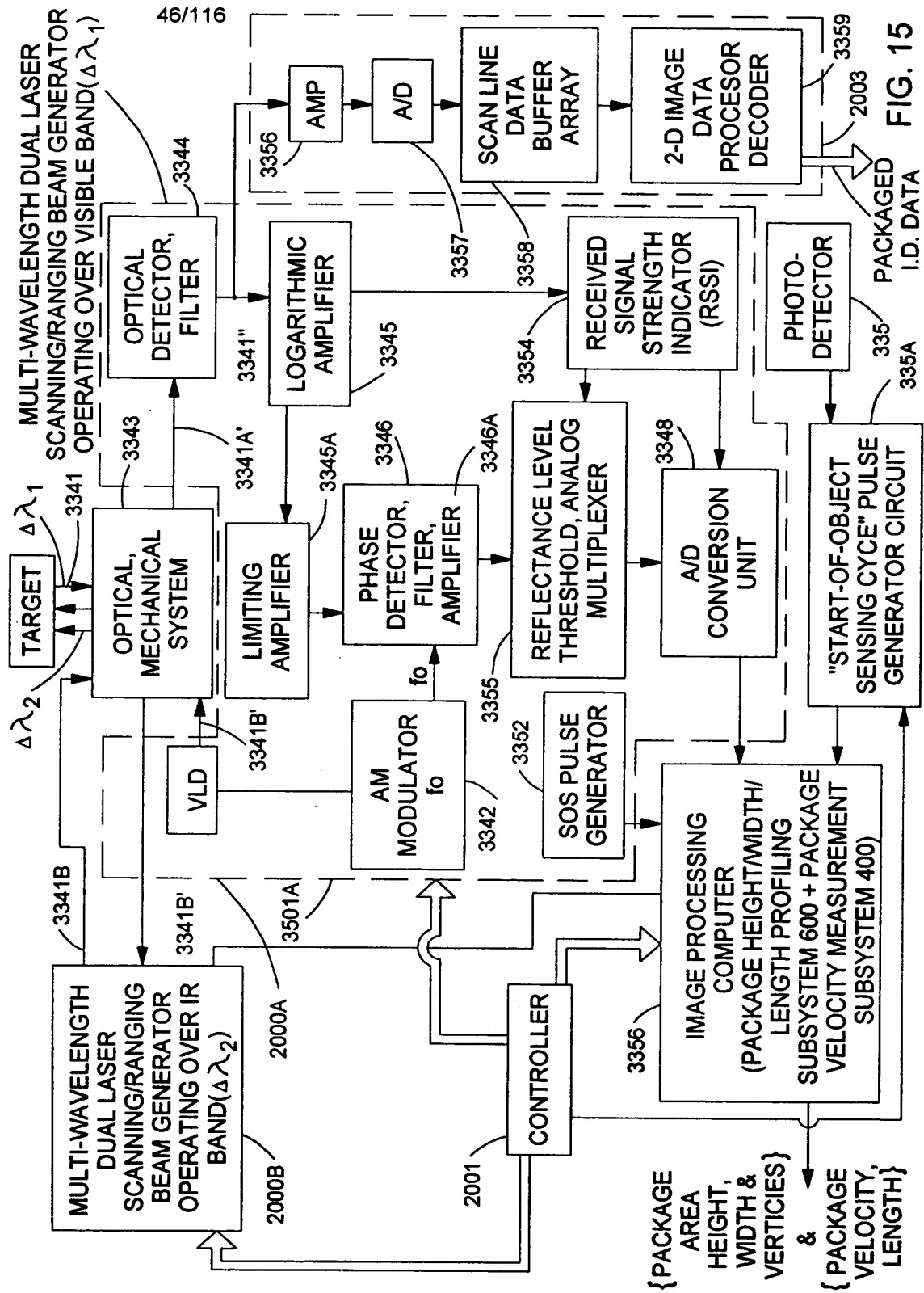


FIG. 15

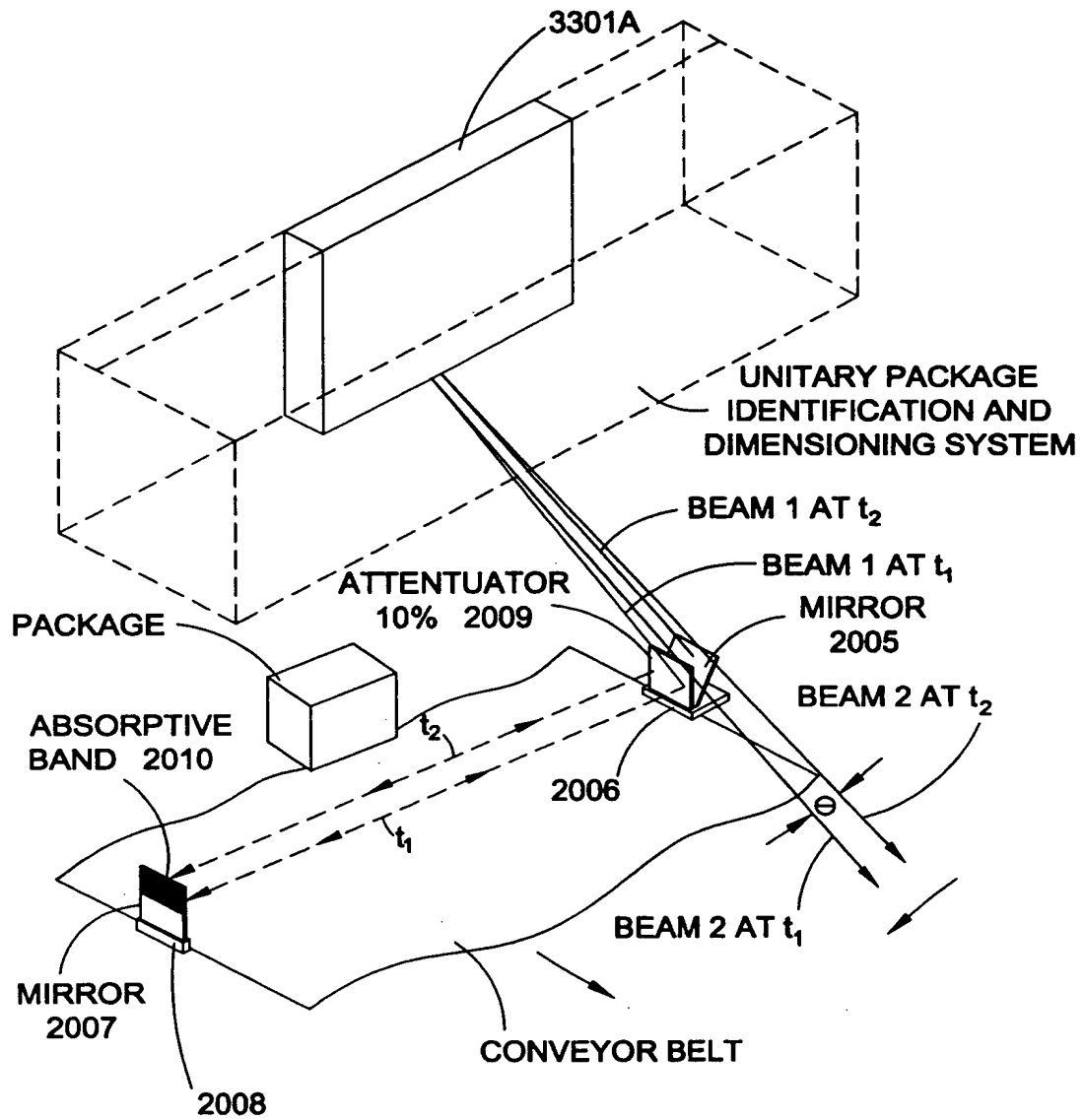


FIG. 15A

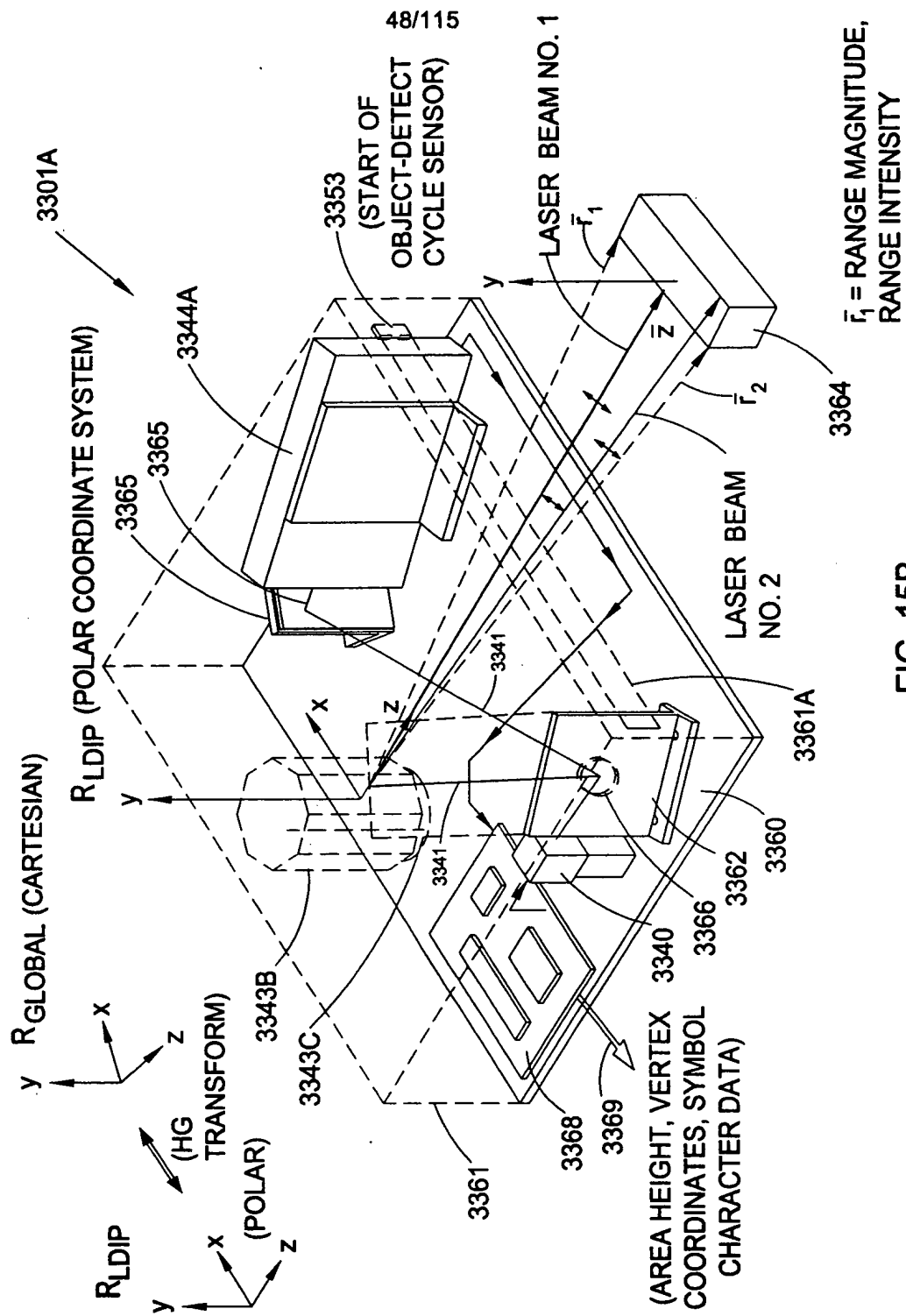


FIG. 15B

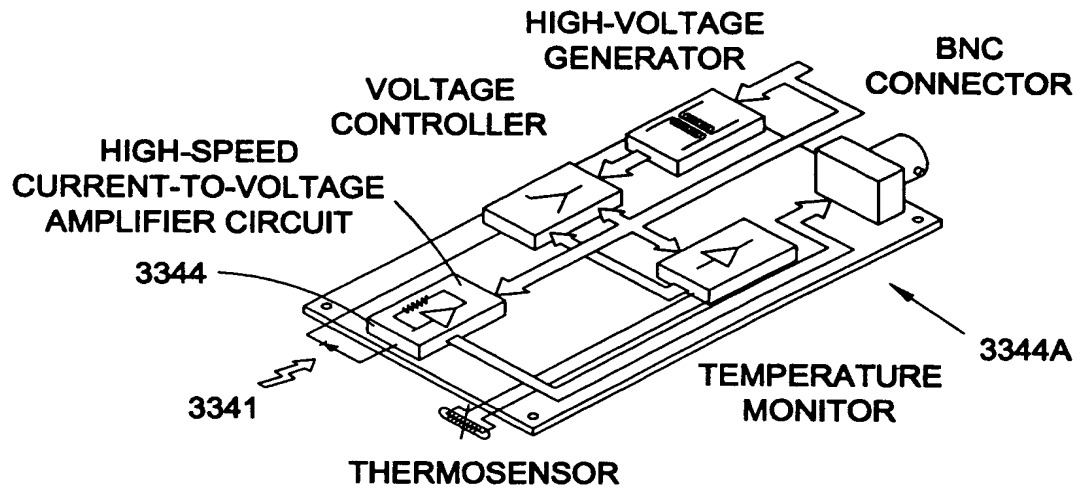


FIG. 15C

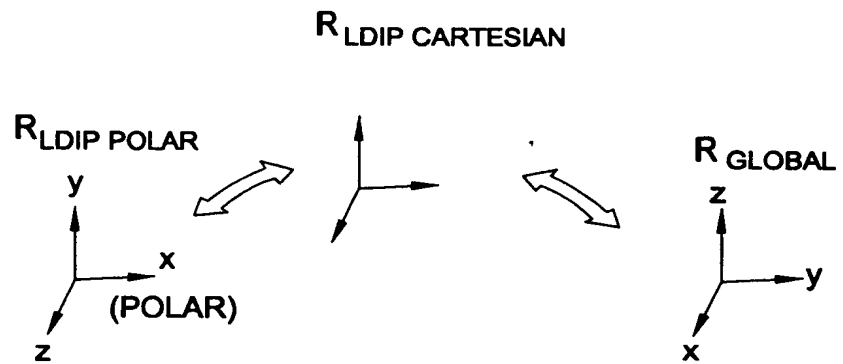


FIG. 15D

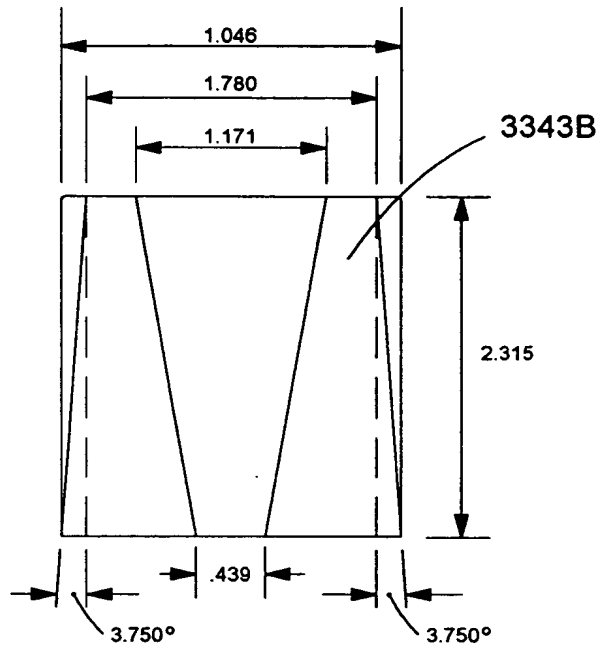


FIG. 15E1

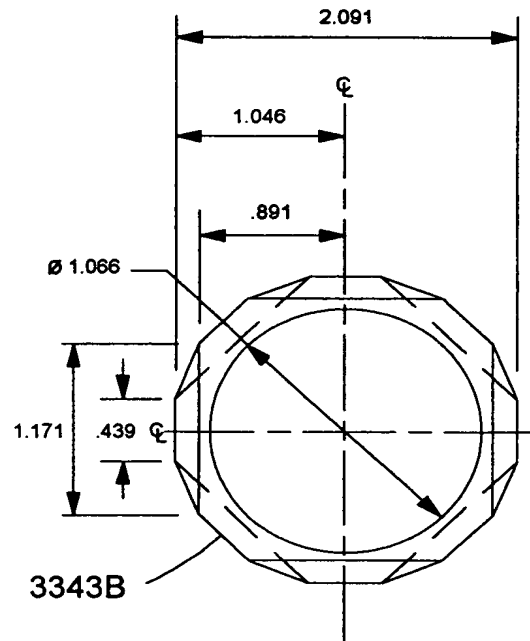


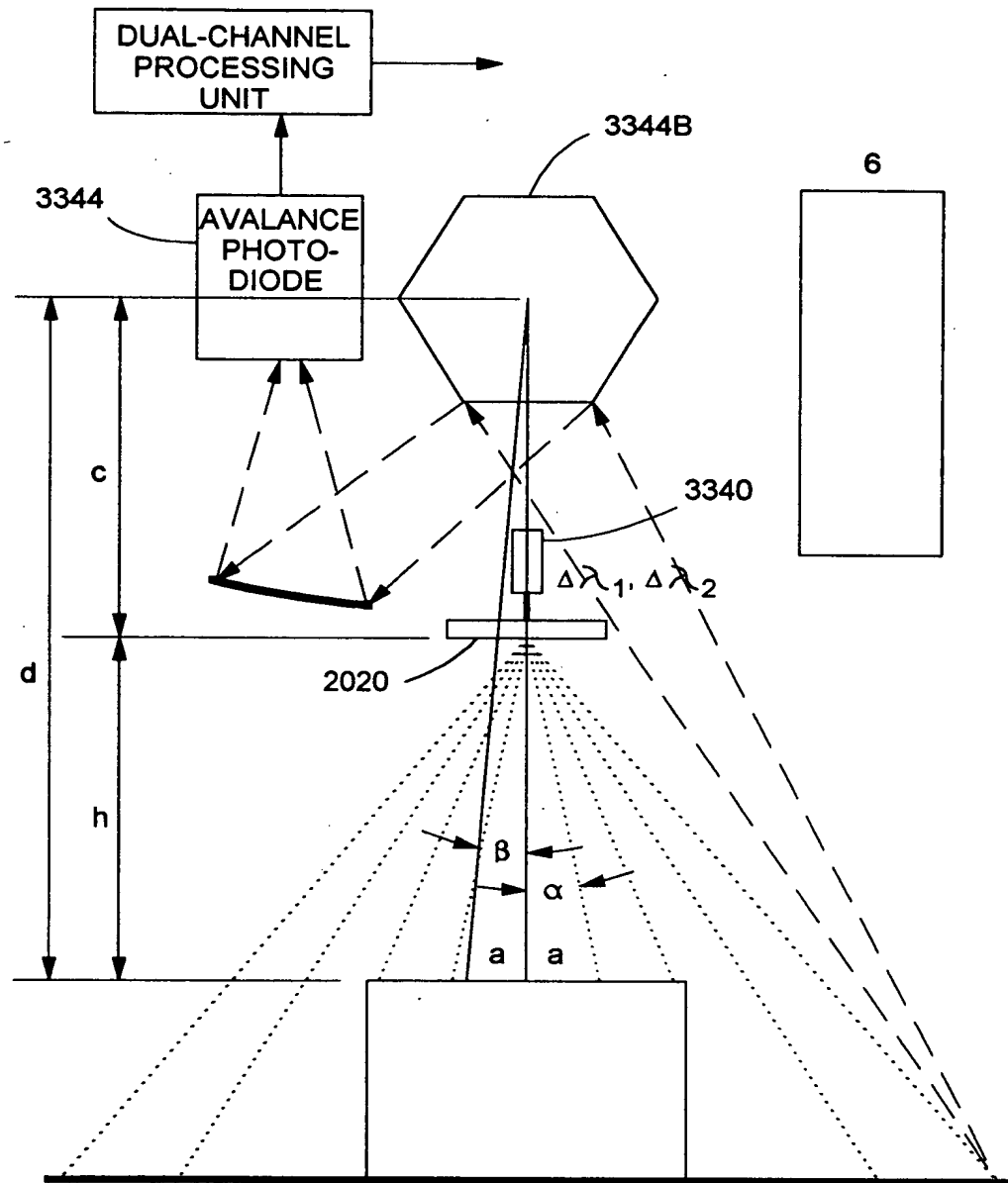
FIG. 15E2

FACE #	ANGLE (DEGREES)
1	3.75
2	-3.75
3	3.75
4	-3.75
5	3.75
6	-3.75
7	3.75
8	-3.75

FIG. 15E3

BEAM NO. 1	1	$\Delta\lambda_1$
	3	$\Delta\lambda_2$
	5	
	7	
BEAM NO. 2	2	$\Delta\lambda_1$
	4	$\Delta\lambda_2$
	6	
	8	

FIG. 15E4



THE EQUATION FOR THE CALCULATION OF THE DISTANCE
FROM THE DEVICE TO THE OBJECT:

$$a = h \tan \alpha, \quad a = d \tan \beta, \quad d = h - c$$

$$h = (c \tan \beta) (\tan \alpha - \tan \beta)$$

FIG. 15F

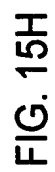


FIG. 15H

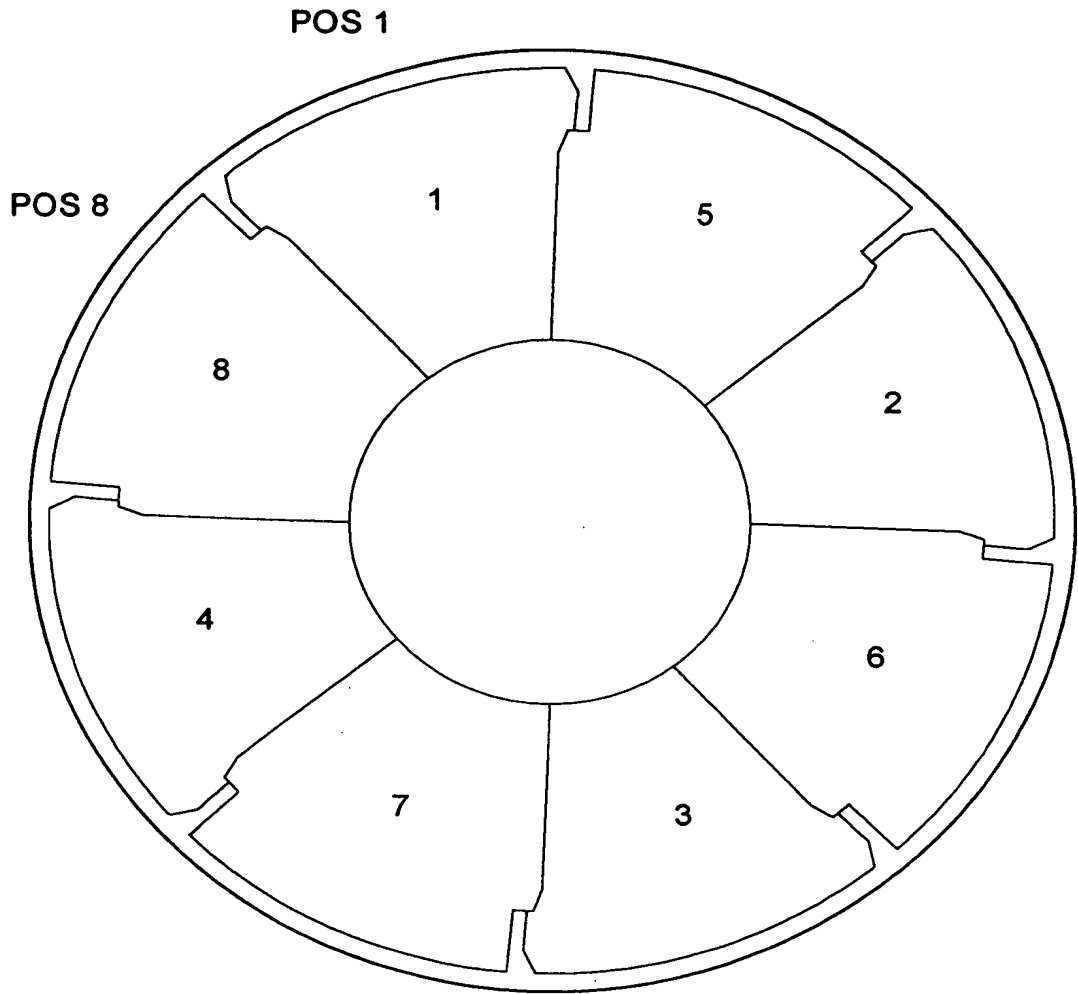
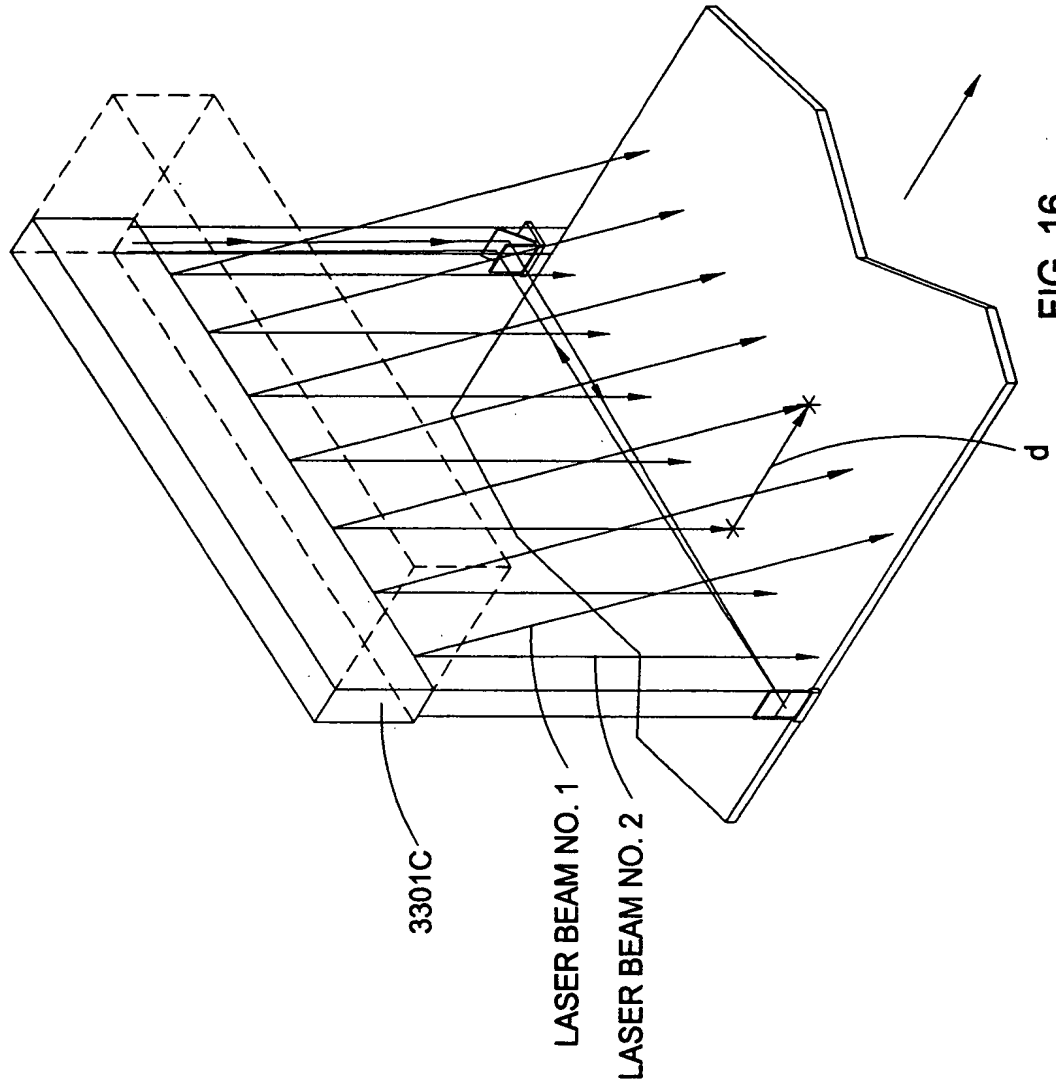
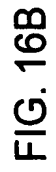
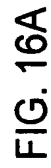


FIG. 15I

BEAM NO.	FACET NOS.	
1	1	$\Delta\lambda_1, \Delta\lambda_2$
	2	
	3	
	4	
2	5	$\Delta\lambda_1, \Delta\lambda_2$
	6	
	7	
	8	

FIG. 15K





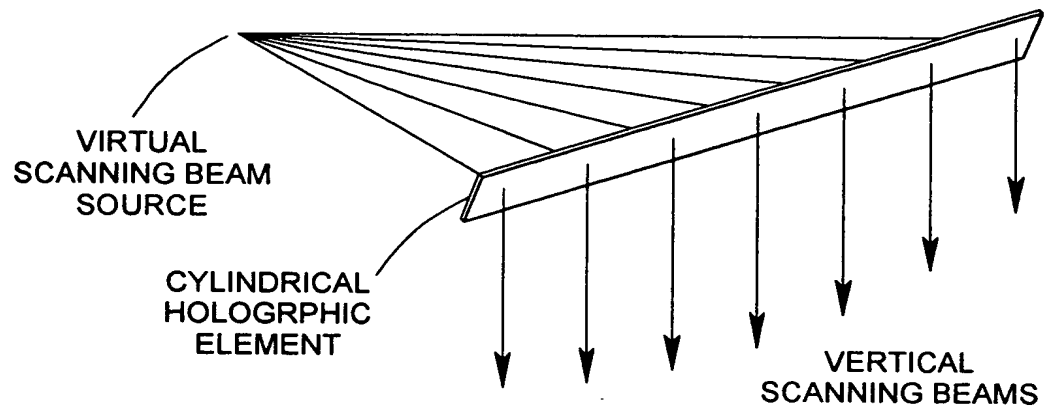


FIG. 16D

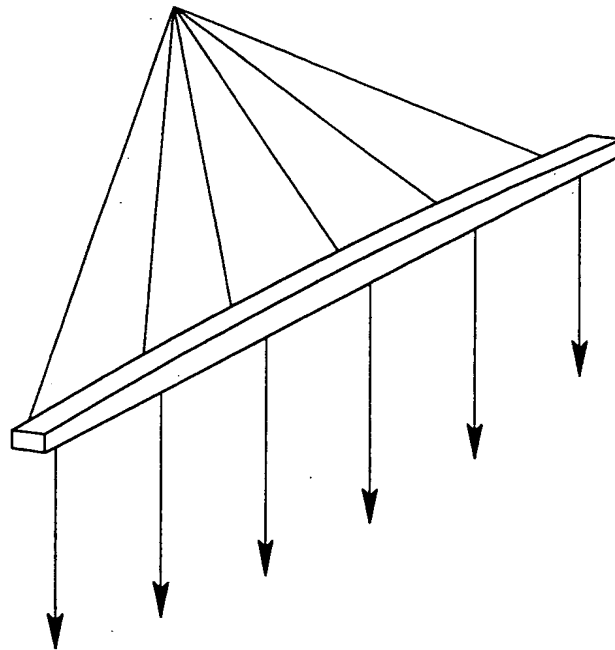
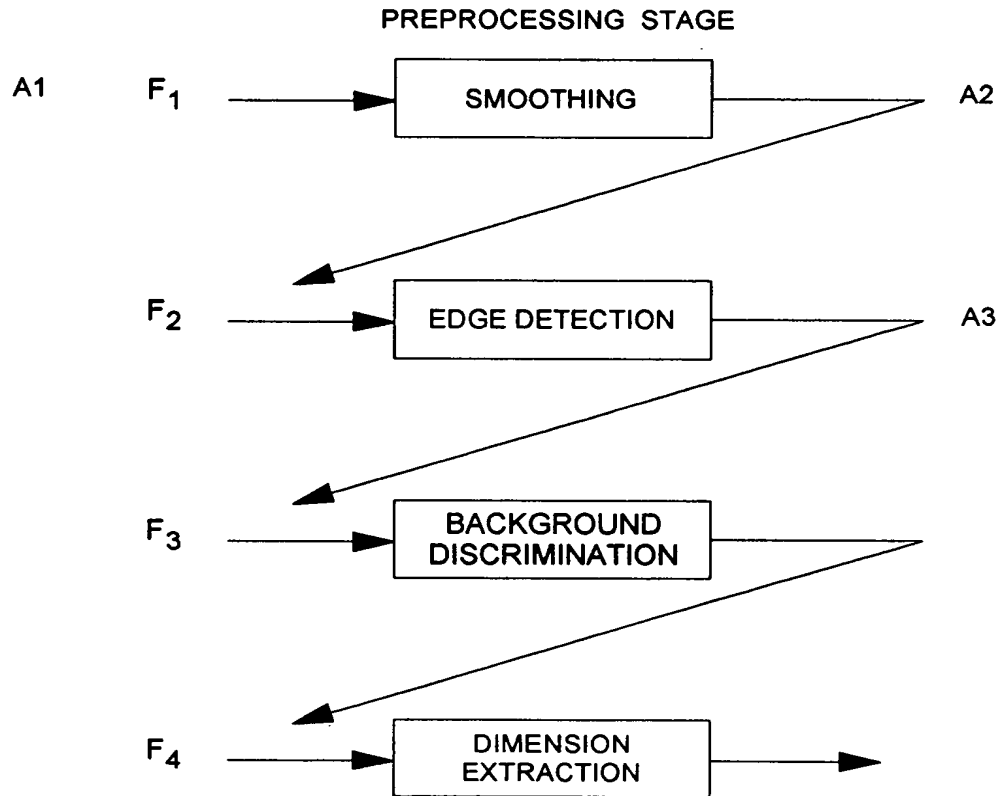


FIG. 16E

HEIGHT/WIDTH/PROFILING
PACKAGE DIMENSIONING SUBSYSTEM

(600) FIGS. 17 - 29B



F₁ = RAW IMAGE

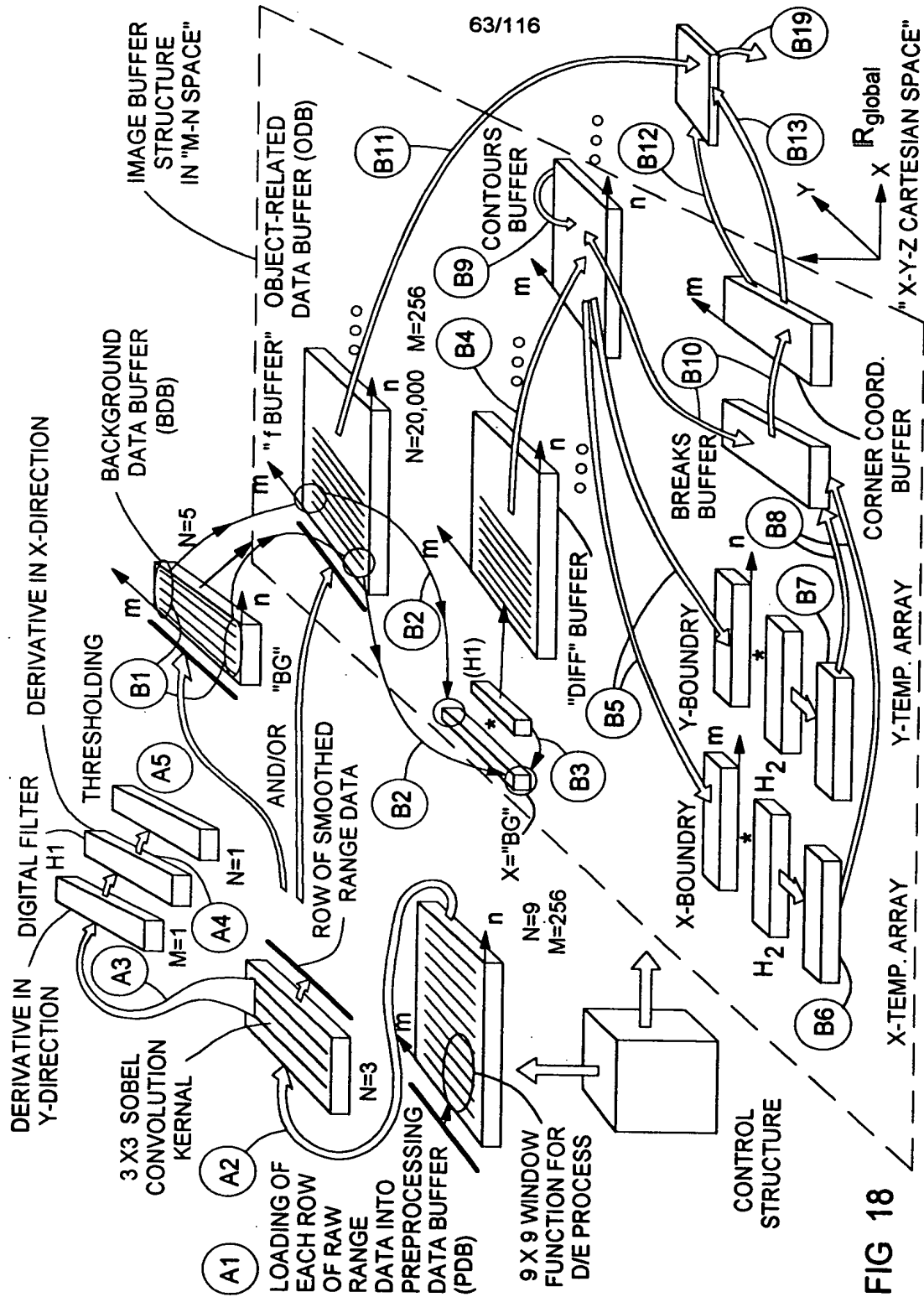
F₂ = SMOOTH IMAGE

F₃ = EDGE IMAGE

F₄ = OBJECT IMAGE

F₅ = AREA HEIGHT, AND CORNER COORDINATES

FIG. 17



CONTROL STRUCTURES

INPUT OF OPERATOR PARAMETERS AND INITIALIZATIONS

```

FOR z := 1 TO n DO
  READ ROW z OF f INTO THE IMAGE ROW STORE
  BUF(1...M, IND(z));
FOR y := k + 1 to N - k DO BEGIN
  FOR x := k + 1 TO M - k DO BEGIN
    FOR z := 1 TO a DO
      F(z) := BUF(x + xind(z), ind(k + 1 + yind(z)));

```

PROCESSING OF THE PICTURE WINDOW $F(f, (x, y))$ WITH A SPECIFIC
 OPERATOR KERNEL ARGUMENTS: $F(z)$, WITH $1 \leq z \leq a$, OR $F(i, j)$,
 WITH $-k \leq i, j \leq k$
 RESULT: GRAY VALUE v

```

⊕      IF (PARSEQ = 0) THEN
⊕          BUFOUT(x) := v
⊕      ELSE BUF(x, IND(k+1)) := v
⊕          END{for};
⊕      IF (PARSEQ = 0) THEN
⊕          WRITE ROW BUFFER STORE BUFOUT(1...M) INTO
⊕          ROW y OF THE RESULTANT IMAGE FILE OUT
⊕      ELSE
⊕          WRITE IMAGE ROW STORE BUF(1...M, IND(K+ 1)) INTO
⊕          ROW y OF THE RESULTANT IMAGE FILE OUT;
⊕      IF (y N - k) THEN BEGIN
          READ ROW y + k + 1 OF THE INPUT IMAGE FILE INTO
          THE IMAGE ROW STORE BUF(1...M, IND(1));
          LINK := IND(1);
          FOR z := 1 TO n - 1 DO IND(z) := IND(z + 1)
          IND(n) := LINK
          END {if}
      END {for}

```

CONTROL STRUCTURE FOR THE COMPUTATION OF LOCAL
 OPERATORS, USING ROW-WISE BUFFERING, THE CENTERED
 ij-COORDINATE SYSTEM, AND THE SPATIAL ARRANGEMENT FOR
 THE WINDOW CONTENT IF THE ONE-DIMENSIONAL ARRAY $F(z)$
 IS USED. PROGRAM LINES LABELED WITH \oplus ARE SUPERFLUOUS
 IF A PARALLEL OPERATOR HAS TO BE IMPLEMENTED

FIG. 19

STEP A1 INVOLVES CAPTURING LINES (ROWS) OF DIGITIZED RANGE DATA PRODUCED BY THE LASER SCANNING/RANGING UNIT DURING EACH SWEEP OF THE AMPLITUDE MODULATED LASER BEAM ACROSS THE WIDTH OF THE CONVEYER BELT. EACH ROW OF RAW RANGE DATA HAS A PREDETERMINED NUMBER OF RANGE VALUE SAMPLES (E.G. $M=256$) TAKEN DURING EACH SCAN ACROSS THE CONVEYOR BELT. EACH SUCH RANGE DATA SAMPLE REPRESENTS THE MAGNITUDE OF THE POSITION VECTOR POINTING TO THE CORRESPONDING SAMPLE POINT ON THE SCANNED PACKAGE, REFERENCED WITH RESPECT TO A POLAR-TYPE COORDINATE SYSTEM SYMBOLICALLY EMBEDDED WITHIN THE LADAR-BASED IMAGING AND DIMENSIONING SUBSYSTEM. STEP A1 ALSO INVOLVES LOADING A PREDETERMINED NUMBER OF RAW RANGE DATA SAMPLES INTO A FIFO-TYPE PREPROCESSING DATA BUFFER (e.g. $M=9$) FOR BUFFERING 9 ROWS OF RANGE DATA AT ANY INSTANT OF TIME.

STEP A2 INVOLVES USING, AT EACH PROCESSING CYCLE AND SYNCHRONIZED WITH THE CAPTURE OF EACH NEW ROW OF RAW RANGE DATA, A 2-D (9X9) WINDOW FUNCTION EMBEDDED INTO A GENERAL CONTROL STRUCTURE (e.g. PIXEL PROGRAM LOOP), TO SMOOTH EACH LINE (OR ROW) OF RAW RANGE DATA BUFFERED IN THE PROCESSING DATA BUFFER USING DILUTION AND EROSION (D/E) PROCESS BASED ON NON-LINEAR TYPE MIN/MAX METHODS. THE OUTPUT FROM THIS NON-LINEAR OPERATION IS A SINGLE ROW OF SMOOTH RANGE DATA OF LENGTH $M=256$ WHICH IS INPUT TO A THREE ROW FIFO BUFFER, AS SHOWN IN FIG. 44G.

STEP 3A INVOLVES USING, AT EACH PROCESSING CYCLE, A 2-D (3X3) CONVOLUTION KERNEL BASED ON THE SOBEL OPERATOR, AND EMBEDDED INTO A GENERAL CONTROL STRUCTURE (e.g. PIXEL PROGRAM LOOP), TO EDGE-DETECT EACH BUFFERED ROW OF SMOOTH EDGE DATA OF LENGTH $M=256$ WHICH IS INPUT TO A FIRST ONE ROW ($N=1$) FIFO BUFFER AS SHOWN IN FIG. 44G. THE OUTPUT ROW OF "EDGE DETECTED" RANGE DATA REPRESENTS THE FIRST SPATIAL DERIVATIVE A OF THE BUFFERED ROWS OF RANGE DATA ALONG THE n DIRECTION OF THE $N=9$ FIFO (CORRESPONDING TO THE FIRST SPATIAL DERIVATIVE OF THE RANGE DATA CAPTURED ALONG THE Y DIRECTION OF THE CONVEYER BELT).

A

FIG. 20A

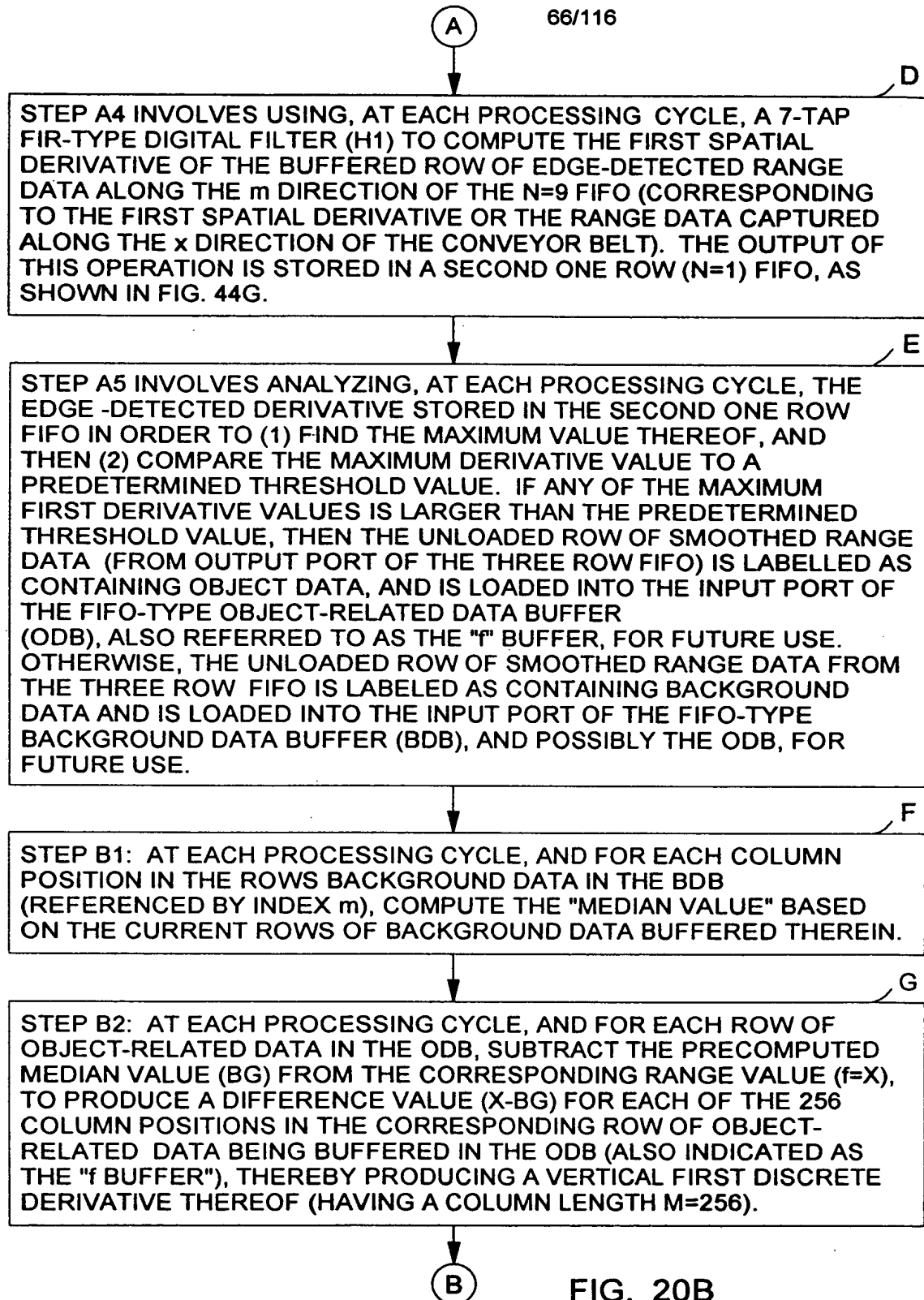


FIG. 20B

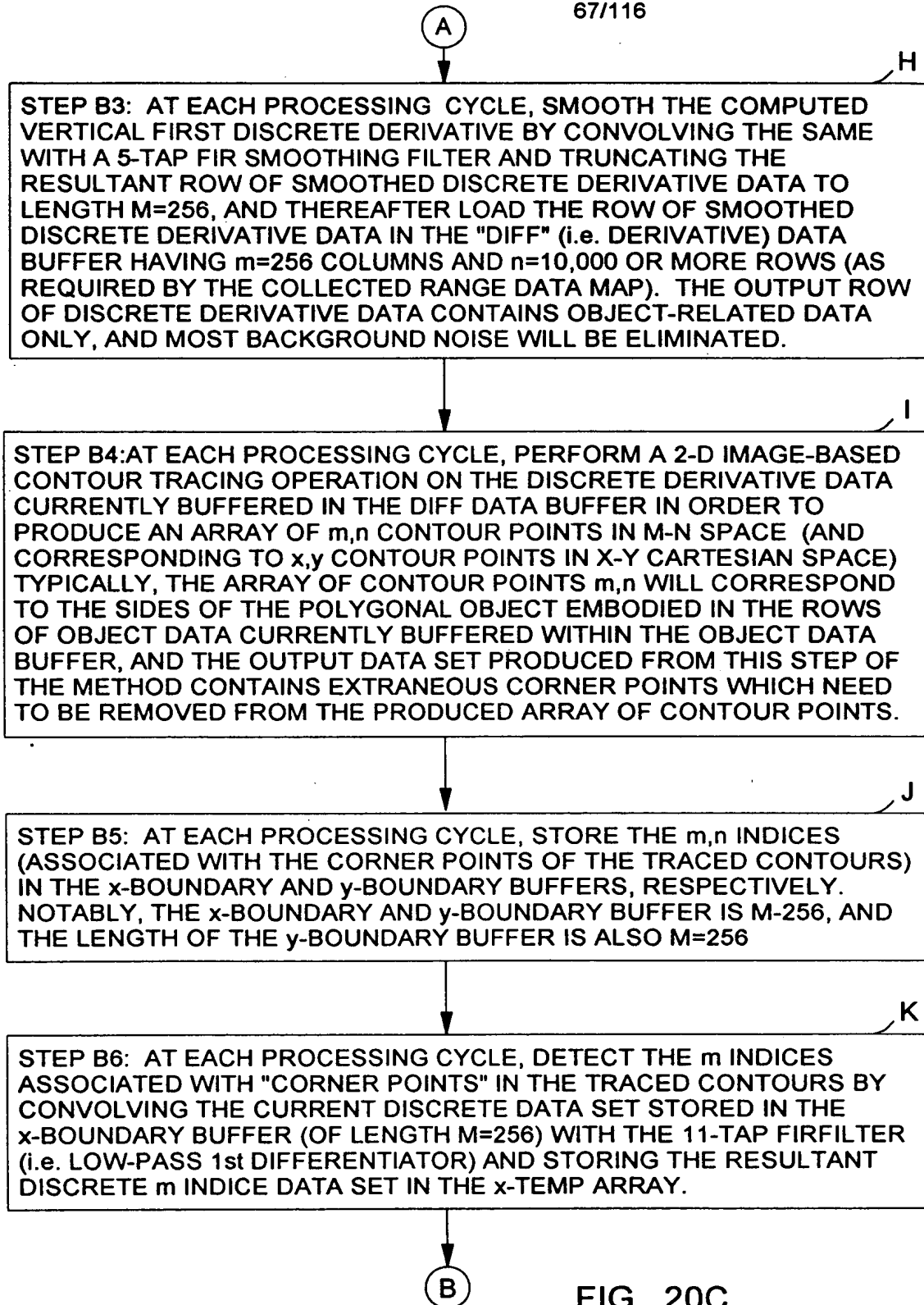


FIG. 20C

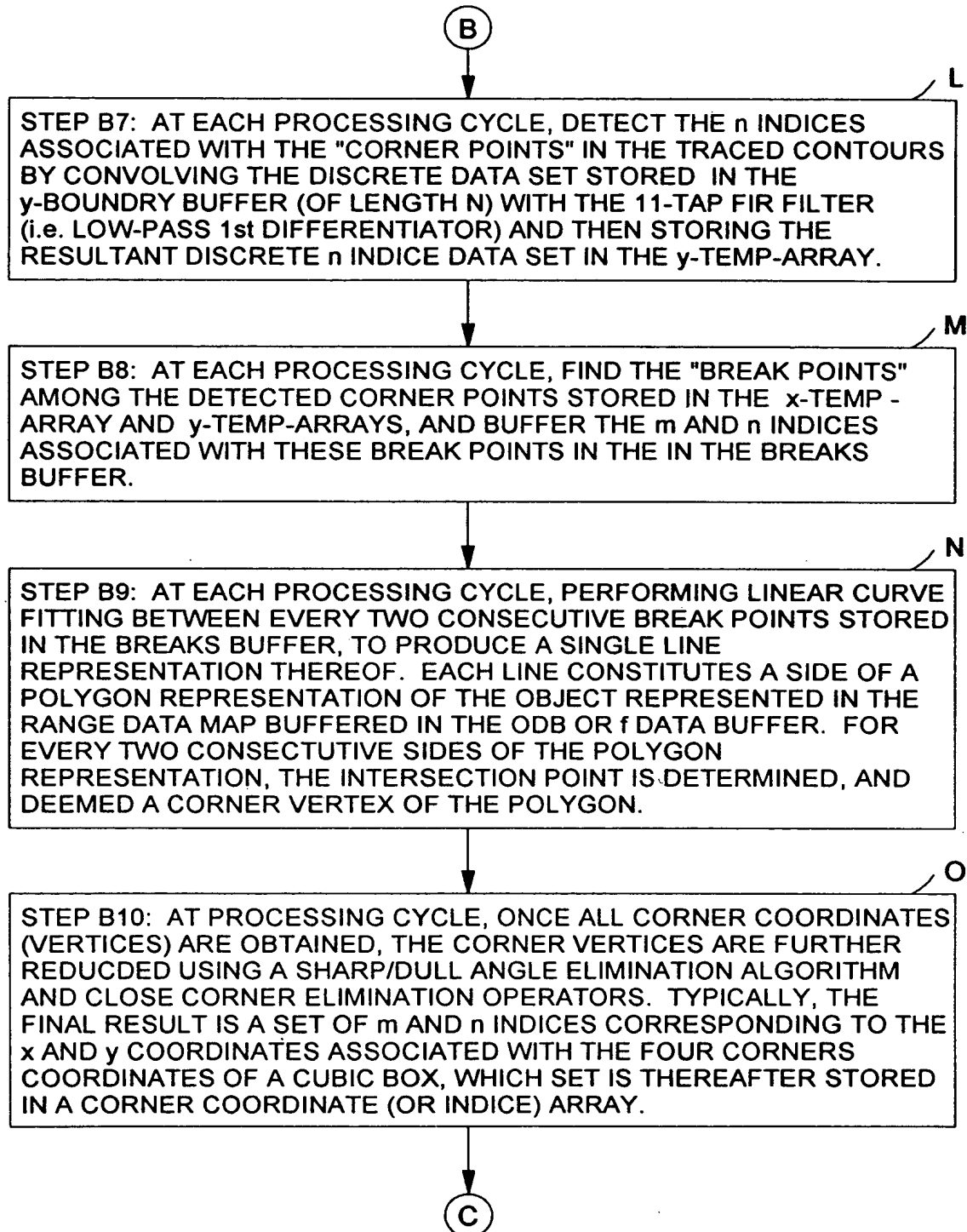


FIG. 20D

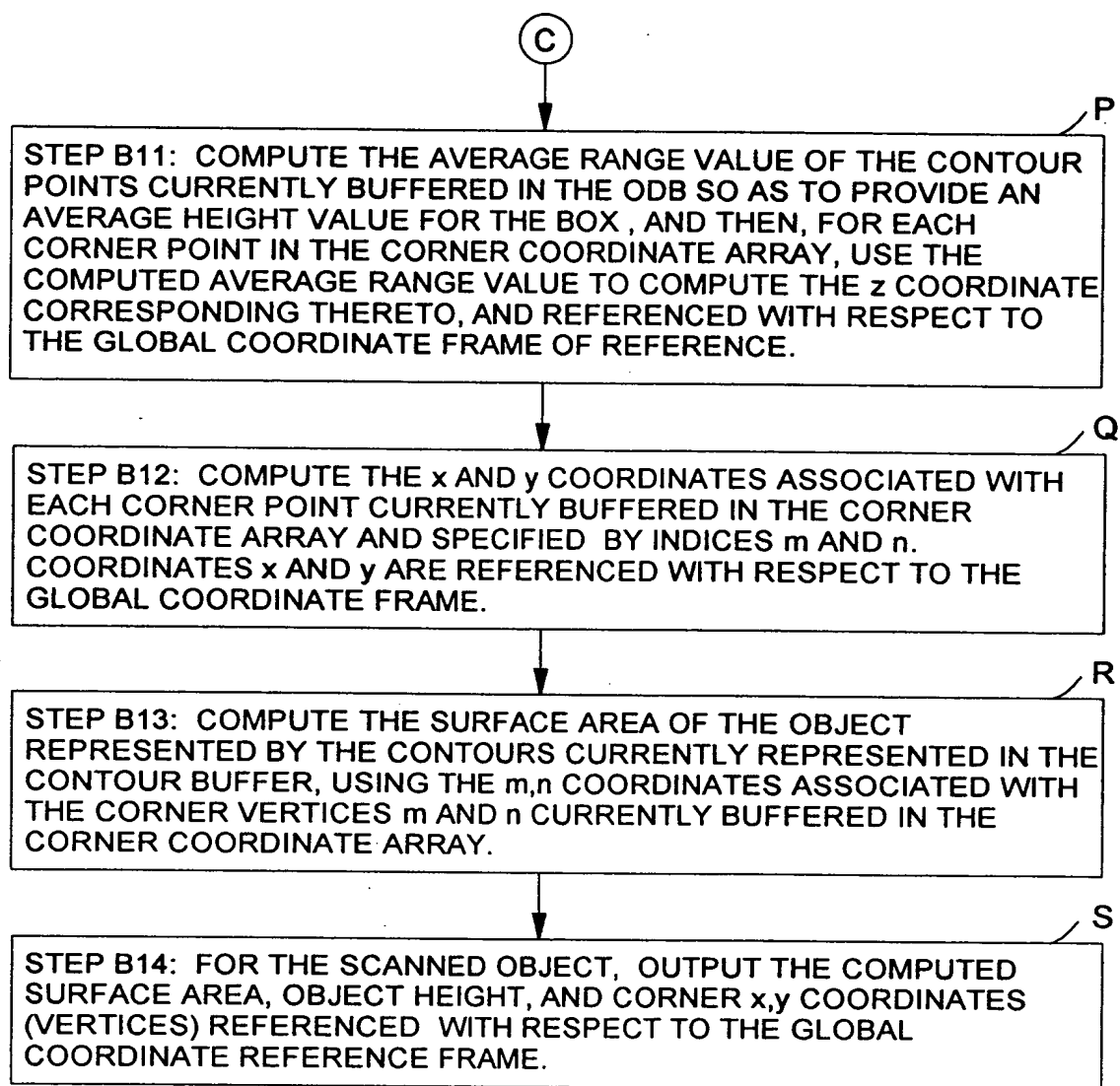


FIG. 20E

70/116

RAW RANGE DATA

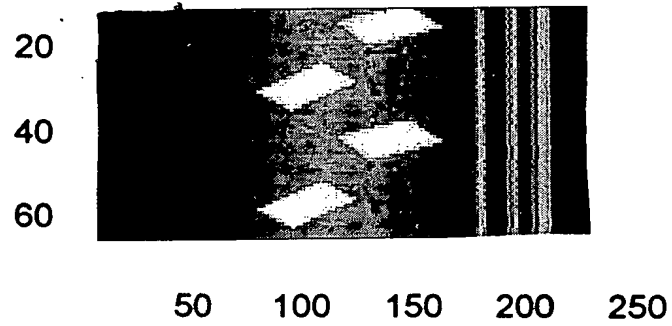


FIG. 21A

SMOOTHED RANGE DATA

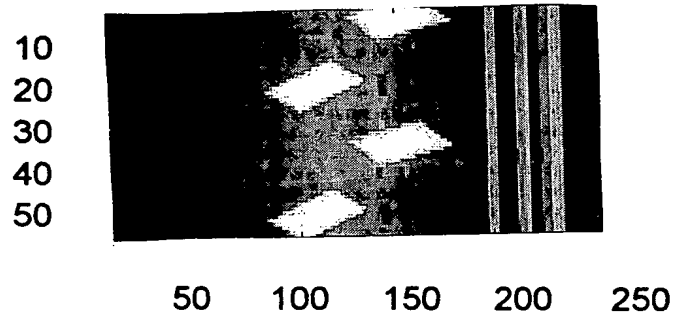


FIG. 21B

VERTICAL EDGE

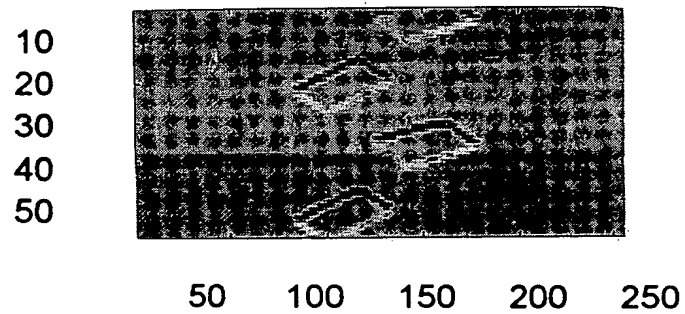


FIG. 21C

71/116

BACKGROUND FOUND

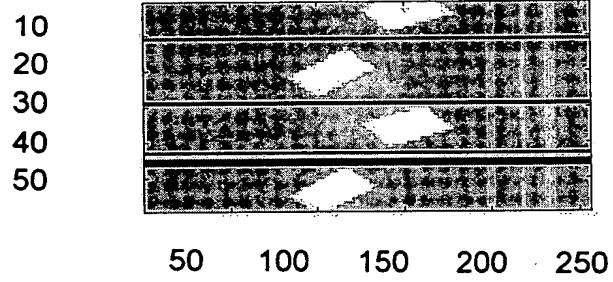


FIG. 21D

BACKGROUND ELIMINATED

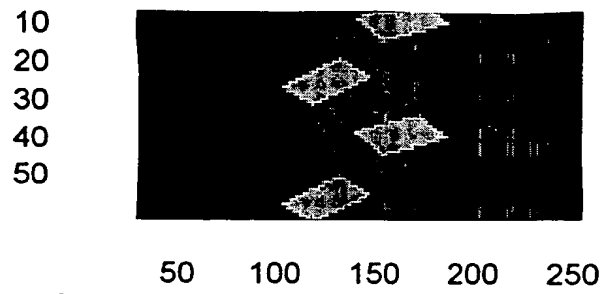
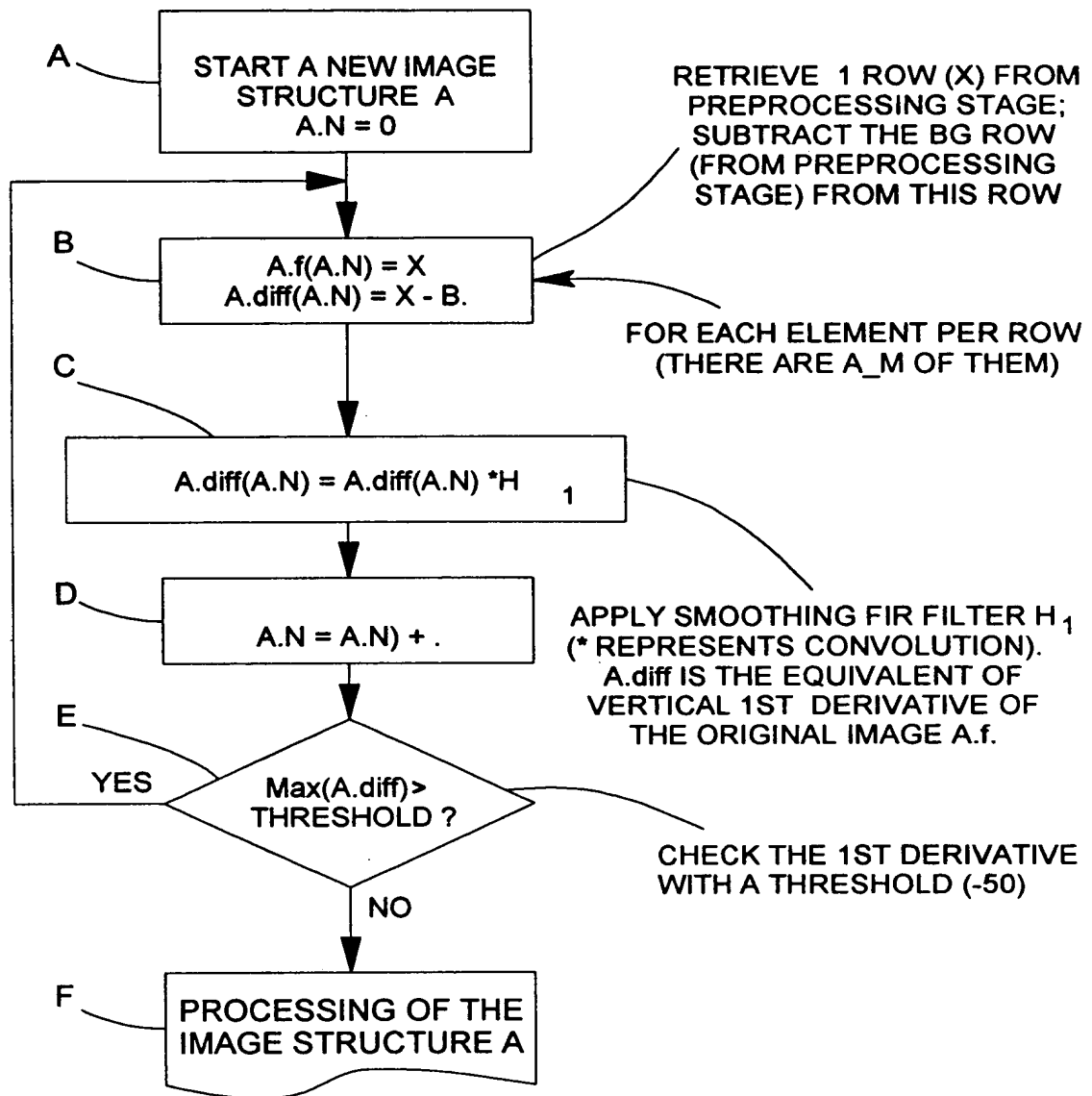


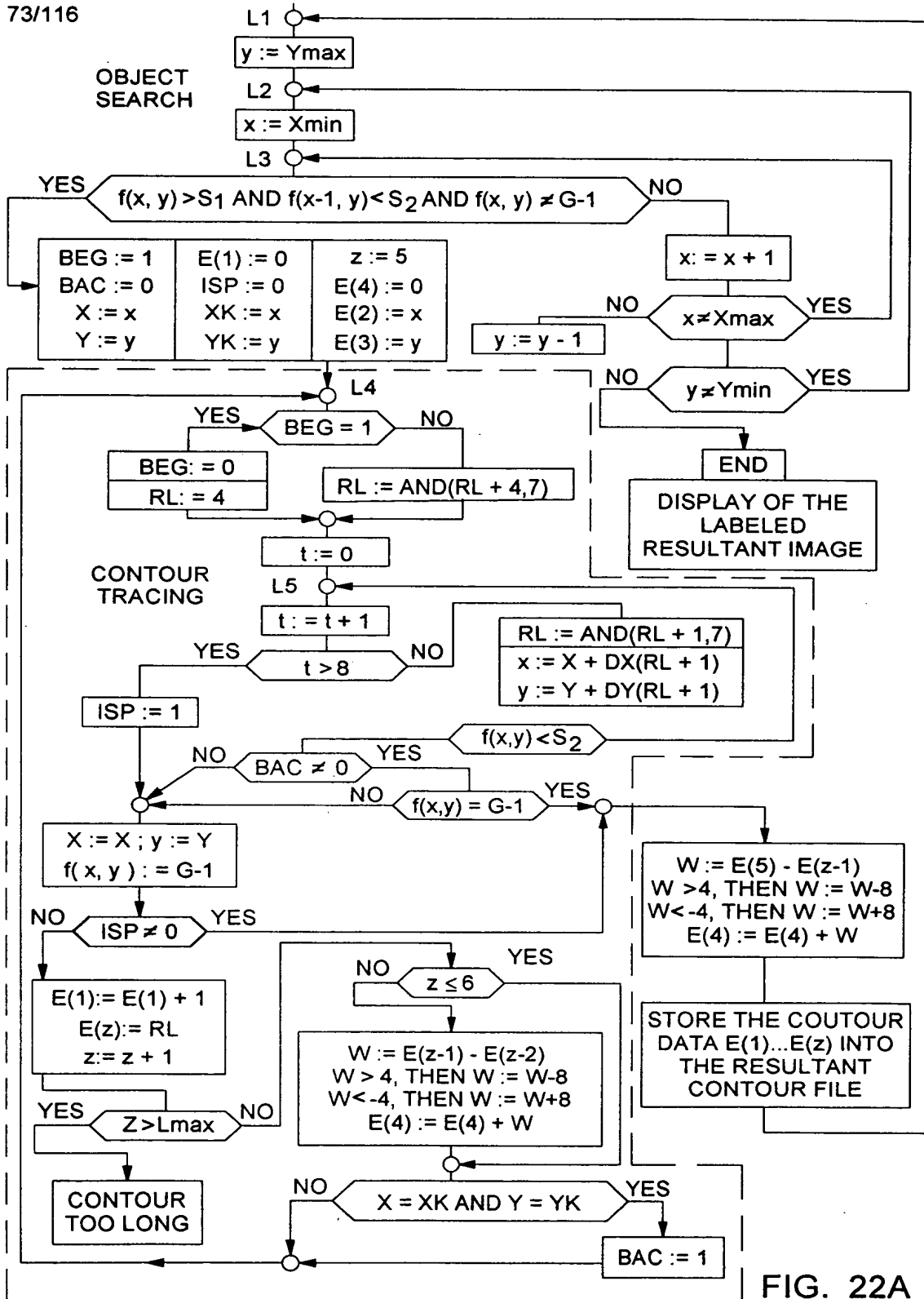
FIG. 21E

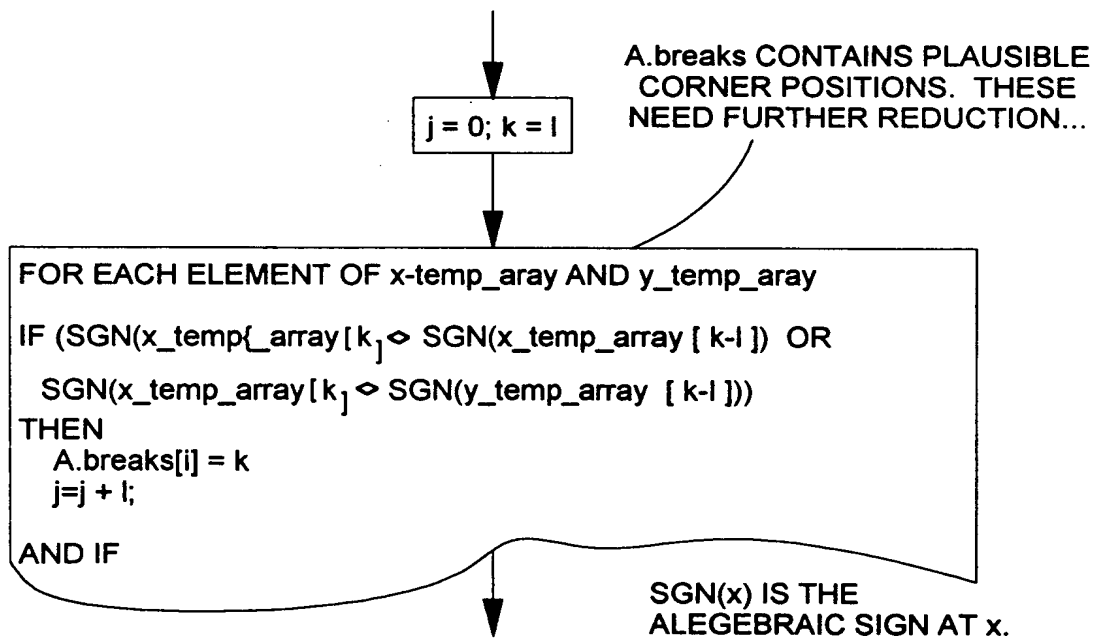
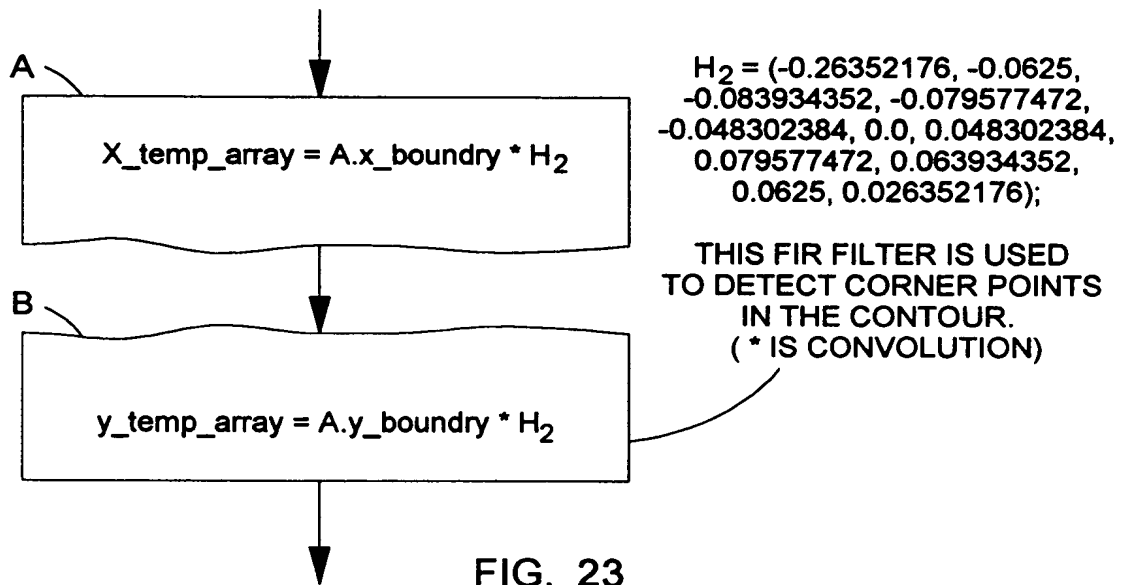


$$H_1 = (0.15 \ 0.25 \ 0.2 \ 0.25 \ 0.15)$$

THIS FUNCTIONAL BLOCK RETRIEVES DATA ALREADY PRE-PROCESSED, COMPUTES VERTICAL FIRST DERIVATIVE, AND STORES THE RESULTS IN AN IMAGE STRUCTURE FOR FURTHER PROCESSING, SUCH AS COMPUTER TRACING, ETC.

FIG. 22





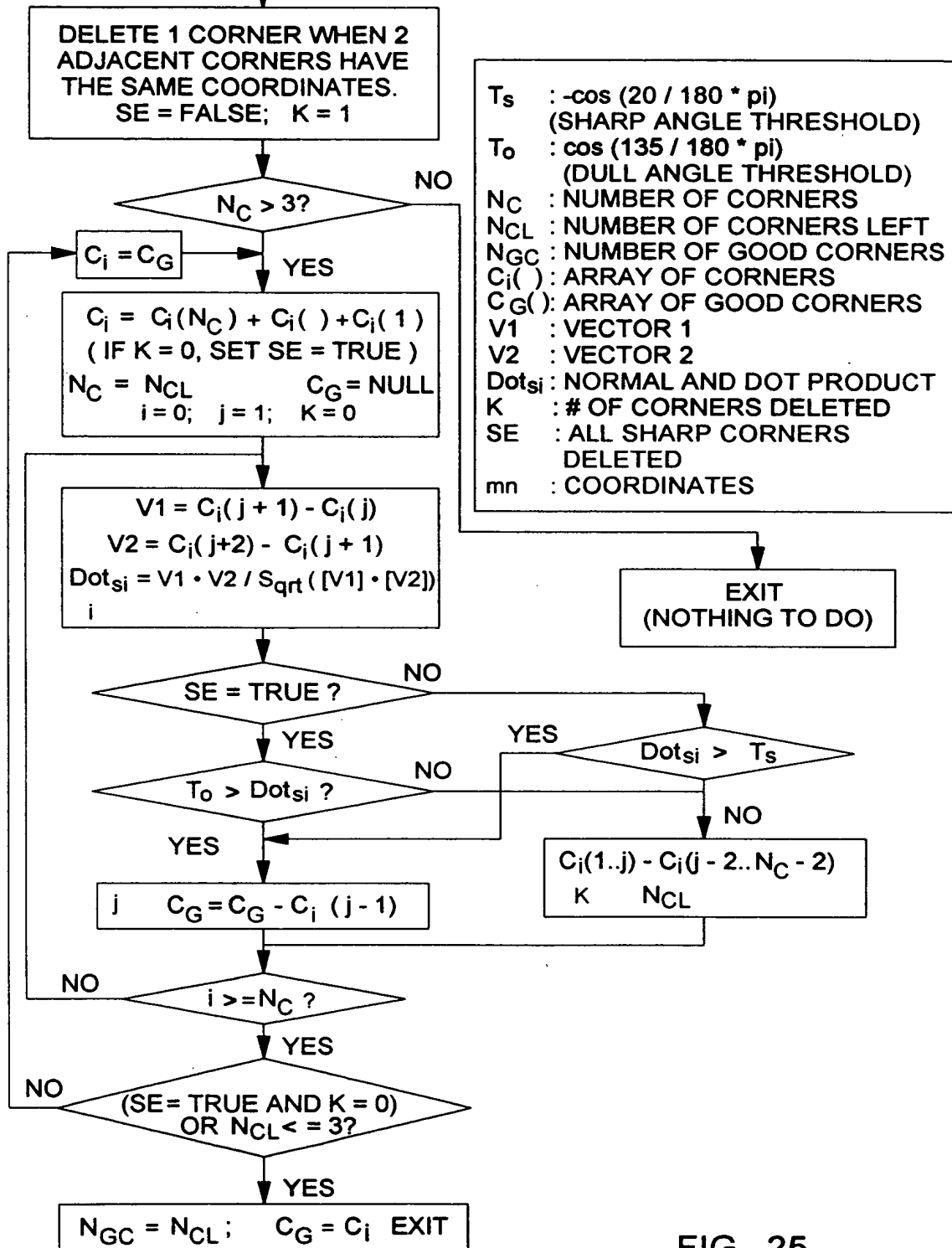
$N_C, C_i()$ FLOW CHART FOR DELETION OF
SHARP AND DULL ANGLES

FIG. 25

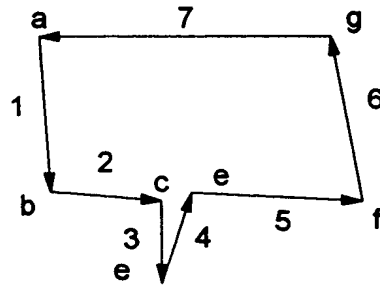


FIG. 26A

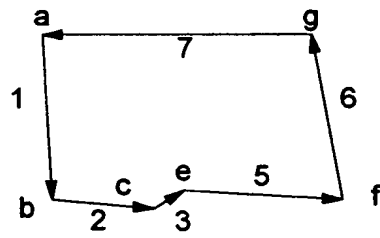


FIG. 26B

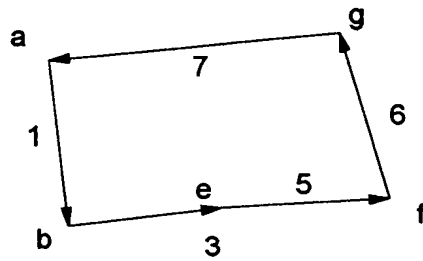


FIG. 26C

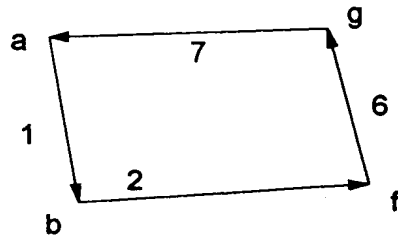


FIG. 26D

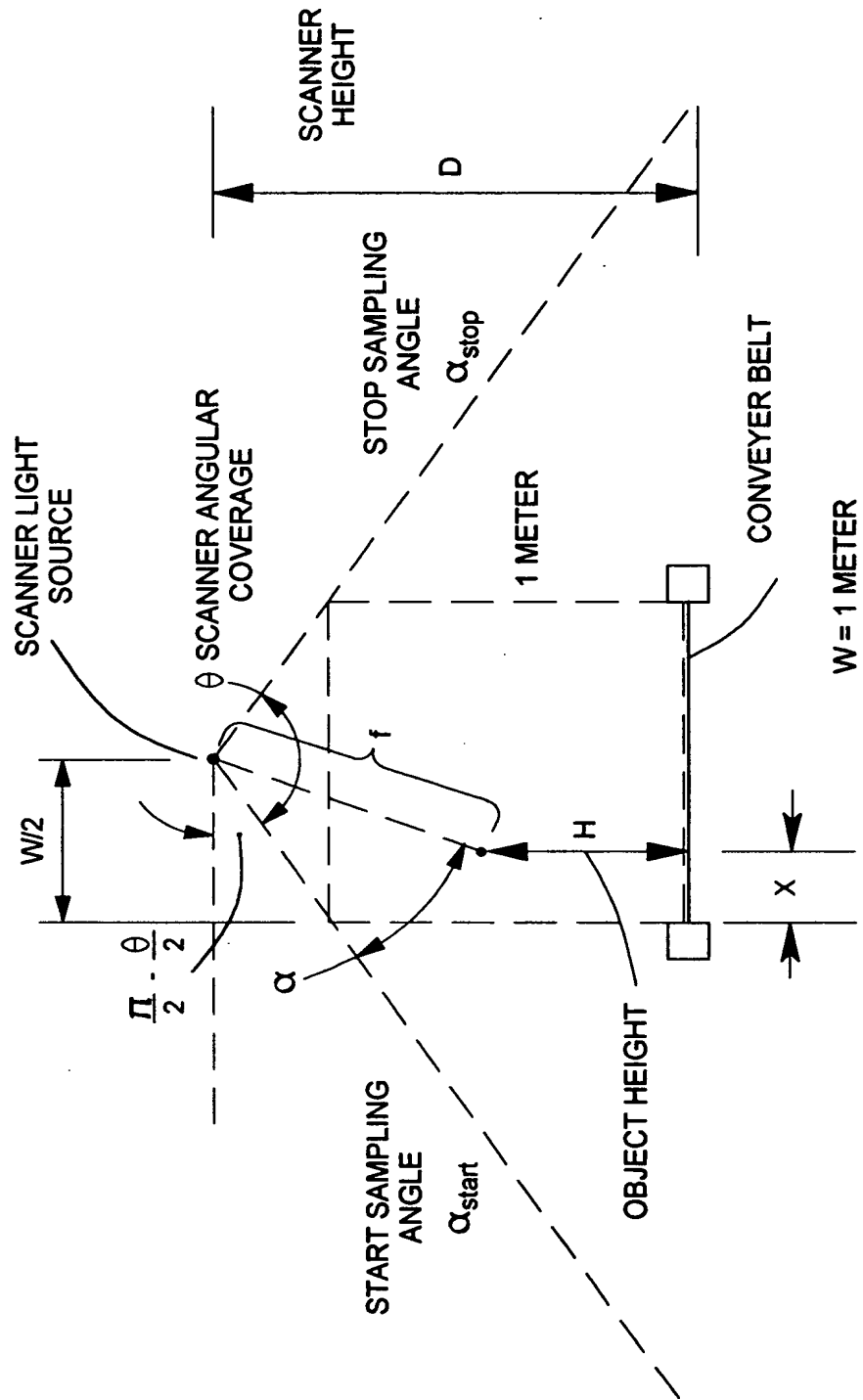


FIG. 27

FLOW CHART FOR PACKAGE AREA COMPUTATION

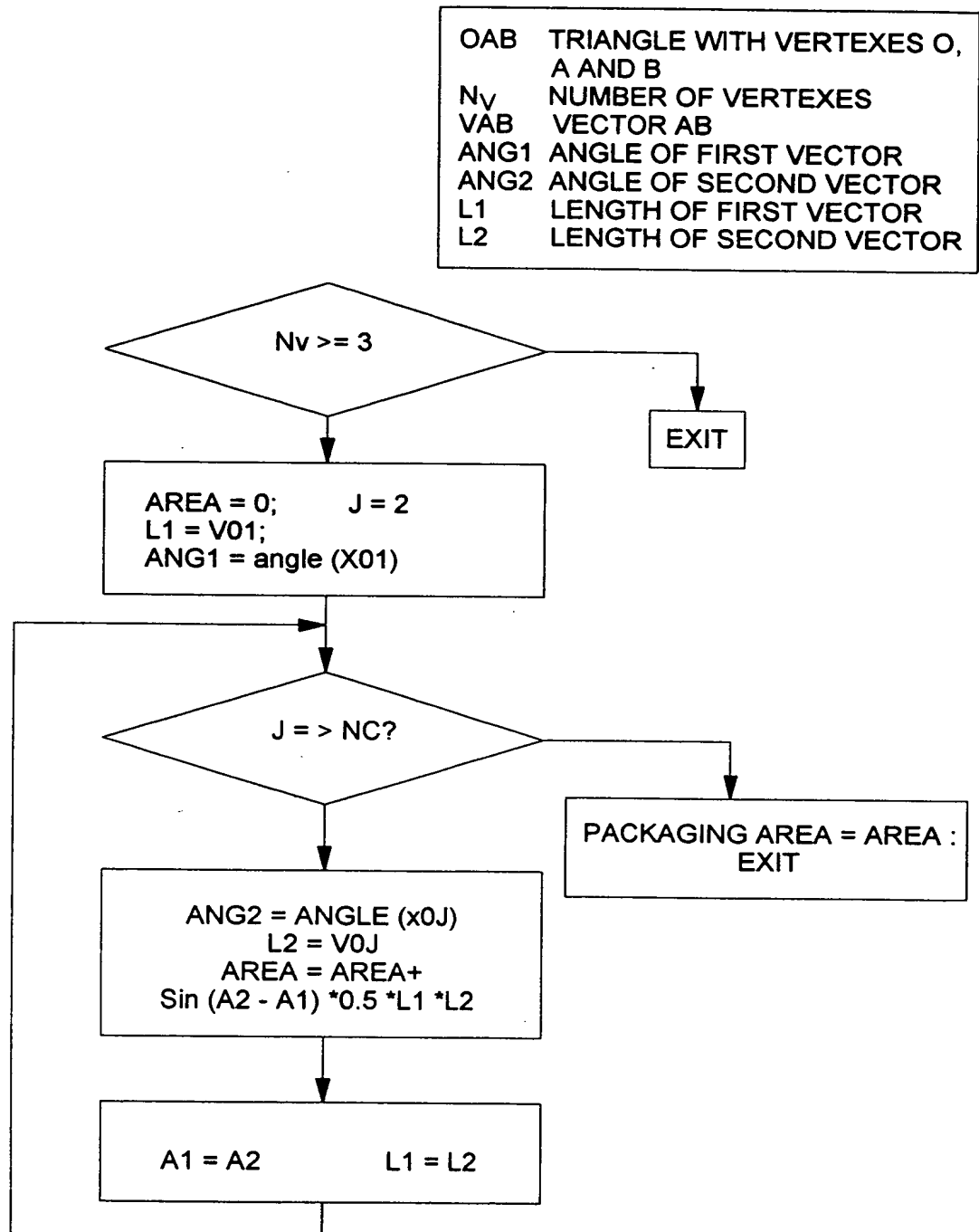


FIG. 28

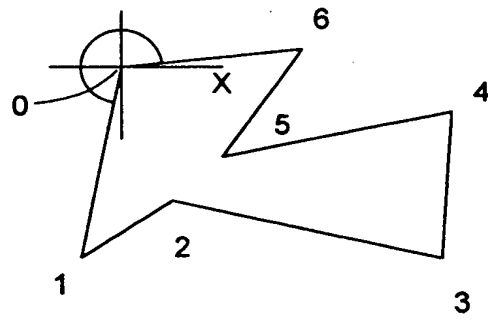


FIG. 29A

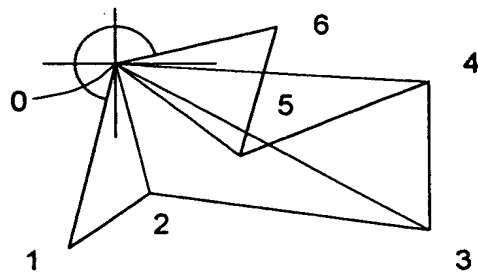


FIG. 29B

PACKAGE VELOCITY MEASUREMENT SUBSYSTEM (400)

80/116

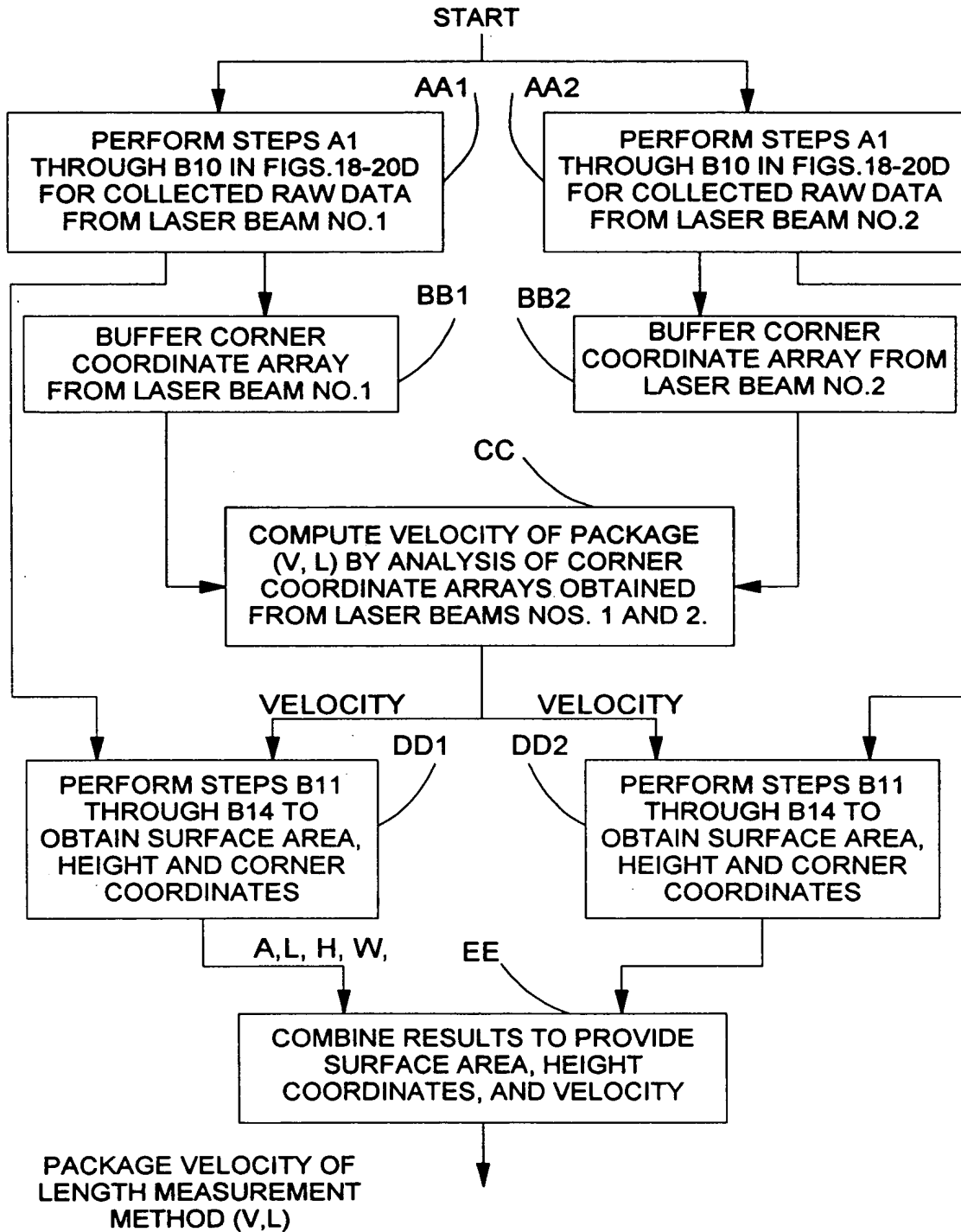


FIG. 30

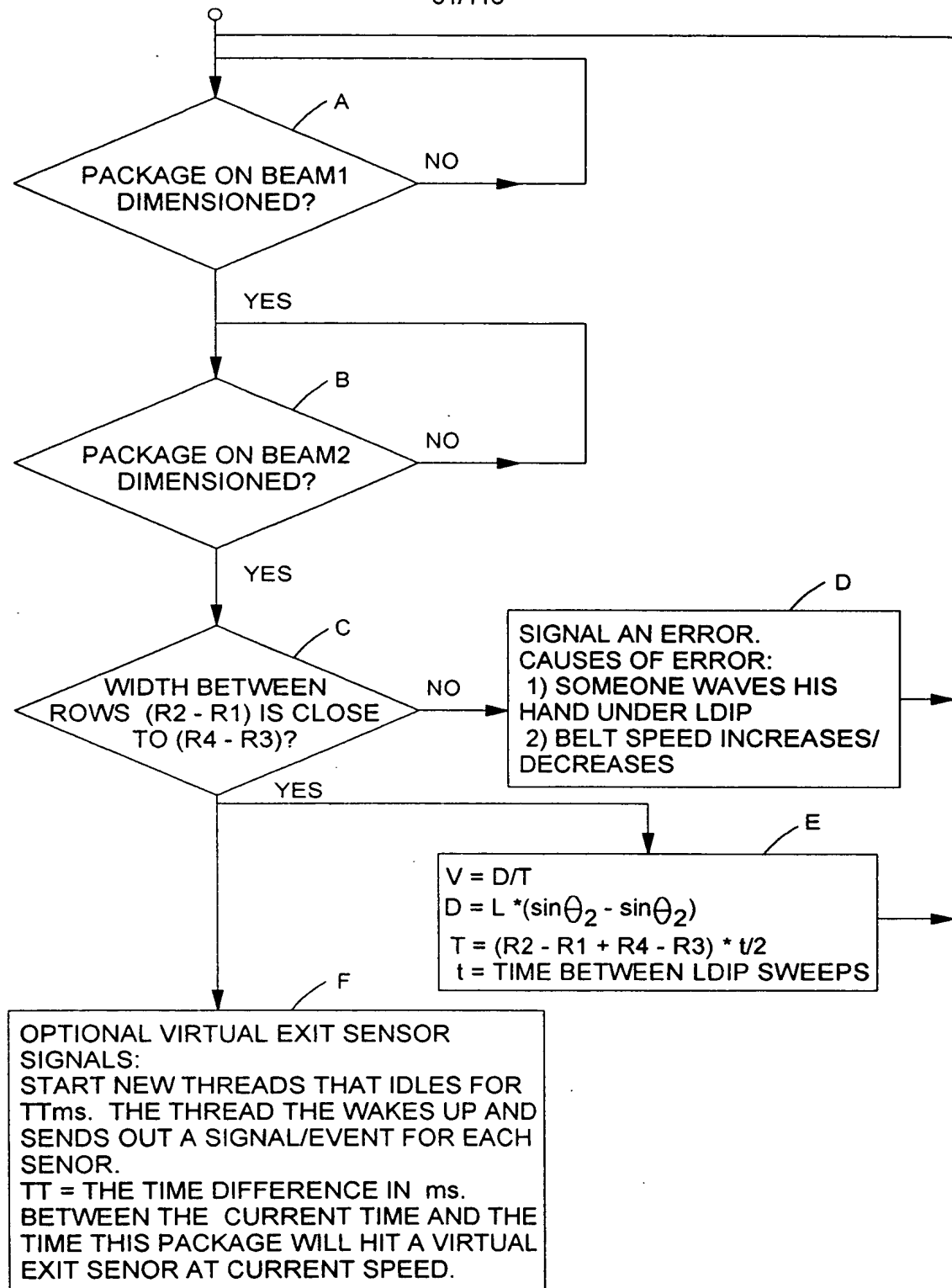


FIG 31

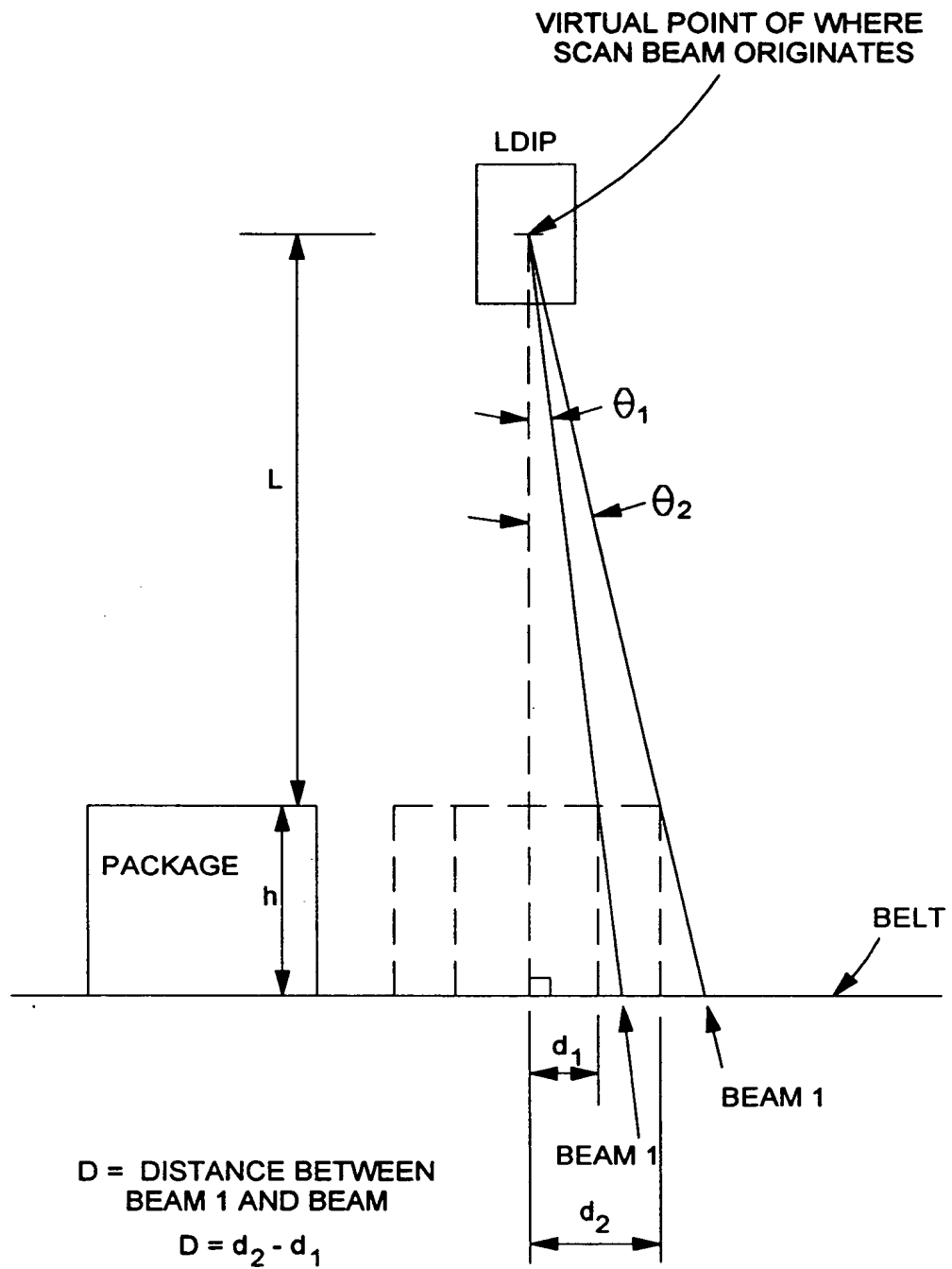


FIG. 32

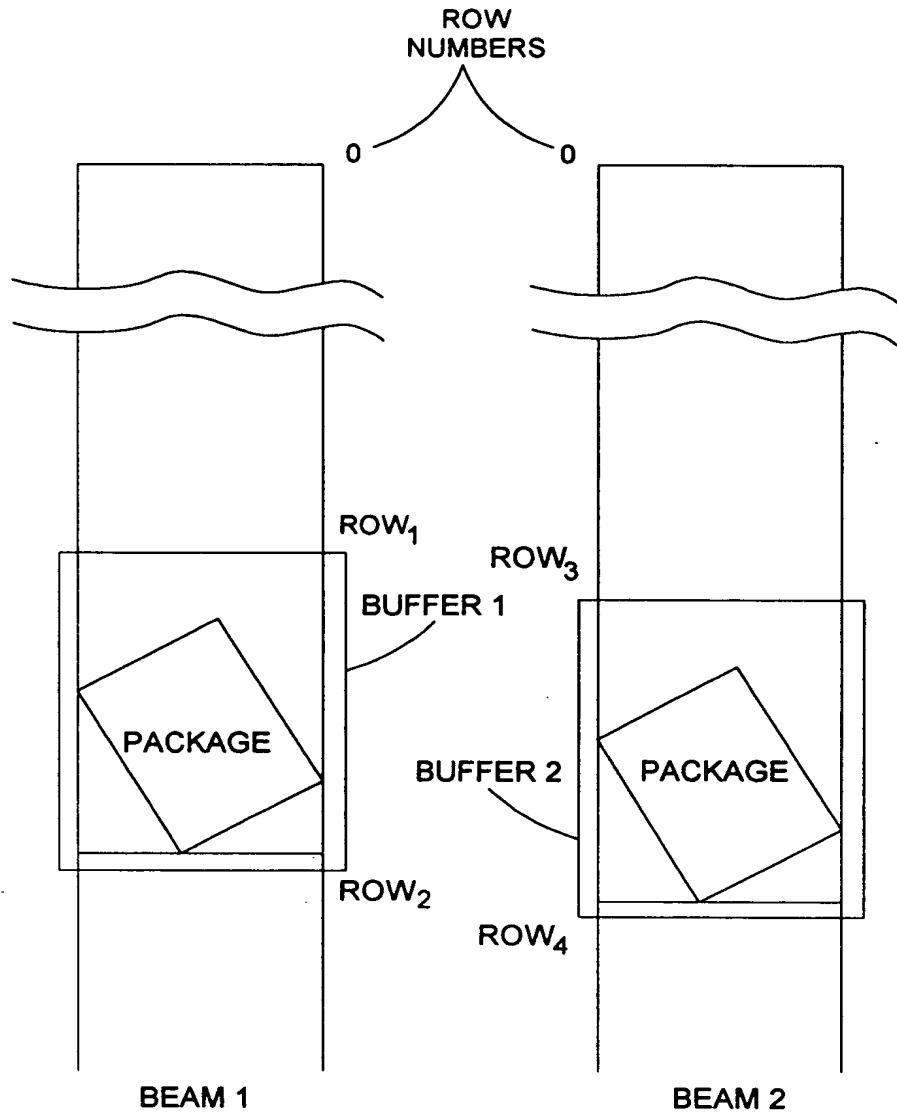


FIG. 33A

FIG. 33B

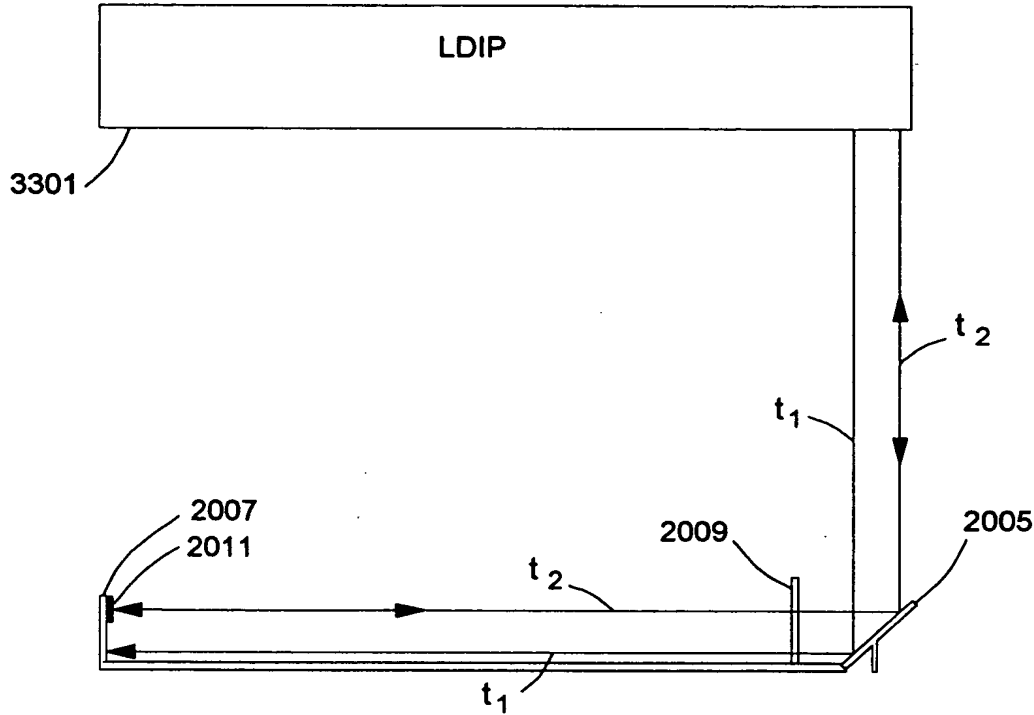


FIG. 33B

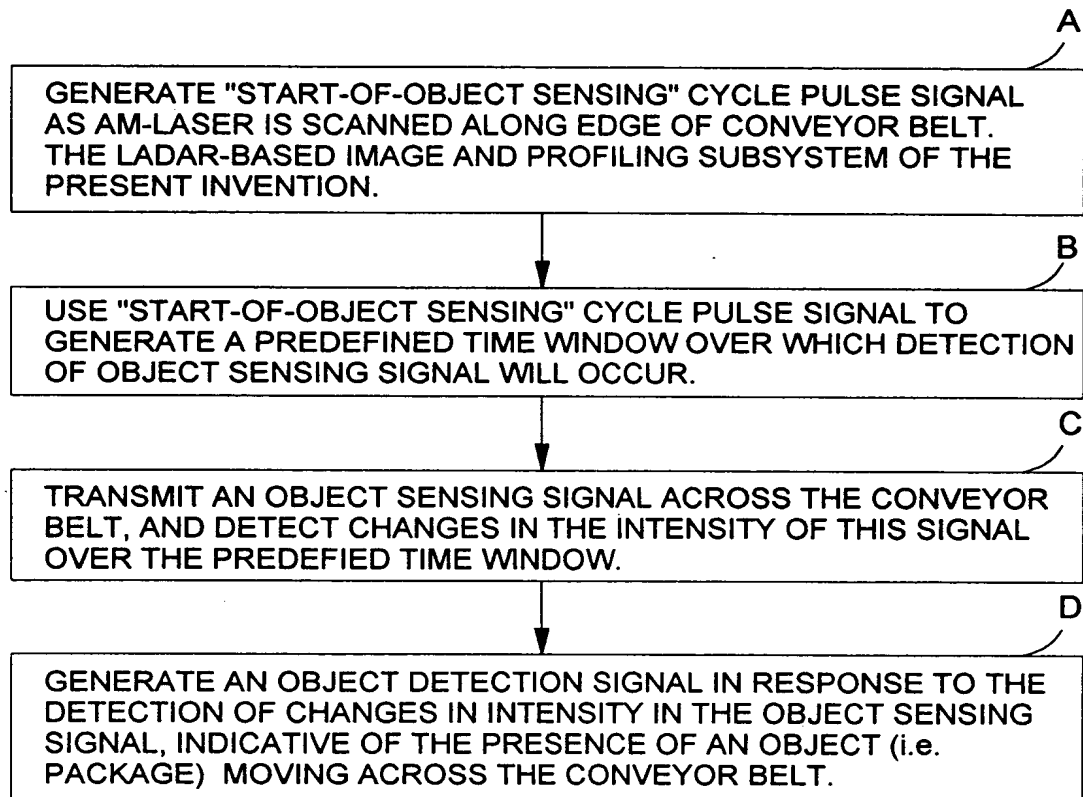


FIG. 34

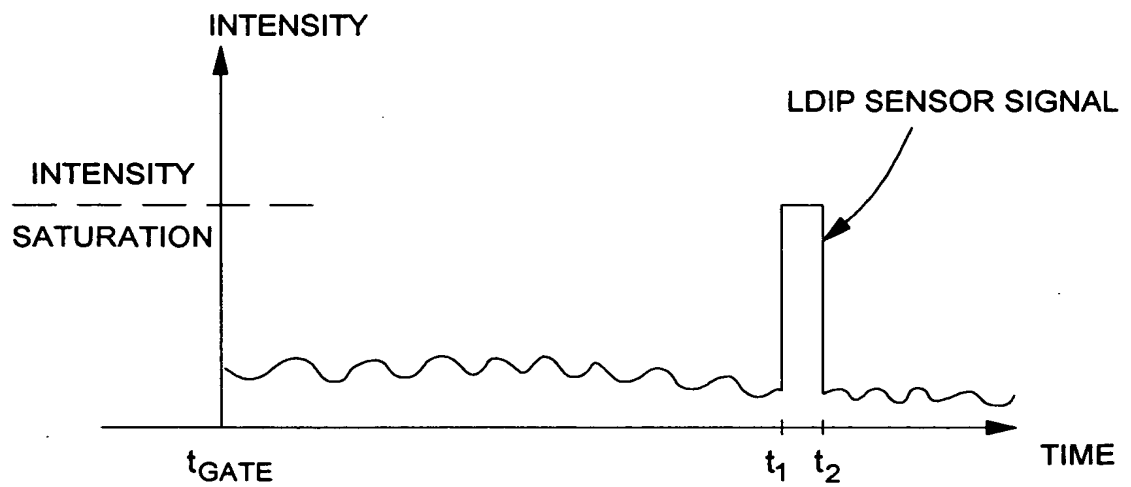


FIG. 35A

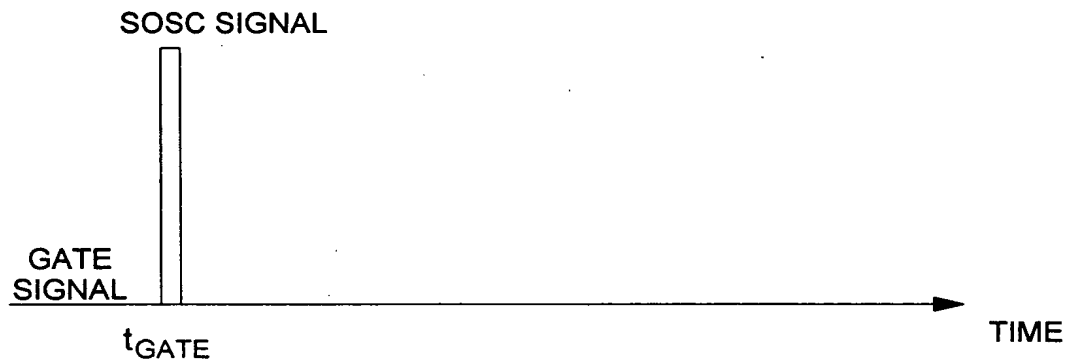


FIG. 35B

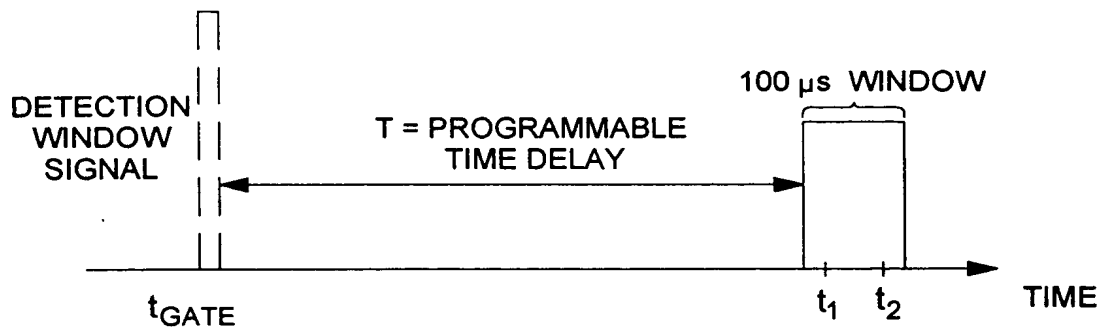


FIG. 35C

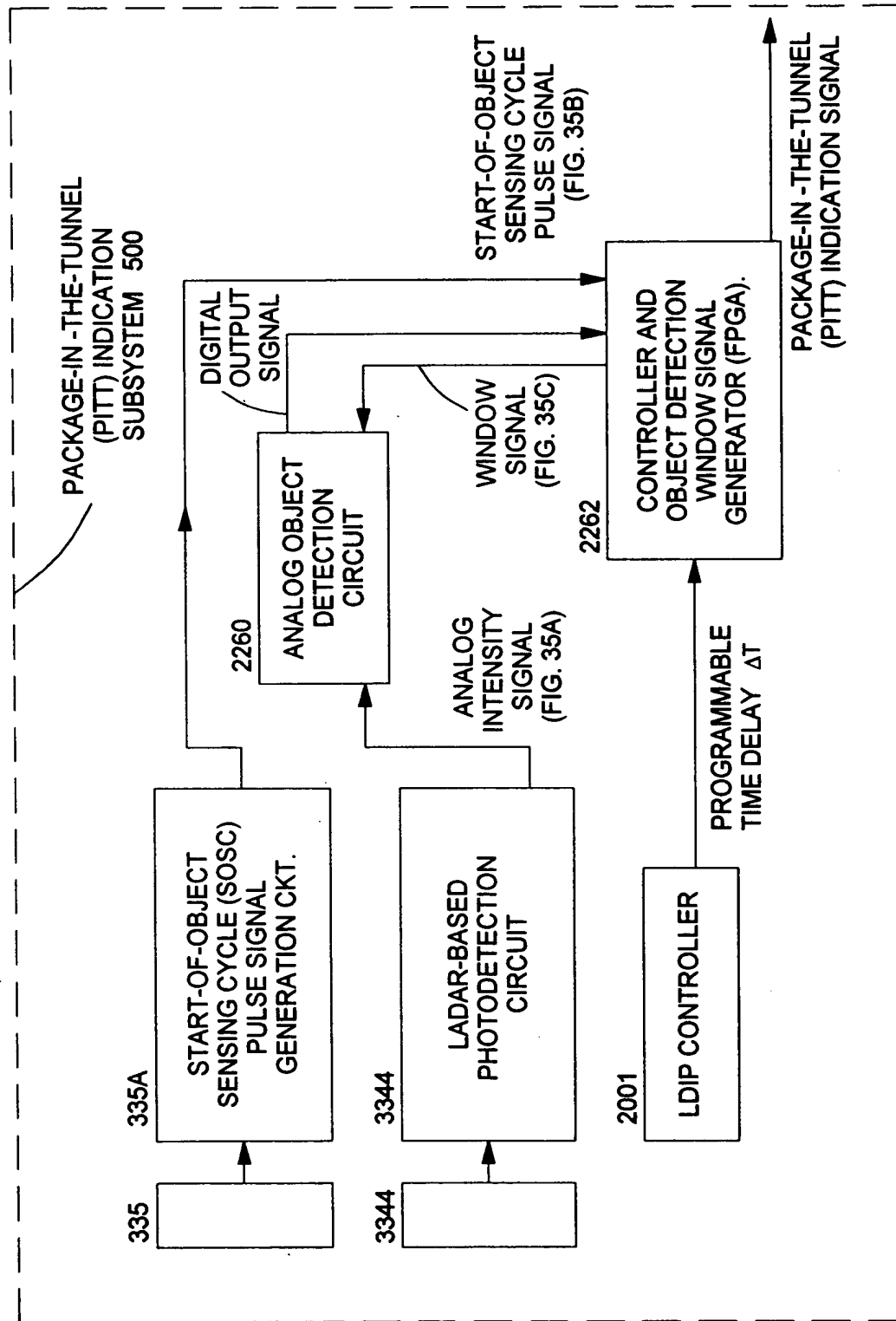
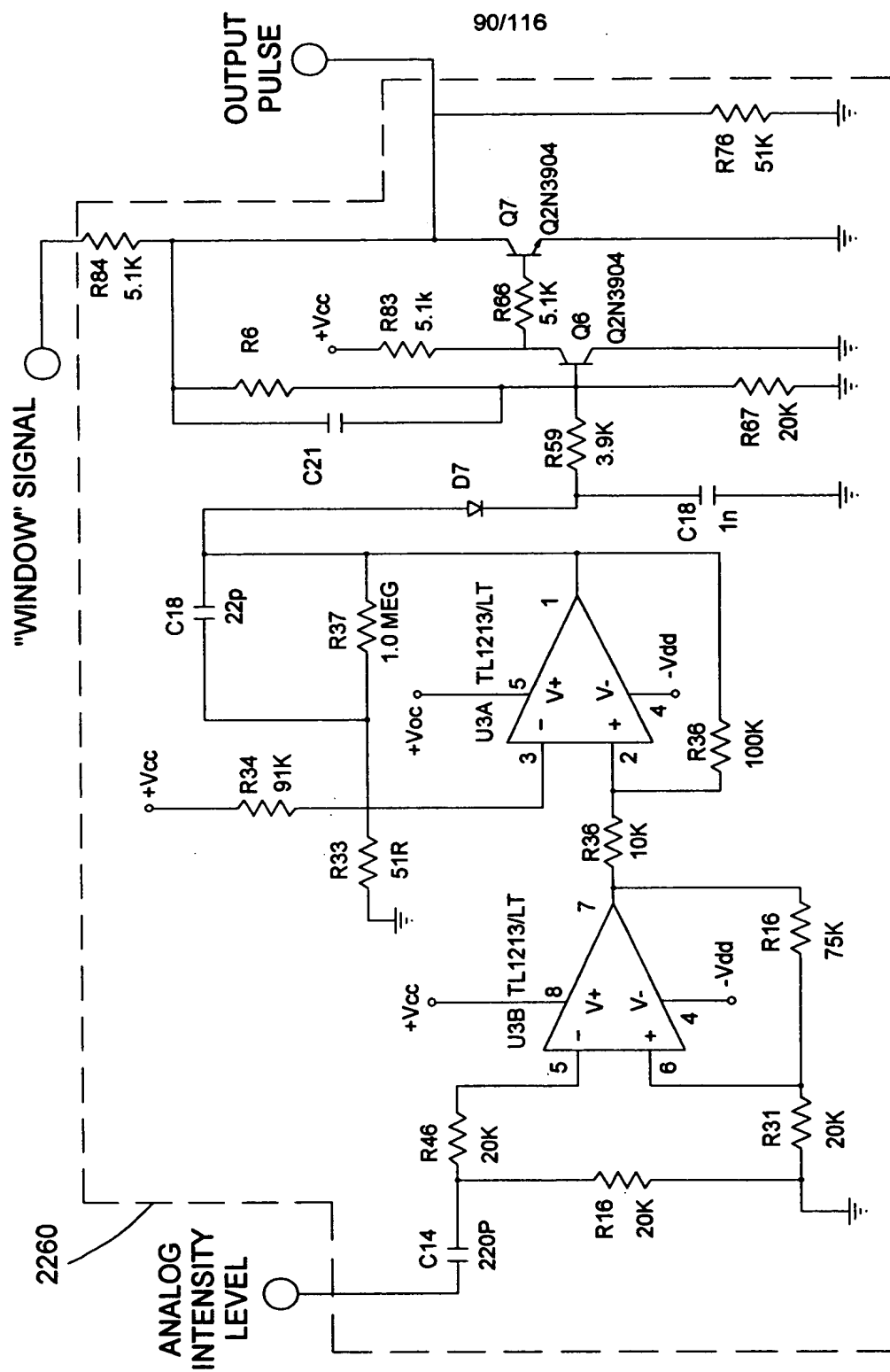


FIG. 37



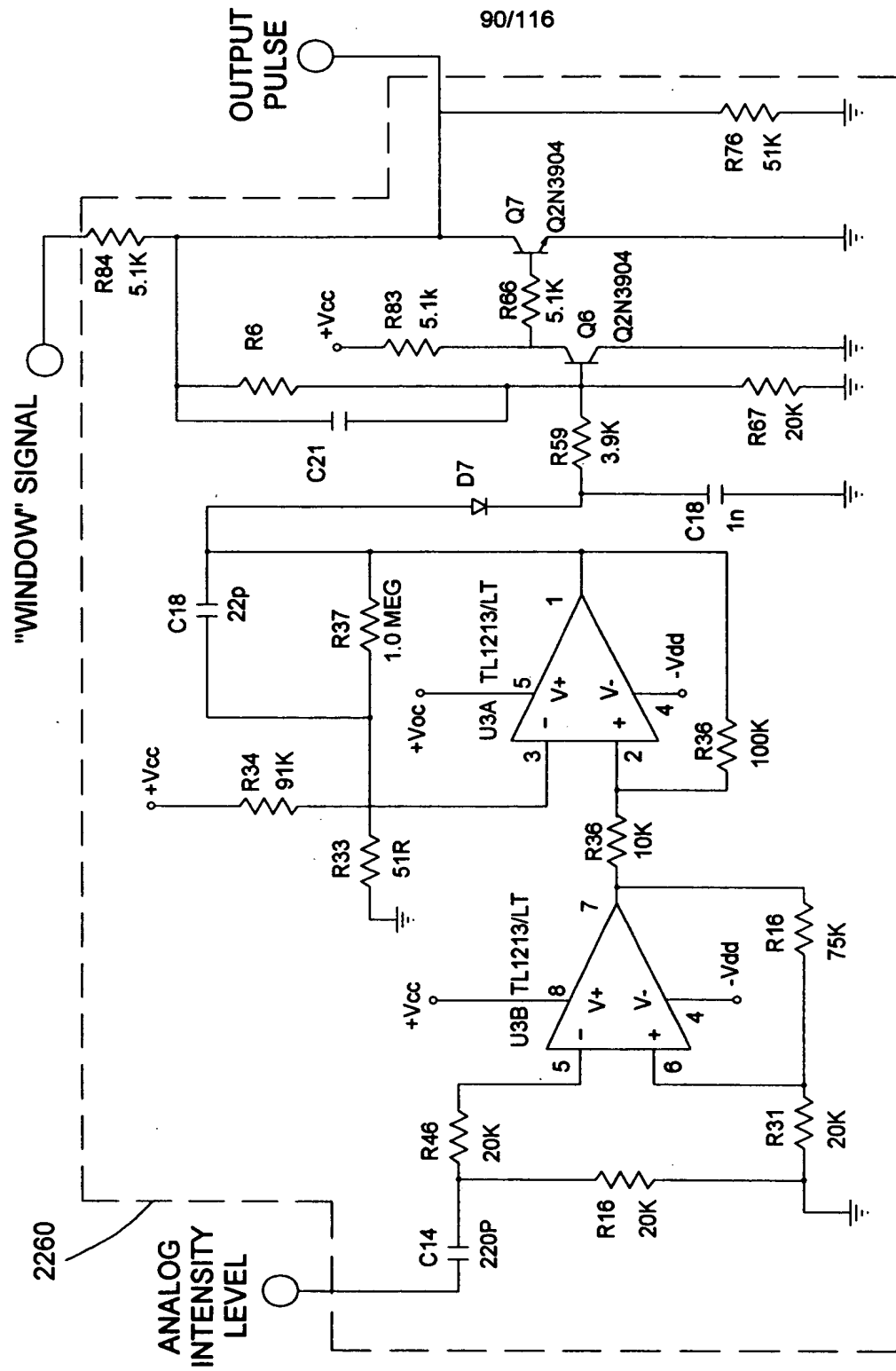


FIG. 38

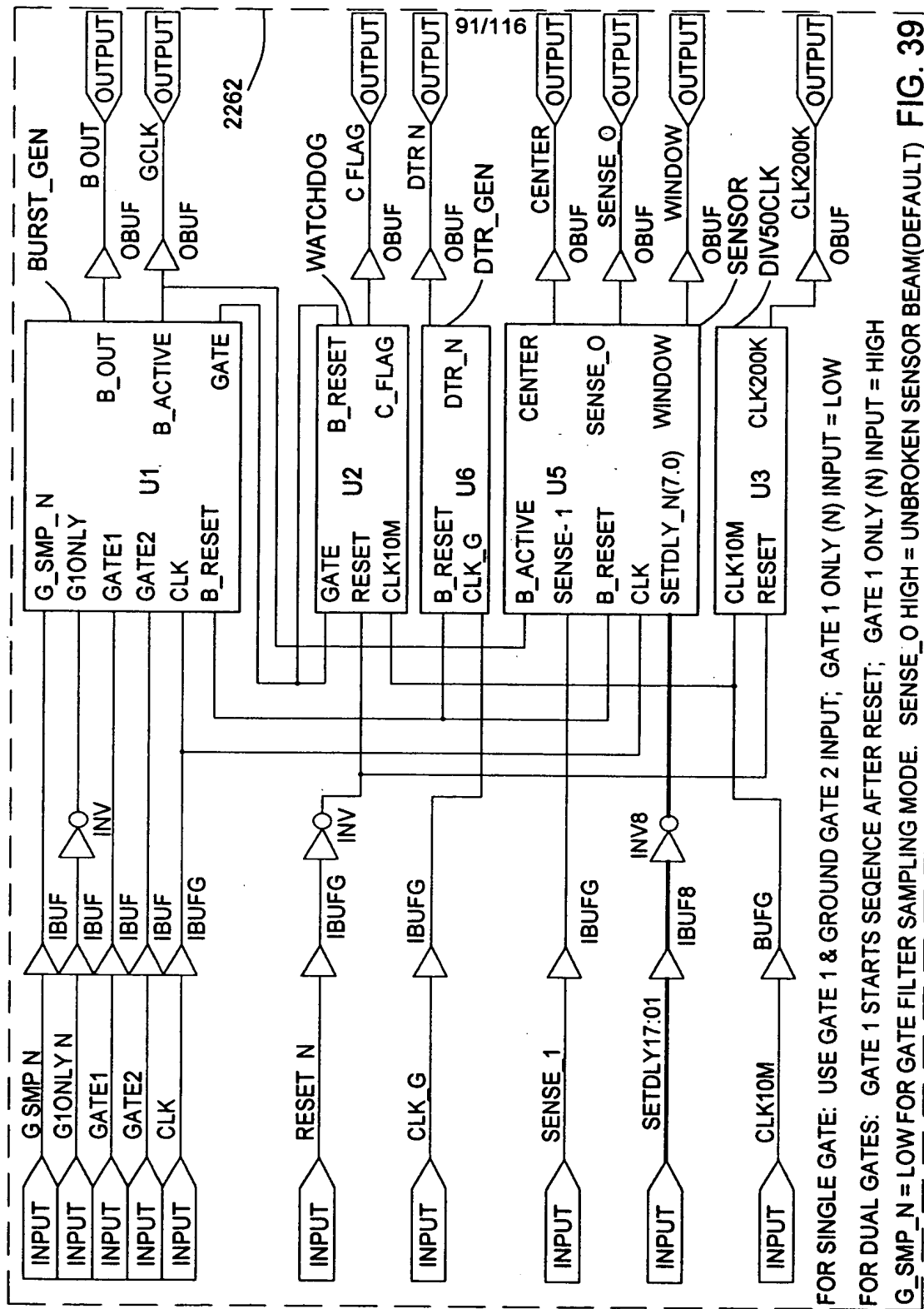


FIG. 39

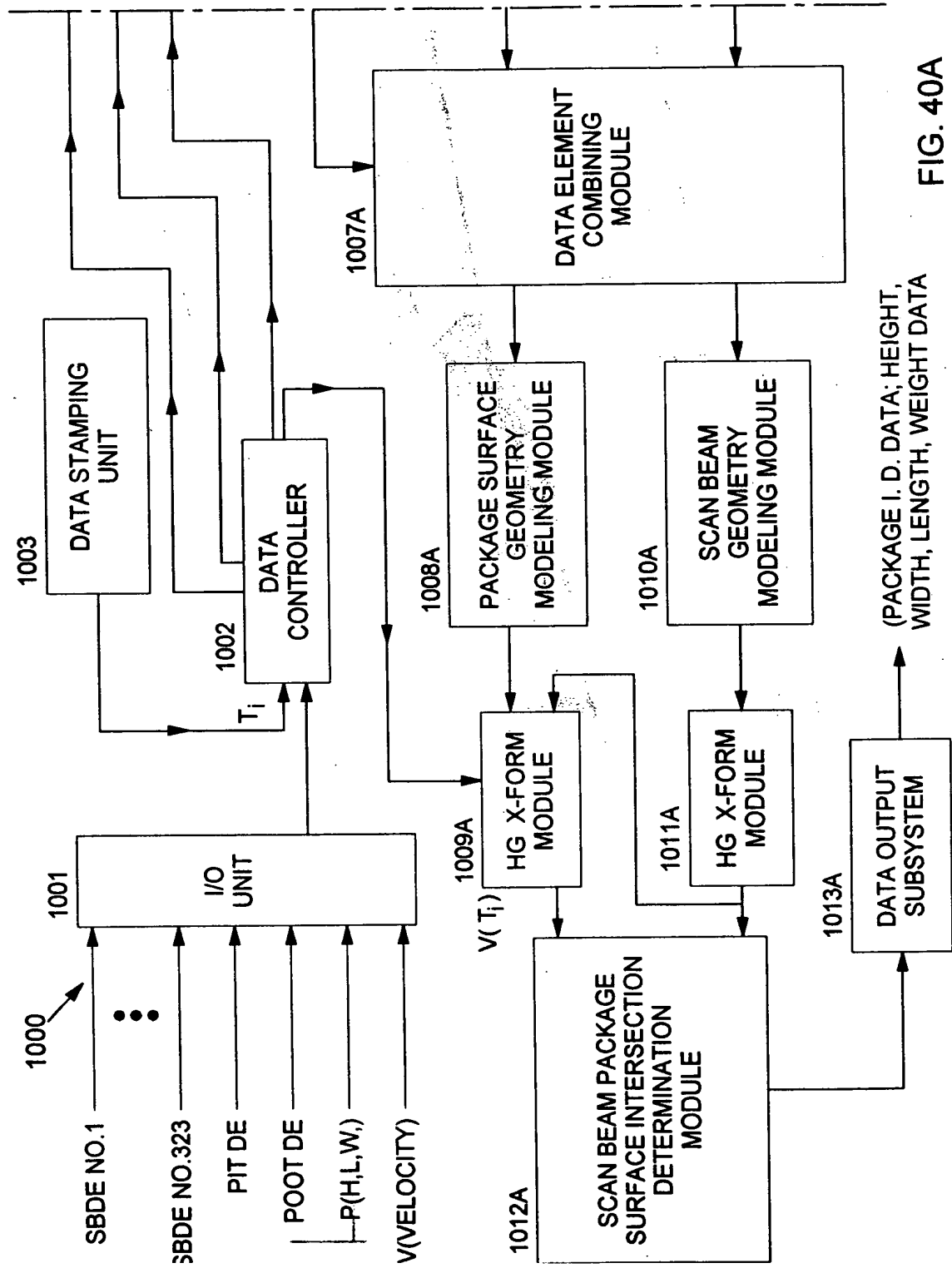


FIG. 40A

DATA ELEMENT TYPES:

- PACKAGE MEASUREMENT DATA ELEMENT
- SCAN BEAM DATA ELEMENT
- PACKAGE-IN-TUNNEL (PIT) DATA ELEMENT
- PACKAGE-OUT-TUNNEL (POOT) DATA ELEMENT

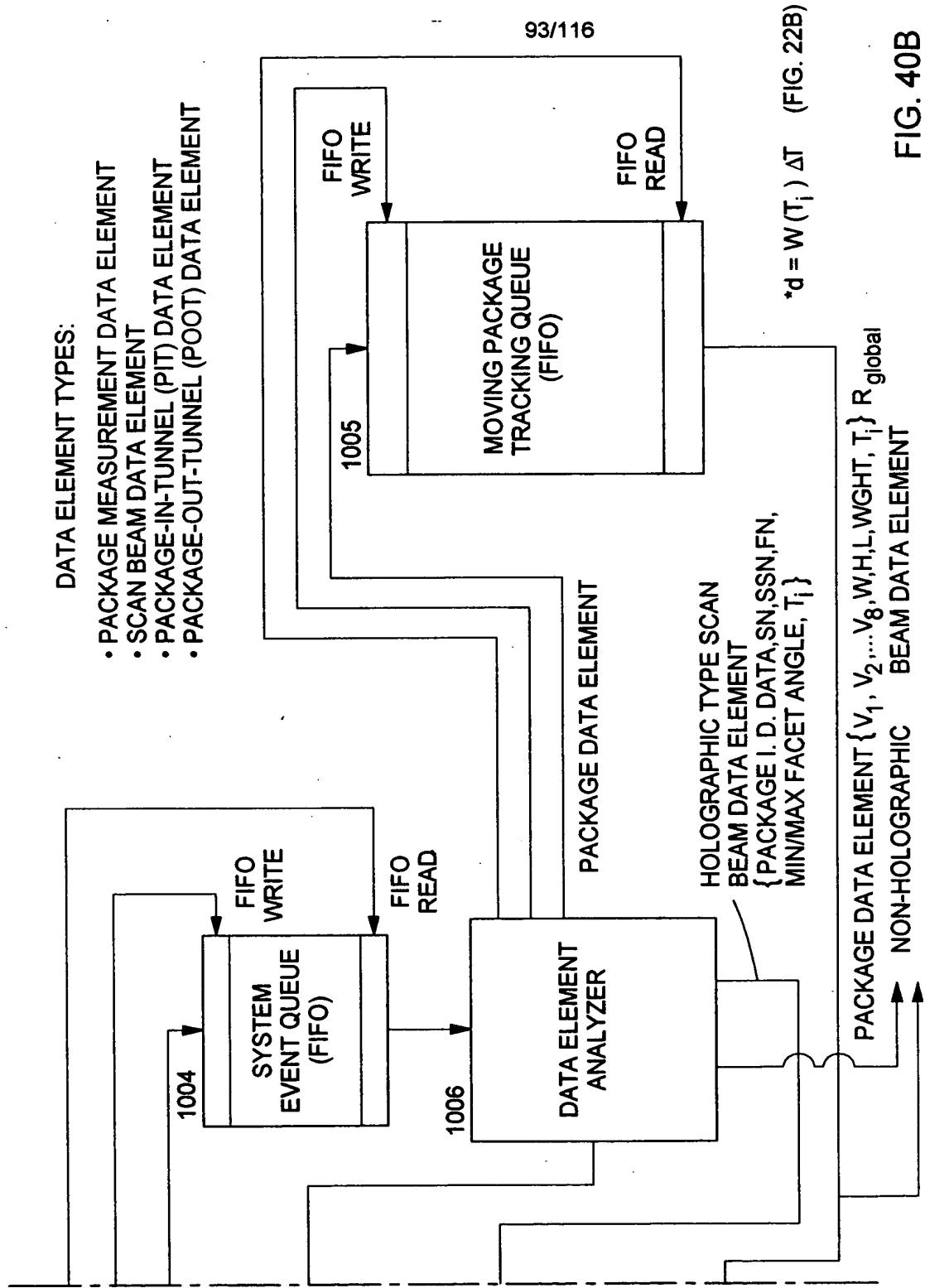


FIG. 40B

DATA ELEMENT HANDLING RULES

1. WHEN A PACKAGE DATA ELEMENT (PDE) OF ANY TYPE IS REMOVED FROM THE SYSTEM EVENT QUEUE, THEN IT IS PLACED IN THE MOVING PACKAGE TRACKING QUEUE
2. WHEN A SCAN BEAM DATA ELEMENT (SBDE) IS REMOVED FROM THE SYSTEM EVENT QUEUE, THEN IT IS COMBINED WITH EACH PACKAGE DATA ELEMENT IN THE MOVING PACKAGE TRACKING QUEUE AND THEN EACH RESULTING DATA ELEMENT PAIR IS PROCESSED ALONG THE PACKAGE DATA ELEMENT CHANNEL AND SCAN DATA ELEMENT CHANNEL AS SHOWN IN FIGS. 40A & 40B
3. WHEN A PACKAGE-IN-TUNNEL (PIT) DATA ELEMENT IS REMOVED FROM THE SYSTEM EVENT QUEUE, THEN THE OLDEST PACKAGE DATA ELEMENT IN THE MOVING PACKAGE TRACKING QUEUE IS REMOVED THERE FROM
4. WHEN A PACKAGE OUT-OF TUNNEL (POOT) DATA ELEMENT IS REMOVED FROM THE SYSTEM EVENT QUEUE, THEN THE FOLLOWING OPERATIONS ARE CARRIED OUT

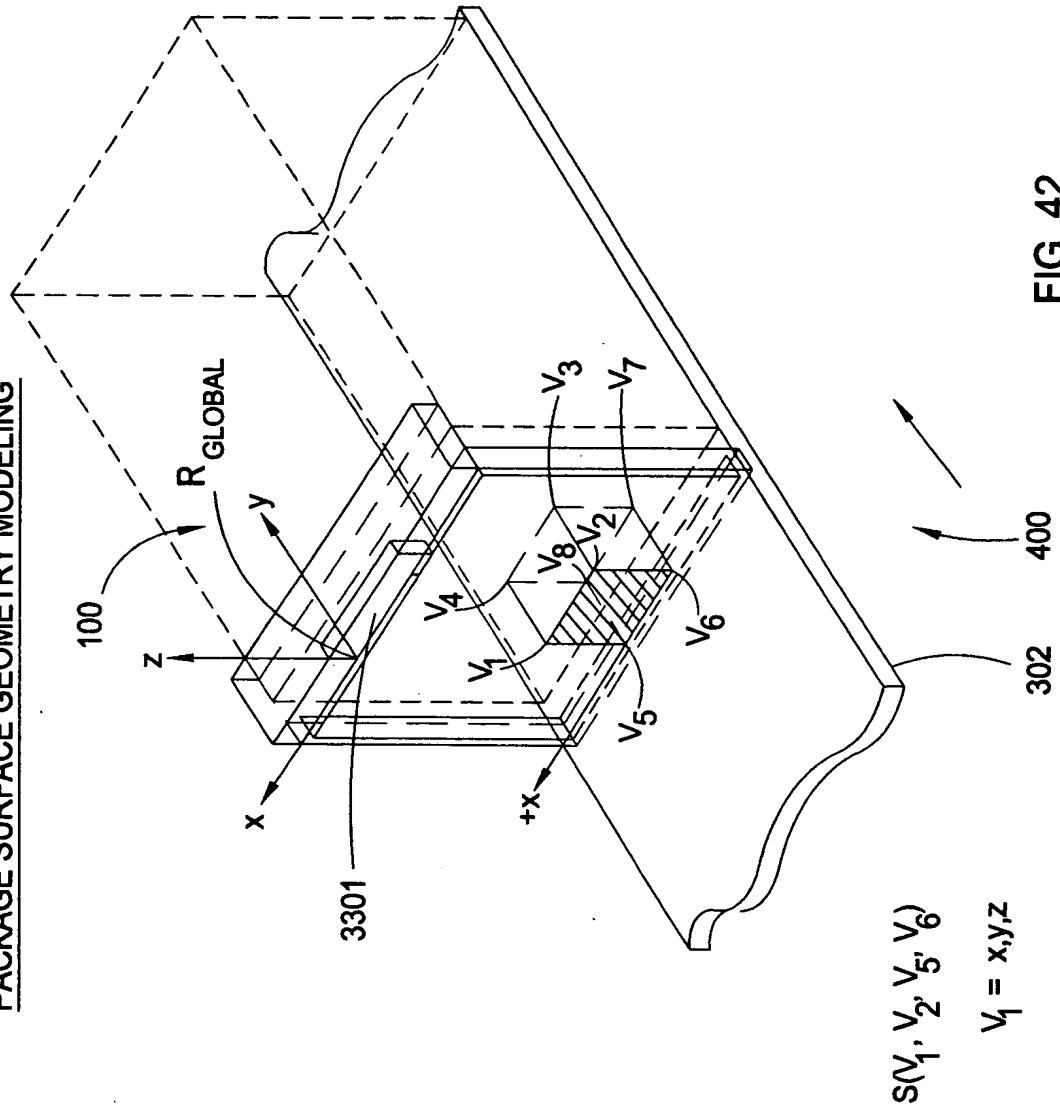
FIG. 41A

(a) IF THE TIME STAMP T_i ON THE REMOVED POOT DATA ELEMENT INDICATES THAT CORRESPONDING PACKAGE HAS MOVED OUT OF THE SCANNING TUNNEL, THEN REMOVE THE OLDEST PACKAGE DATA ELEMENT IN MOVING PACKAGE TRACKING QUEUE

(b) IF THE TIME STAMP T_i ON THE REMOVED POOT DATA ELEMENT INDICATES THAT THE CORRESPONDING PACKAGE IS STILL MOVING THROUGH THE SCANNING TUNNEL, THEN DO NOT REMOVE ANY PACKAGE DATA ELEMENT FROM THE MOVING PACKAGE TRACKING QUEUE.

FIG. 41B

PACKAGE SURFACE GEOMETRY MODELING



**VECTOR-BASED SURFACE MODELING OF PACKAGES MOVING
IN SCANNING TUNNEL**

**MATHEMATICAL FORM OF EACH SURFACE ON THE PACKAGE:
VECTOR-BASED MODEL CONSISTING OF (1) AT LEAST THREE
VERTICE POINTS WITHIN THE PLANE OF THE PACKAGE SURFACE,
AND (2) NORMAL VECTOR FOR THE PLANE.**

PROCEDURE:

- (1) USE POSITION VECTOR (REFERENCED TO $X=0, Y=0, Z=0$ IN R_{global}), FOR SPECIFYING THE POSITION OF EACH VERTEX IN THE PACKAGE SURFACE PLANE; AND**
- (2) USE NORMAL VECTOR FOR SPECIFYING THE SURFACE DIRECTION OF THE PACKAGE SURFACE (AT WHICH LIGHT REFLECTS)**
- (3) THESE FOUR VECTORS SPECIFY THE SURFACE OF THE PACKAGE IN COORDINATE REFERENCE FROM R_{global}**

FIG. 43

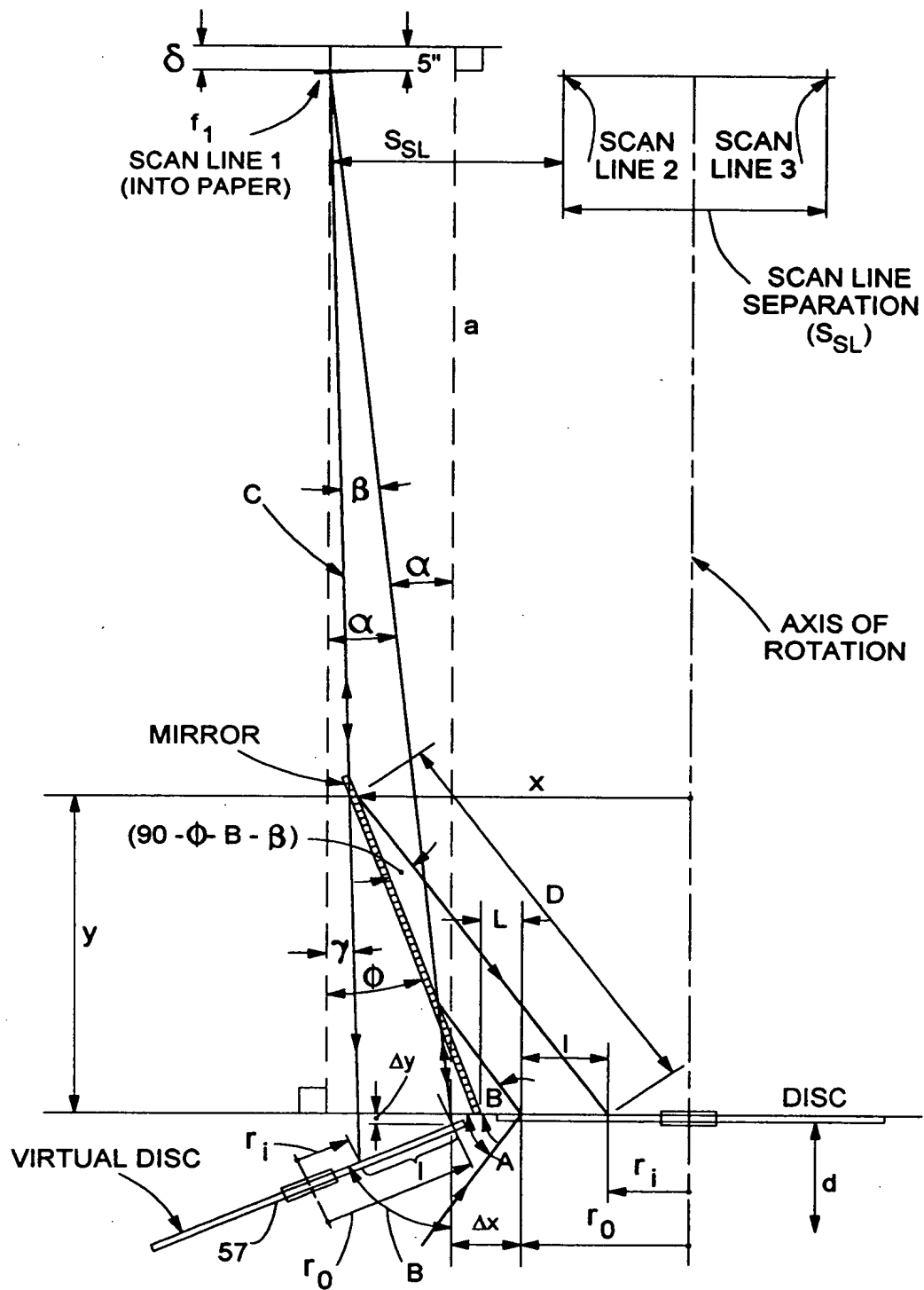


FIG. 44A1

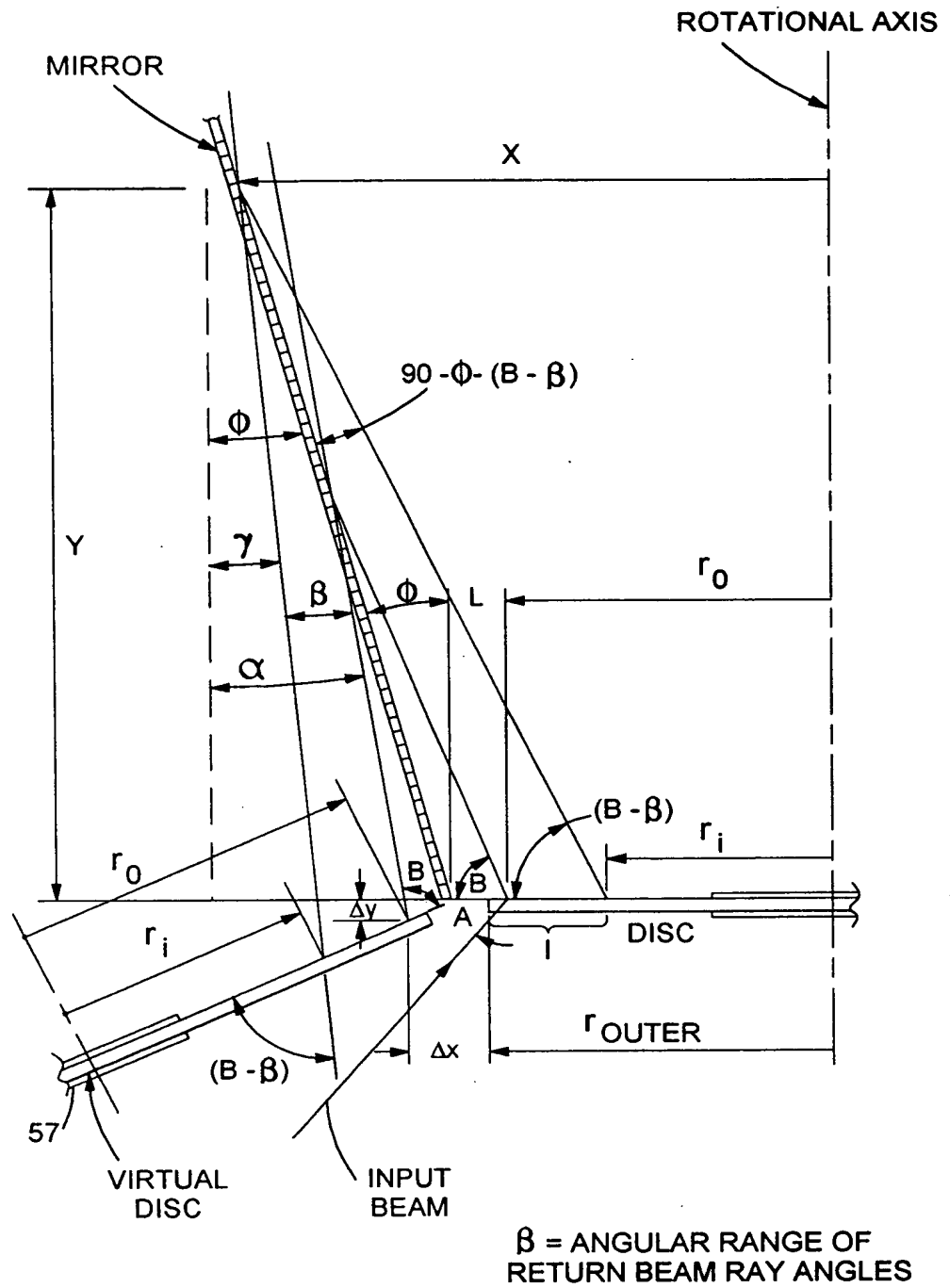


FIG. 44A2

- (1) THE RADIUS TO BEAM-INCIDENT-POINT ON THE HOLOGRAPHIC SCANNING DISC, ASSIGNED THE SYMBOLIC NOTATION " r_0 "
- (2) SCANLINE SEPARATION BETWEEN ADJACENT SCANLINES AT THE FOCAL PLANE OF THE (i,J)-TH SCANLINE, ASSIGNED THE SYMBOLIC NOTATION " s_{SL} "
- (3) THE SCANLINE LENGTH (MEASURED INTO PAPER) FOR THE (i,J)-TH SCANLINE, ASSIGNED THE SYMBOLIC NOTATION " L_{SL} "
- (4) THE DISTANCE MEASURED FROM THE SCANNING DISC TO THE FOCAL PLANE OF THE (i,J)-TH SCANLINE, ASSIGNED THE SYMBOLIC NOTATION a_i
- (5) THE DISTANCE FROM RADIUS TO BEAM-INCIDENT-POINT r_0 TO BEAM FOLDING MIRROR, ASSIGNED THE SYMBOLIC NOTATION " L "
- (6) THE TILT ANGLE OF THE J-TH BEAM FOLDING MIRROR ASSOCIATED WITH GENERATION OF THE (i,J)-TH SCANLINE, ASSIGNED THE SYMBOLIC NOTATION " ϕ_j "
- (7) THE TILT ANGLE OF THE VIRTUAL SCANNING DISC, ASSIGNED THE SYMBOLIC NOTATION " 2ϕ "
- (8) THE LATERAL SHIFT OF THE BEAM INCIDENT POINT ON THE VIRTUAL SCANNING DISC, ASSIGNED THE SYMBOLIC NOTATION " Δx "
- (9) THE VERTICAL SHIFT OF THE BEAM INCIDENT POINT ON THE VIRTUAL SCANNING DISC, ASSIGNED THE SYMBOLIC NOTATION " Δy "
- (10) THE DISTANCE FROM THE ROTATION AXIS TO THE BEAM INCIDENT POINT ON THE VIRTUAL SCANNING DISC, ASSIGNED THE SYMBOLIC NOTATION " $r_0 + \Delta x$ "
- (11) THE DISTANCE FROM THE BEAM INCIDENT POINT ON THE VIRTUAL SCANNING DISC TO THE FOCAL PLANE WITHIN WHICH THE (i,J)-TH SCANLINE RESIDES, ASSIGNED THE SYMBOLIC NOTATION " f_i "
- (12) THE DIAMETER OF THE CROSS-SECTION OF THE LASER BEAM SCANNING STATION, ASSIGNED THE SYMBOLIC NOTATION " d_{BEAM} "
- (13) THE ANGULAR GAP BETWEEN ADJACENT HOLOGRAPHIC SCANNING FACETS, ASSIGNED THE SYMBOLIC NOTATION " d_{GAP} "
- (14) THE OUTER RADIUS OF THE AVAILABLE LIGHT COLLECTION REGION ON THE HOLOGRAPHIC SCANNING DISC, ASSIGNED THE SYMBOLIC NOTATION " r_{OUTER} "

FIG. 44B1

(15) THE INNER RADIUS OF THE AVAILABLE LIGHT COLLECTION REGION ON THE HOLOGRAPHIC SCANNING FACET, ASSIGNED THE SYMBOLIC NOTATION " r_{INNER} "

(16) ONE-HALF OF THE DEPTH OF FIELD OF THE (i, j)-TH SCANLINE, ASSIGNED THE SYMBOLIC NOTATION " δ "

(17) THE DISTANCE FROM THE MAXIMUM READ DISTANCE ($f_i + 5$) TO THE INNER RADIUS r_i OF THE SCANNING FACET, ASSIGNED THE SYMBOLIC NOTATION "c"

(18) THE OUTER RAY ANGLE MEASURED RELATIVE TO THE NORMAL TO THE i-TH HOLOGRAPHIC FACET, ASSIGNED THE SYMBOLIC NOTATION " α "

(19) THE INNER RAY ANGLE MEASURED RELATIVE TO THE NORMAL TO THE i-TH HOLOGRAPHIC FACET, ASSIGNED THE SYMBOLIC NOTATION " γ "

(20) THE LIGHT COLLECTION ANGLE MEASURED FROM THE FOCAL POINT OR THE i-TH FACET TO THE LIGHT COLLECTION AREA OF THE SCANNING FACET, ASSIGNED THE SYMBOLIC NOTATION " β "

(21) THE INTERSECTION OF THE BEAM FOLDING MIRROR AND LINE C, ASSIGNED THE SYMBOLIC NOTATION "x"

(21A) THE INTERSECTION OF THE BEAM FOLDING MIRROR AND LINE C, ASSIGNED THE SYMBOLIC NOTATION "y"

(22) THE DISTANCE MEASURED FROM THE INNER RADIUS TO THE POINT OF MIRROR INTERSECTION, ASSIGNED THE SYMBOLIC NOTATION "d"

(23) THE DISTANCE MEASURED FROM THE BASE OF THE SCANNER HOUSING TO THE TOP OF THE j-TH BEAM FOLDING MIRROR, ASSIGNED THE SYMBOLIC NOTATION "h"

(24) THE DISTANCE MEASURED FROM THE SCANNING DISC TO THE "d" BASE OF THE HOLOGRAPHIC, ASSIGNED THE SYMBOLIC NOTATION

(25) THE FOCAL LENGTH OF THE i-TH HOLOGRAPHIC SCANNING FACET FROM THE CORRESPONDING FOCAL PLANE WITHIN THE SCANNING VOLUME, ASSIGNED THE SYMBOLIC NOTATION " f_i "

(26) INCIDENT BEAM ANGLE, ASSIGNED THE SYMBOLIC NOTATION " A_i "

(27) DIFFRACTED BEAM ANGLE, ASSIGNED THE SYMBOLIC NOTATION " B_i "

FIG. 44B2

- (28) THE ANGLE OF THE J-TH LASER BEAM MEASURED FROM THE VERTICAL, ASSIGNED THE SYMBOLIC NOTATION " $-\alpha$ "
- (29) THE SCAN ANGLE OF THE LASER BEAM, ASSIGNED THE SYMBOLIC NOTATION " θ_{si} "
- (30) THE SCAN MULTIPLICATION FACTOR FOR THE I-TH HOLOGRAPHIC FACET, ASSIGNED THE SYMBOLIC NOTATION " M_i "
- (31) THE FACET ROTATION ANGLE FOR THE I-TH HOLOGRAPHIC FACET, ASSIGNED THE SYMBOLIC NOTATION " θ_{ROTi} "
- (32) ADJUSTED FACET ROTATION ANGLE ACCOUNTING FOR DEADTIME, ASSIGNED THE SYMBOLIC NOTATION " θ'_{ROTi} "
- (33) THE LIGHT COLLECTION EFFICIENCY FACTOR FOR THE I-TH HOLOGRAPHIC FACET, NORMALIZED RELATIVE TO THE 16TH FACET, ASSIGNED THE SYMBOLIC NOTATION " ξ_i "
- (34) THE MAXIMUM LIGHT COLLECTION FOR THE I-TH HOLOGRAPHIC FACET, ASSIGNED THE SYMBOLIC NOTATION " $Area_i$ "
- (35) THE BEAM SPEED AT THE CENTER OF THE (i, j)-TH SCANLINE, ASSIGNED THE SYMBOLIC NOTATION " V_{CENTER} "
- (36) THE ANGLE OF SKEW OF THE DIFFRACTED LASER BEAM AT THE CENTER OF THE I-TH HOLOGRAPHIC FACET, ASSIGNED THE SYMBOLIC NOTATION " ϕ_{SKEW} "
- (37) THE MAXIMUM BEAM SPEED OF ALL LASER BEAMS PRODUCED BY THE HOLOGRAPHIC SCANNING DISC, ASSIGNED THE SYMBOLIC NOTATION " V_{MAX} "
- (38) THE MINIMUM BEAM SPEED OF ALL LASER BEAMS PRODUCED BY THE HOLOGRAPHIC SCANNING DISC, ASSIGNED THE SYMBOLIC NOTATION " V_{MIN} "
- (39) THE RATIO OF THE MAXIMUM BEAM SPEED TO THE MINIMUM BEAM SPEED, ASSIGNED THE SYMBOLIC NOTATION " V_{MAX} / V_{MIN} "
- (40) THE DEVIATION OF THE LIGHT RAYS REFLECTED OFF THE PARABOLIC LIGHT REFLECTING MIRROR BENEATH THE SCANNING DISC, FROM THE BRAGG ANGLE FOR THE FACET, ASSIGNED THE SYMBOLIC NOTATION " δ_e "

FIG. 44B3

PARAMETER EQUATION USED IN THE SPREADSHEET
DESIGN OF THE SCANNER

$$(1) \quad \Delta x \quad := L (1 + \cos (2 \Phi))$$

$$(2) \quad \Delta y \quad := L \sin (2 \Phi)$$

$$(3) \quad \Delta y \quad := r_0 + \Delta x$$

$$(4) \quad C \quad := \sqrt{ (f + \delta)^2 + l^2 + 2 (f + \delta) l \cos (B) }$$

LAW OF COSINES, WHERE : $l = r_{\text{outter}} - r_{\text{inner}}$

$$\beta = \alpha - \gamma = B + 2\Phi - 90 - \gamma$$

$$(5) \quad \alpha \quad := B - 90 + 2\Phi$$

$$(6) \quad r \quad := \alpha - \cos \left[\frac{ (f + \delta)^2 + C^2 - l^2 }{ 2 (f + \delta) C } \right]$$

$$(7) \quad \beta \quad := \alpha - \gamma$$

$$(8) \quad X \quad := D \cos (B - \beta) + r_i$$

$$(9) \quad Y \quad := D \sin (B - \beta)$$

$$(10) \quad D \quad := \frac{ [r_0 + L - r_i] \sin (90 +) }{ \sin (90 - B + \beta - \Phi) } \quad \text{LAW OF SINES}$$

$$(11) \quad h \quad := Y + d$$

FIG. 44C1

$$(12) \quad f_i := \sqrt{a_i^2 + [m S_{SL} - [r_0 + \Delta x]]^2}$$

m IS A FACTOR THAT VARIES FROM SCAN LINE TO SCAN LINE AND DETERMINED BY SCAN LINE SEPARATION AND DISTANCE FROM THE ROTATIONAL AXIS OF THE DISC.

$$(13) \quad B_i := \text{atan} \left[\left[\frac{m S_{SL} - [r_0 + \Delta x]}{a_i} \right] \right] + 90 - 2\phi$$

$$(14) \quad \phi_{Si} := 2 \text{atan} \left[\left[\frac{\frac{1}{2} \text{ScanLineLength}}{f_i} \right] \right]$$

$$(15) \quad M_i := \frac{r_0}{f_i} + \cos(\lambda_1) + \cos(B_i)$$

$$(16) \quad \Theta_{\text{roti}} := \frac{\Theta_{Si}}{M_i}$$

$$(17) \quad \Theta'_{\text{roti}} := \Theta_{\text{roti}} + \underbrace{\frac{d_{\text{beam}}}{r_0} + \frac{d_{\text{gap}}}{r_0}}_{\Theta_{\text{dead}}}$$

$$(18) \quad \xi_i := \left[\frac{f_i}{f_{16}} \right]^2 \frac{\sin[B_{16}]}{\sin(B_i)} H_i$$

$$(19) \quad \text{Area}_i := \pi \left[r_{\text{outer}}^2 + r_{\text{inner}}^2 \right] \frac{\xi_i}{\sum_{i=1}^{16} [\xi_i]}$$

$i = 1, 2, \dots, 16$

FIG. 44C2

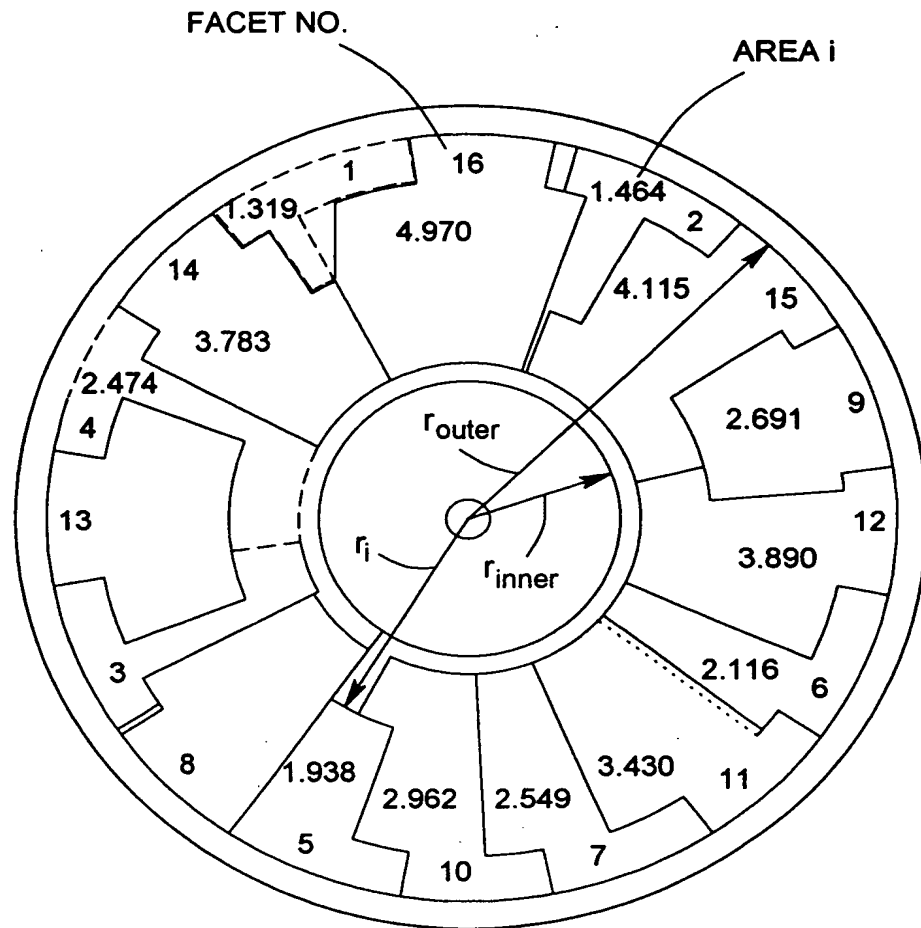


FIG. 44D

**VECTOR MODELING OF LASER SCAN BEAMS IN
HOLOGRAPHIC SCANNING SUBSYSTEMS**

**MATHEMATICAL FORM FOR EACH LASER SCAN BEAM:
VECTOR-BASED MODEL OF OPTICAL PATH OF BEAM FROM DISC TO
MIRROR TO FOCAL PLANE (∞)**

PROCEDURE:

- (1) USE POSITION VECTOR REFERENCED FROM $X=0, Y=0, Z=0$ IN $R_{\text{local scanner}}$ FOR SPECIFYING THE STARTING POINT OF LASER SCAN BEAM ON DISC, AND DIRECTION VECTOR FOR SPECIFYING THE DIRECTION OF LASER BEAM THE BEAM FOLDING MIRROR; AND
- (2) USE POSITION VECTOR FOR SPECIFYING POINT ON MIRROR WHERE BEAM IS REFLECTED FROM BEAM FOLDING MIRROR TOWARDS FOCAL PLANE OF FACET, EXTENDING TO INFINITY, AND DIRECTION VECTOR FOR SPECIFYING THE DIRECTION OF LASER BEAM TOWARDS DESIGNATED FOCAL PLANE
- (3) THESE FOUR VECTORS SPECIFY THE LASER BEAM RAY IN LOCAL COORDINATE REFERENCE $R_{\text{local scanner}}$

FIG. 45

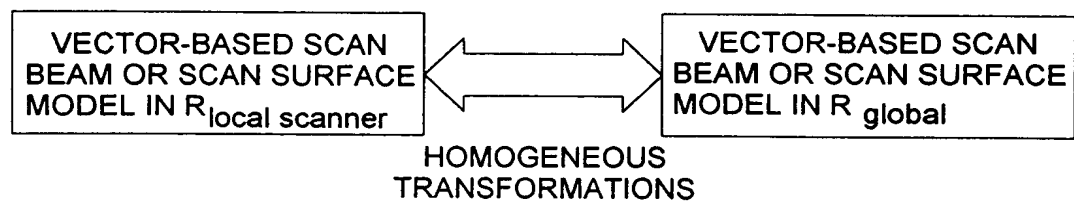
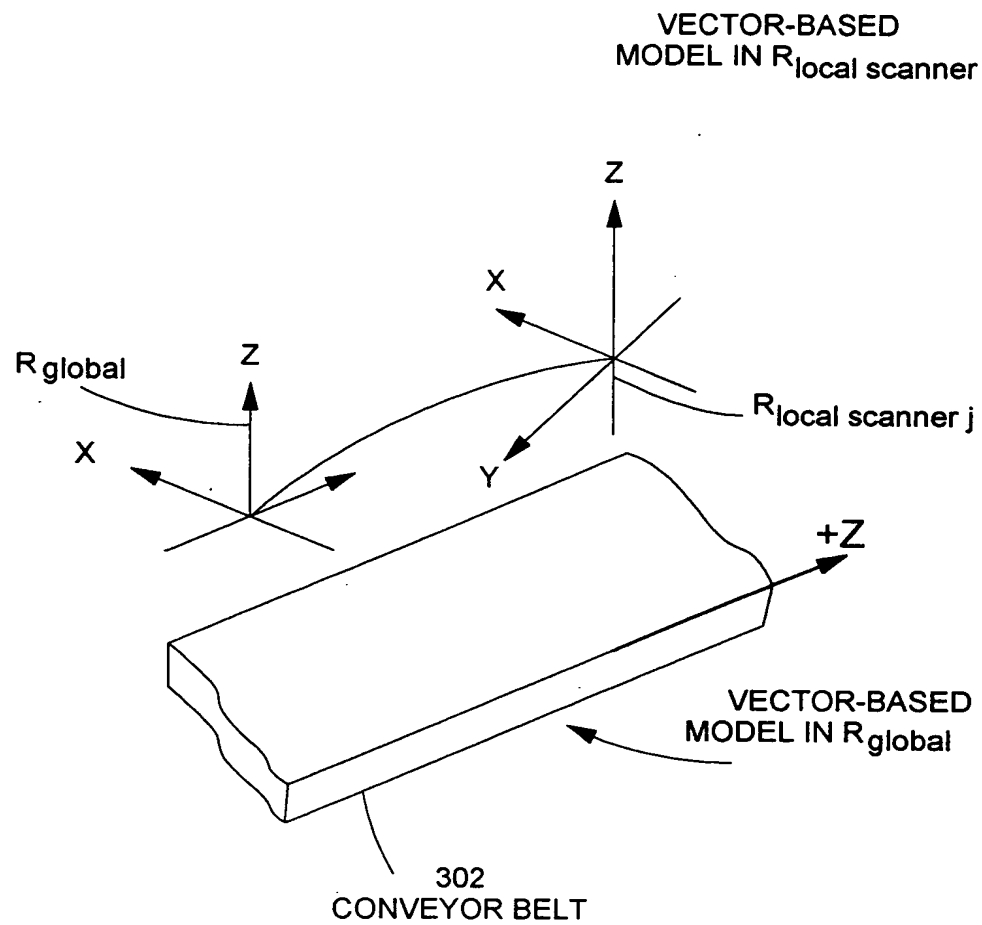
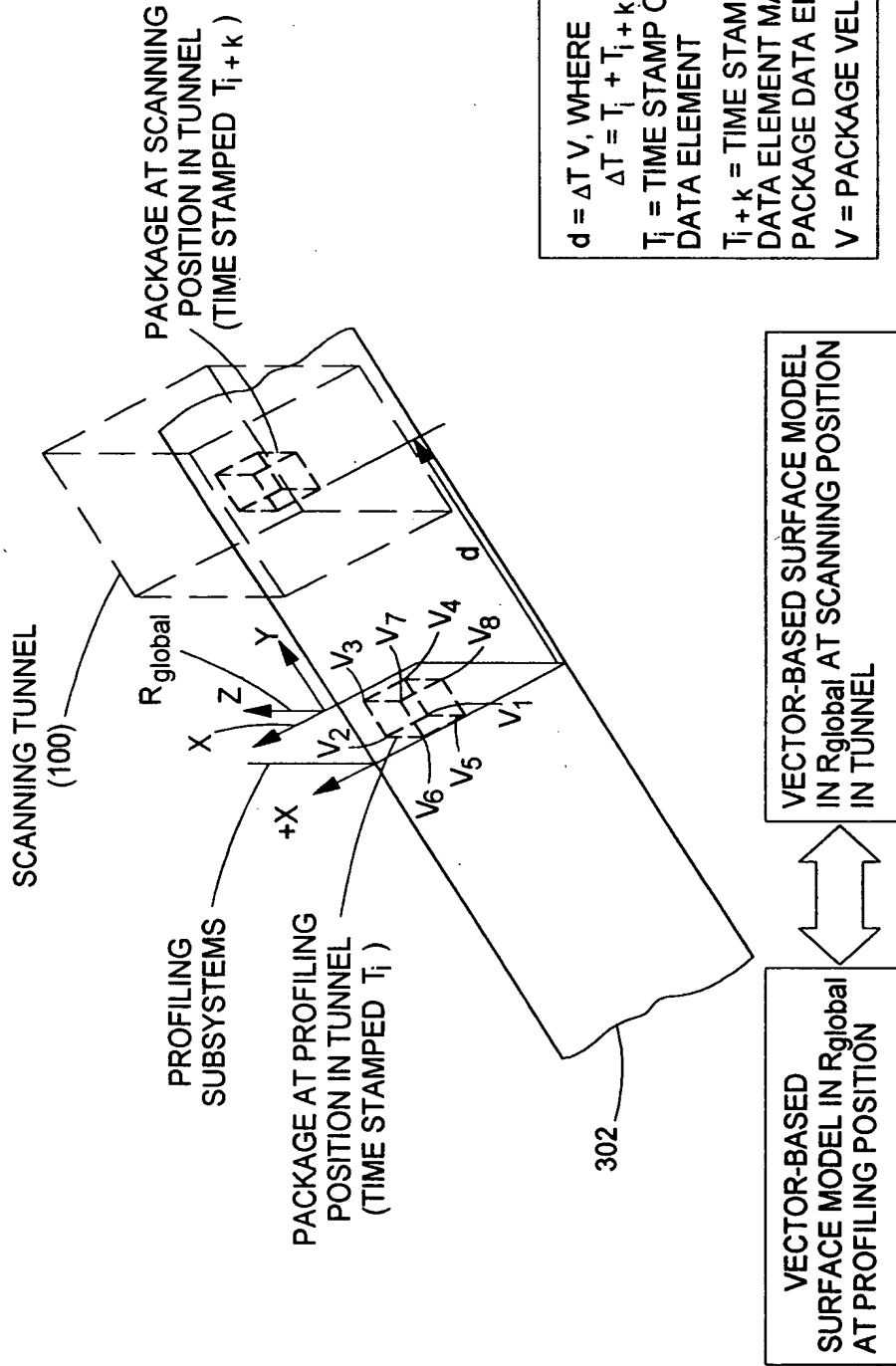


FIG. 46

COORDINATE CONVERSION OF VECTOR-BASED MODELS OF PACKAGE SURFACES



108/116

FIG. 47

SCAN BEAM/PACKAGE SURFACE INTERSECTION DETERMINATION
METHOD FOR SCAN DATA ELEMENTS PRODUCED FROM
HOLOGRAPHIC SCANNING SUBSYSTEMS

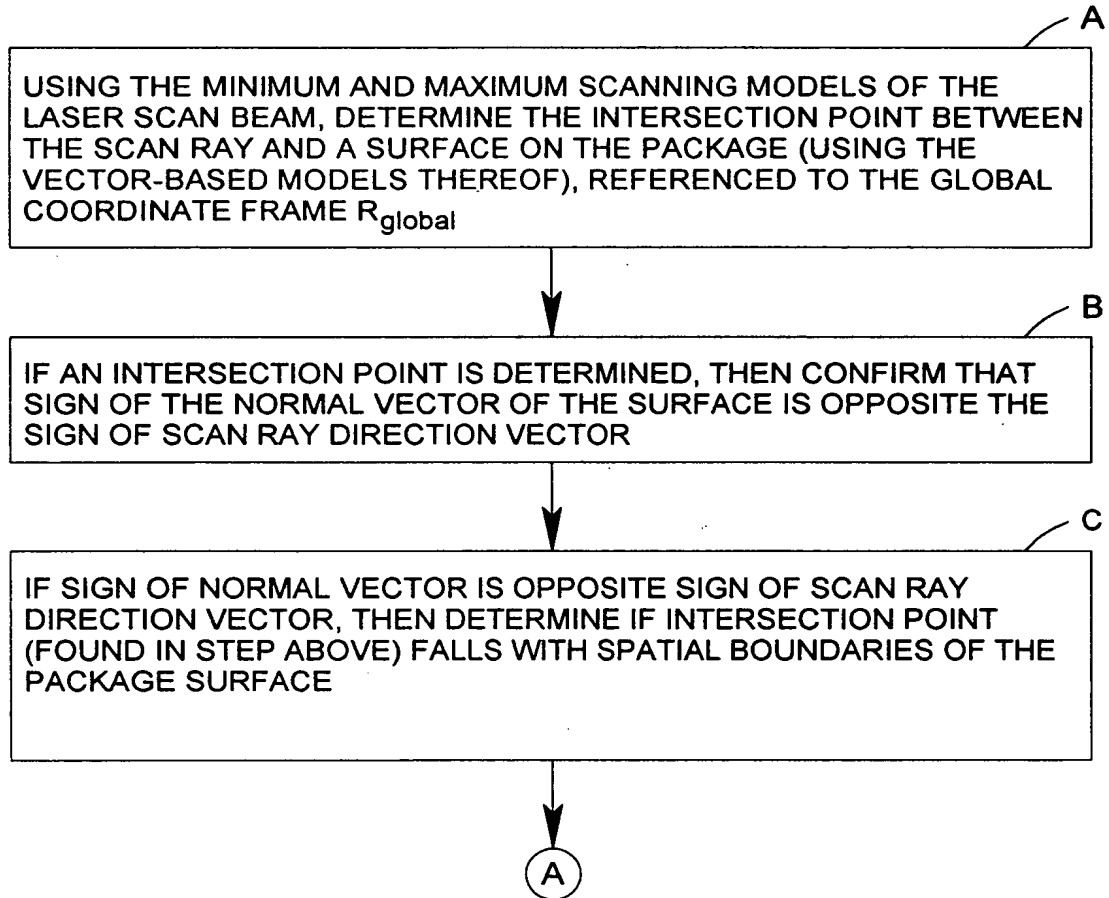


FIG. 48A

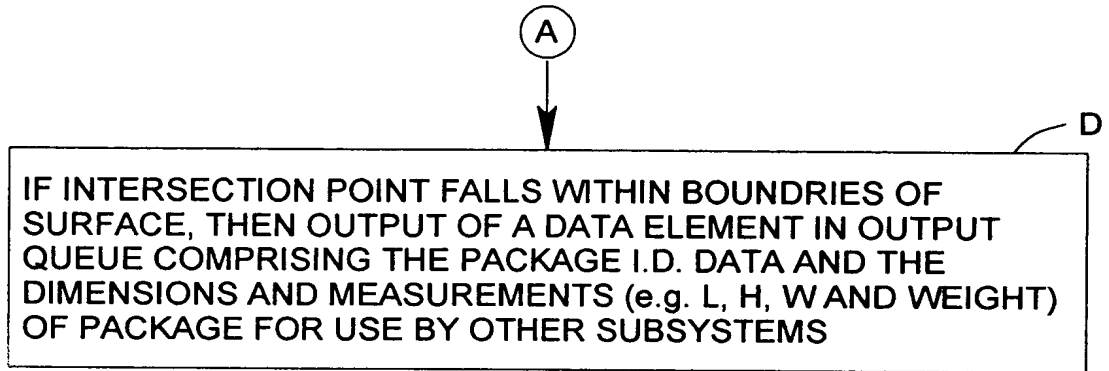


FIG. 48B

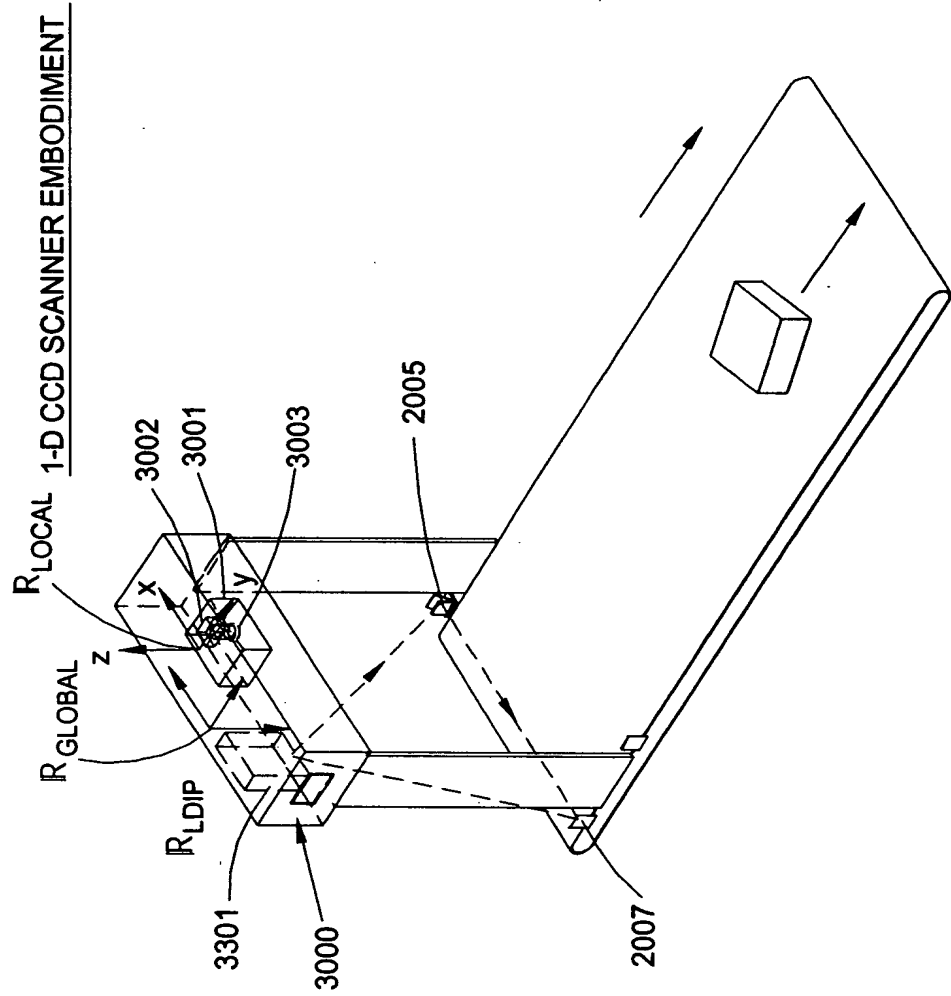


FIG. 49

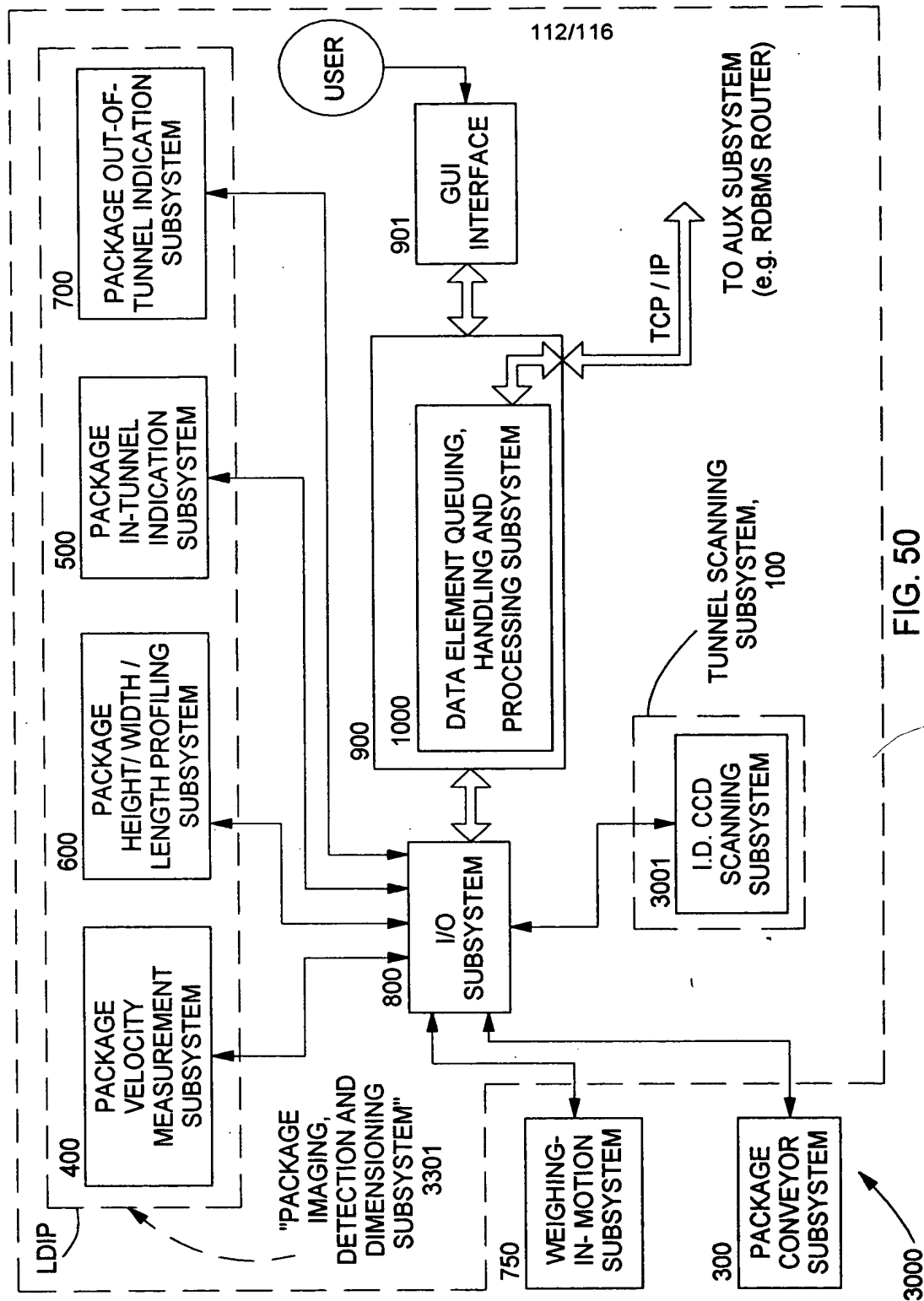


FIG. 50

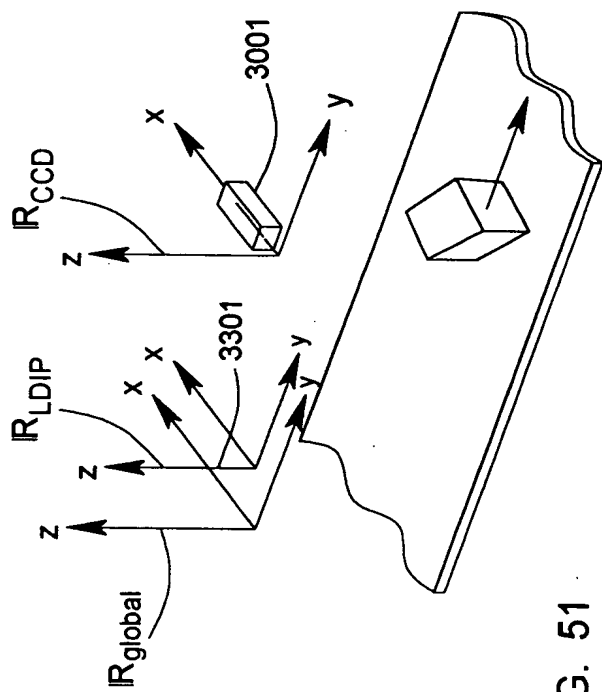


FIG. 51

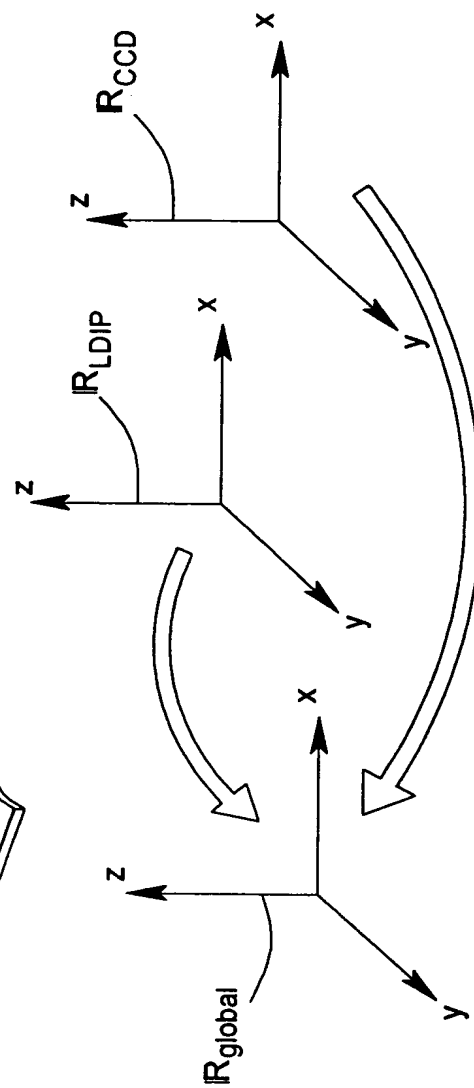


FIG. 52

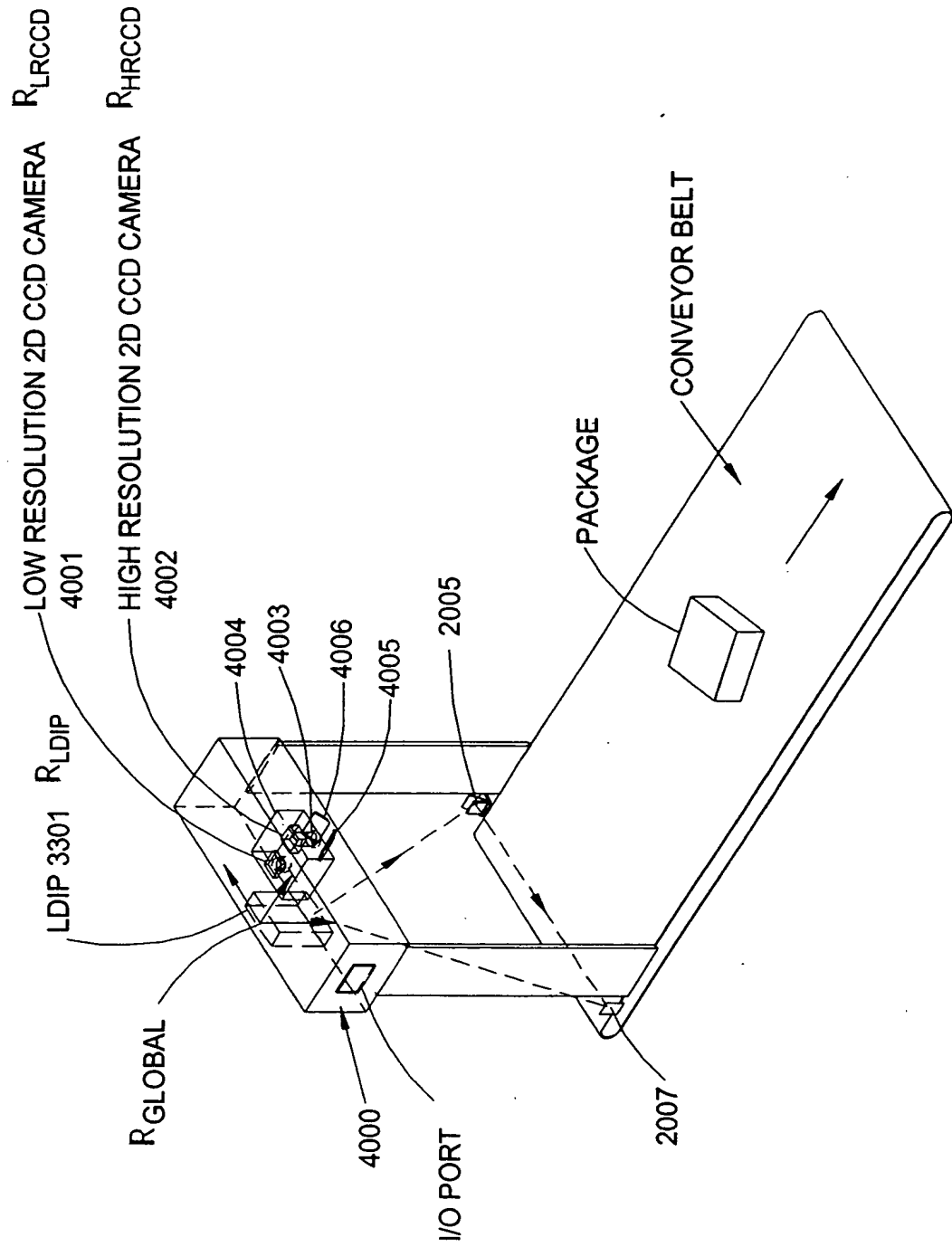


FIG. 53

